SOLID ROCKET PLANT

61 p.

N63 18207

TWENTY-SECOND MONTHLY PROGRESS REPORT
ALGOL SOLID ROCKET MOTOR PROGRAM

Contract No. NAS 1-1330

Period Covered: March 1963

Report 0498-01M-22 15 April 1963

NASA LANGLEY RESEARCH CENTER
MAY 2 1963
LIBRARY BRANCH

OTS PRICE
XEROX $ 6.60
MICROFILM $ 2.25

15 April 1963

TWENTY-SECOND MONTHLY PROGRESS REPORT
ALGOL SOLID ROCKET MOTOR PROGRAM

Prepared by

AEROJET-GENERAL CORPORATION
SOLID ROCKET PLANT
Sacramento, California

Report 0498-01M-22

Contract No. NAS 1-1330

Period Covered: March 1963

Prepared for

National Aeronautics and Space Administration
Langley Research Center
Langley Field, Virginia

AEROJET-GENERAL CORPORATION
A SUBSIDIARY OF THE GENERAL TIRE & RUBBER COMPANY

TABLE OF CONTENTS

		Page
I.	Introduction	1
II.	Summary	2
III.	Program Status	4
	A. Design	4
	B. Fabrication	5
	C. Motor Processing and Shipping	5
	D. Tooling	6
IV.	Testing	6
	A. Objectives	6
	B. Motor Ballistic Performance	7
	C. Motor Components	8
	D. Jet-Vane Performance	12
	E. Flight-Type-Transducer Performance	12
	F. Accelerometer Data	13
V.	Future Work	16

FIGURE LIST

	Figure
Algol II Production and Delivery Schedule	1
Algol IIA-3 (Rehab) Igniter Chamber	2
Modified Igniter Chamber	3
Tooling Schedule	4
Comparison of Algol IIA-3 (Rehab) Pressure and Thrust vs Time	5
Algol IIA-3 (Rehab) Data	6
Pressure-Transducer-Comparison Curve	7
Prefiring and Postfiring Nozzle Contours	8
Contours of Algol IIA-1 and IIA-2 Nozzle-Entrance Erosion	9
Prefiring vs Postfiring Contour, Algol IIA-1 and IIA-2 Exit Cones	10
Algol IIA-3 Thermocouple Locations	11
Nozzle Temperature, Thermocouple TN-090-37.5	12
Nozzle Temperature, Thermocouples TN-180-7.5, -22.5, -37.5	13
Nozzle Temperature, Thermocouples TN-000-1.5, -15.0, -37.5	14
Prefiring and Postfiring Insulation Contour	15
Chamber Temperature, Thermocouples TCF-135-10.0, -16.0	16
Chamber Temperature, Thermocouples TCF-180-10.0, -16.0	17
Chamber Temperature, Thermocouples TCC-180-12.0, -90.0	18
Chamber Temperature, Thermocouples TCC-000-162.0, TCC-045-110.0, TCC-045-162.0	19
Chamber Temperature, Thermocouple TCC-000-275.0, TCC-045, -275.0	20
Chamber Temperature, Thermocouple TCC-270-12.0	21
Comparison of Igniter Performance With and Without Initiator Seal	22
Performance of Igniters With Initiator Seal	23
Prefiring View of Phenolic-Refrasil Jet Vane	24
Prefiring View of Tungsten-Molybdenum Jet Vane	25
Postfiring View of Tungsten-Molybdenum Jet Vane	26
Postfiring View of Tungsten-Molybdenum Jet Vane	27
Postfiring View of Tungsten-Molybdenum Jet Vane	28
Postfiring View of Phenolic-Refrasil Jet Vane	29

FIGURE LIST (cont.)

	Figure
Postfiring View of Phenolic-Refrasil Jet Vane	30
Prefiring and Postfiring Vane Profiles	31
Jet-Vane Thermocouple Locations	32
Jet-Vane Thermocouple Locations	33
Jet-Vane Thermocouple Locations	34
Jet-Vane Temperature, Thermocouples TJV1-1-V1, -2-V2, -3-V3, -4-V4, and -5-V5	35
Jet-Vane Temperature, Thermocouples TJV1-6-P1, -7-P2, -8-P3, -9-P4, and -10-P5	36
Jet-Vane Temperature, Thermocouples TJV1-11-F1, -12-F2 -13-F3, -14-F4, and -15	37
Jet-Vane Temperature, Thermocouples TJV2-7-P2, -9-P4, -11-F1, -13-F3	38
Jet-Vane Temperature, Thermocouples TJV2-6-P1, -8-P3, -10-P5, and -12-F2	39
Jet-Vane Temperature, Thermocouples TJV1-22-B4, -23-B5, and -24-B6	40
Jet-Vane Temperature, Thermocouples TJV1-16-F6, -17-F7, -18-F8, -19-B1, -20-B2, and -21-B3	41
Jet-Vane Temperature, Thermocouples TVJ2-18-F8 and -15-F5	42
Jet-Vane Temperatures, Thermocouples TVJ2-4-V4 and TJV2-5-V5	43
Jet-Vane Temperatures, Thermocouple TJV2-16-F6	44
Jet-Vane Temperature, Thermocouple TJV2-14-F4	45
Jet-Vane Temperature, Thermocouple TJV2-2-V2	46
Jet-Vane Temperature, Thermocouples TSCV-1 and TSSV-1	47
Jet-Vane Force Data	48
Thermocouple Locations, Bourns Transducer Plumbing	49
Transducer Temperature, Thermocouples T_{TT} -3, -5, -7, and -11	50
Transducer Temperature, Thermocouples T_{TT}-8, -9, and -11	51
Transducer Temperature, Thermocouples T_{TT}-2, -4, and -6	52
Transducer Temperature, Thermocouple T_{TT}-1	53
Comparison of Bourns and Taber Transducer Pressure Recordings	54

FIGURE LIST (cont.)

	Figure
Accelerometer Locations	55
Vibration Data, Accelerometer GCFy-0-20.0	56
Vibration Data, Accelerometer GCFy-0-2.0	57
Vibration Data, Accelerometer GCAy-225-20	58
Vibration Data, Accelerometer GCAy-45-20	59
Vibration Data, Accelerometer G1GNy	60
Vibration Data, Accelerometer GCCz-90-304	61
Vibration Data, Accelerometer GCCz-90-160	62
Sound Pressure Level, SPL-30-200	63
Power Spectral Density, Accelerometer GCFy-0-20	64
Power Spectral Density, Accelerometer GCAy-45-20	65
Power Spectral Density, Accelerometer GCFy-0-2	66
Power Spectral Density, Accelerometer GCAy-225-20	67
Power Spectral Density, Accelerometer GCCz-90-304	68
Power Spectral Density, Accelerometer GCLz-90-160	69

I. INTRODUCTION

This is the twenty-second monthly progress report to the National Aeronautics and Space Administration (NASA) under Contract NAS 1-1330. This report covers the fabrication, testing, and delivery of Algol solid-rocket motors for the Scout vehicle during March 1963. The program has undergone numerous redirections since it was initiated; a summary of the program history is as follows:

PROGRAM MILESTONES

Date	Event
June 1961	The Algol I phase of the program was established with the receipt of a Letter of Intent covering 17 Algol I motors: 16 delivery motors and 1 motor for static firing.
November 1961	Direction was received for the development of a new motor (designated Algol IIA) and the reduction of the number of motors in the Algol I phase.
January 1962	An amendment to the contract was received that reduced the number of Algol I motors to nine. The original Algol II phase consisted of the design, development, and testing of 14 Algol IIA motors: 10 delivery motors and 4 motors for static firings; delivery of three Algol Dual Transporters; and tooling for processing four units per month.
February 1962	Contract negotiations were completed on the scope of work defined in January.
April 1962	Contract Change Notification (CCN) No. 1 was received for the fabrication and delivery of two borescopes.
June 1962	A follow-on contract was negotiated for the delivery of 13 additional Algol IIA motors.

I. Introduction (cont.)

PROGRAM MILESTONES (cont.)

Date	Event
November 1962	Direction was received to reduce the Algol IIA motor delivery rate from four to two units per month, which extended the delivery schedule by 6 months.
December 1962	Authority was received to proceed with rehabilitating the Algol IIA-3 chamber for an additional (fifth) static test.
January 1963	Direction was received for the fifth static test to be conducted as proposed with the Algol IIA-3 rehabilitated chamber.

The Algol I phase of the program was completed in May 1962 and descriptions of this past effort are no longer reported.

The schedule for the Algol IIA program (Figure 1) shows the reduction in the delivery rate for Algol IIA motors from four to two units per month in compliance with the direction received in November 1962. Also scheduled, as a result of a hangfire that occurred during the firing of Algol IIA-3 (Rehab), is a sixth static firing to qualify an igniter with an increased main charge. Algol IIA-18 has been selected for this test, which is scheduled for 25 April 1963.

II. SUMMARY

The fifth full-scale motor static firing was conducted at Aerojet-General, Sacramento, on 12 March 1963. All aspects of the firing were normal except for a 3.7-sec hangfire. The total impulse delivered was 4,740,000 lbf-sec over an action time of 66.5 sec. delivered specific impulse was 223.6 lbf-sec/lbm. The web burning time was 45.1 sec and the web impulse was 4,107,180 lbf-sec. The hangfire was attributed to the smooth grain surface that resulted from the use of the aluminum hard core. On all previously fired motors, ignition had

II, Summary (cont.)

been easily sustained because of the coarse grain surface that resulted from the temporary wood cores with Styrofoam inserts that had been used to simulate the new grain configuration.

The following corrective actions for the hangfire were investigated:

A. Increasing the main charge of the igniter to compensate for the smooth condition of the grain.

B. Providing a rough, ignitible surface by mechanical abrasion.

C. Using a combination of A and B.

As a result of this investigation, a technical discussion with NASA personnel was held at Langley Field, Va., on 21 March 1963 and the first action was selected to improve motor ignition characteristics.

Subsequent to the selection of the corrective action, an ignition-recovery program was initiated. The seven existing igniter chambers will be reworked to accommodate the increased main charge and will be loaded with a 2000-gm main charge. Four of the seven igniters will be qualified in the Little Joe II free-volume chamber, two will be delivered (one to PMR, one to Wallops Island, Va.), and the remaining igniter will be used in the sixth static test, scheduled for 25 April 1963.

Motor IIA-13 is ready for radiographic inspection when shipping equipment is available. Motors IIA-16 and -18 were sent to Naval Ammunition Depot (NAD) Concord, Calif., for radiographic inspection. Motor IIA-17 was delivered to PMR, motor IIA-19 is awaiting shipment to NAD, and motor IIA-20 is being final assembled. Nine motors are now in storage at Aerojet and all available shipping equipment is occupied; thus, motors IIA-13, -19, and -20 cannot be shipped to NAD at this time. The delivery of these motors and the processing

II. Summary (cont.)

of motors subsequent to IIA-20 has been suspended until the ignition-recovery program has been successfully completed.

III. PROGRAM STATUS

A. DESIGN

The basic development phase of the program was completed with the fourth static firing. However, the hangfire of Algol IIA-3 (Rehab) has necessitated modification of the igniter. The igniter main charge will be increased from 1400 to 2000 gm of Alcic pellets and the igniter-chamber will be extended 10 in. to accommodate the increased loading. The existing and modified chamber configurations are shown in Figures 2 and 3, respectively. Also, four 0.750-in.-dia ports are to be drilled in the nozzle end of the chamber 90 degrees apart and oriented so that each port vents down on the grain.

The igniter-recovery program to be conducted will include:

1. Static testing of the two remaining 1400-gm charge igniters in the Little Joe II free-volume chamber.

2. Reworking of seven igniters to the new configuration.

3. Loading of all seven reworked igniters with a 2000-gm main charge.

4. Testing of four reworked igniters in the Little Joe II free-volume chamber.

5. Delivery of two reworked igniters, one to PMR and the other to Wallops Island, Va.

III, A, Design (cont.)

6. Using the remaining reworked igniter in the sixth static test.

Motor IIA-18 will be used for the sixth static test. This motor, which is similar to motor IIA-3 (Rehab) (used in the fifth static test), is scheduled to be fired 25 April 1963. This test will be conducted without jet vanes and with the motor conditioned to +50°F prior to the static firing.

B. FABRICATION

The remaining 15 chambers in the follow-on order have been fabricated. Two of these will be used as manufacturing spares. Thirteen insulated chambers have been received, including the rehabilitated IIA-3 chamber. Since the chamber for IIA-3 (Rehab) was not included on the original order, available funds enable insulating only two of the remaining three chambers. Nozzle fabrication by the second-source vendor, Cincinnati Testing Laboratories (CTL), for the follow-on order has been completed.

C. MOTOR PROCESSING AND SHIPPING

Processing of Algol IIA motors was changed by NASA directive, TWX 337-338 from S. T. Butler to C. H. Parr, dated 30 August 1962. This directive requires that either a radiographic or borescopic inspection be performed on all deliverable motors. Motors IIA-4 through -9 were processed with Styrofoam star points imbedded in the grain. These inserts were originally used to change the configuration of the temporary wood cores for a grain-design modification. Because adequate release agents are unavailable, these inserts are not released from the propellant and stay in the motor. The presence of the Styrofoam in the bore of the grain physically obstructs the use of a borescope for inspecting the motor interior. After several attempts, the Styrofoam was mechanically removed from motors IIA-6 and -7. Motor IIA-7 was borescopically inspected in conjunction with the borescope training program conducted by Aerojet-General for NASA personnel.

III. C. Motor Processing and Shipping (cont.)

Wood inserts were successfully used in motors IIA-10, -11, -12, and -13. An aluminum hard core was used in casting all subsequent motors. The following is a summary of the status of motors IIA-13 and IIA-16 through -20.

Motor	Status	Grain Status	Inspection Status
IIA-13	To be delivered	Wood core, removed	To be radiographically inspected at NAD
IIA-16	To be delivered	Aluminum hard core, removed	Radiographically inspected at NAD
IIA-17	Delivered to PMR	Aluminum hard core, removed	Radiographically inspected at NAD
IIA-18	To be statically tested	Aluminum hard core, removed	Radiographically inspected at NAD
IIA-19	To be delivered	Aluminum hard core, removed	To be radiographically inspected at NAD
IIA-20	In final assembly	Aluminum hard core, removed	To be radiographically inspected at NAD

D. TOOLING

The tooling schedule is shown in Figure 4. The third aluminum hard core was received and accepted during February following rework to eliminate surface irregularities and dimensional discrepancies. Tooling is now complete.

IV. TESTING

A. OBJECTIVES

Algol IIA-3 (Rehab) was successfully fired 12 March 1963 at Sacramento. The chamber used in this test was the refurbished Algol IIA-3 motor chamber. The major objectives of this fifth static test, designated AS-DA-07S-TH, were to:

1. Confirm ballistic performance.
2. Verify acceptability of the aluminum hard core.

IV, A, Objectives (cont.)

3. Qualify the second-source nozzle.

4. Qualify an igniter with an improved initiator seal.

5. Determine the actual temperature increase of the flight-type pressure transducer and plumbing during motor operation.

6. Evaluate two NASA-supplied jet vanes.

7. Obtain vibration data at specific locations on the propulsion system for flight analysis.

8. Obtain sound-level data.

All test objectives were achieved.

B. MOTOR BALLISTIC PERFORMANCE

The pressure and thrust-vs-time curves for this firing are presented in Figure 5. A summary of general motor characteristics and performance data is given in Figure 6.

A hangfire of approximately 3.7 sec occurred in the test.

Ignition transient data show that the igniter performed as designed. In Figure 7, pressure traces of the Taber pressure transducer and the Bourns flight-type pressure transducer during the Algol IIA-3 (Rehab) ignition are compared with pressure monitored by a Taber transducer in the test of Algol IIA-3. Further discussion of motor ignition is presented in IV, C, 3.

The total impulse delivered was 4,740,000 lbf-sec over an action time of 66.5 sec (corrected for the hangfire) and the delivered specific impulse was 223.6 lbf-sec/lbm. The web burning time, also corrected for the hangfire, was 45.1 sec and the web impulse was 4,107,180 lbf-sec. Both the total impulse and the web impulse values given were corrected for the drag imposed by actuation of the two jet vanes.

IV. B. Motor Ballistic Performance (cont.)

The chamber pressure reached a peak value of 681.6 psia at 3.819 sec after fire switch. This overpressurization, approximately 65 psia greater than any previously recorded with the redesigned grain, was due to the deep preignition heating of the propellant during the 3.7-sec hangfire. The chamber pressure decreased to 550 psia after 4.754 sec.

The total impulse, originally determined by adding the measured motor impulse and the drag as calculated from the measured jet vane forces, was 4,763,394 lbf-sec, resulting in a specific impulse of 224.7 lbf-sec/lbm. These values are higher than those reported for previous firings although within the normal three-sigma variation. However, to remain consistent with the conservative approach taken previously, these values were reduced. The validity of this approach will be determined following results of the straight ballistic firing that is scheduled for 25 April 1963.

The motor, complete with jet vanes, was conditioned to +77°F for 5 days before the firing. The temperature-conditioning facility was removed from the motor on the morning of the test and the grain temperature was monitored by thermocouples up to firing time. During this period, the grain temperature changed from the initial +77 to +74°F, which was within the required limits of 77 ± 5°F.

C. MOTOR COMPONENTS

All motor components of Algol IIA-3 (Rehab) were of the flight configuration and performed satisfactorily. The chamber (SN 617664) was the same chamber as that used during the third development firing and had been cleaned, hydrostatically tested, and reinsulated with flight-weight insulation for this test. The nozzle (SN 633055) was the first to be statically tested from the second-source vendor, CTL. The igniter (SN 54-27) had an improved initiator seal but was identical to previous igniters in all other respects.

IV. C. Motor Components (cont.)

1. Nozzles

A postfiring inspection of the nozzle revealed that the exit-cone erosion was uniform and similar to that of the first four development firings. The nozzle was sectioned after firing and the erosion and char depths were measured and compared with data obtained on tests of Algol IIA-1 and -2. Figure 8 shows prefiring and postfiring contours of the Algol IIA-3 (Rehab) nozzle. The erosion contour illustrated was obtained directly in line with the star ray, where conditions are the most extreme. The char depth is a result of delaying the postfiring water quench for 3 min to determine the effect of postfiring burning on motor components. Figures 9 and 10 show the prefiring and postfiring contours of sectioned nozzles of motors Algol IIA-1 and -2.

Erosion of the graphite throat was uniform; the postfiring throat area showed an increase of 5.50%. A circumferential crack, similar to those found in previous nozzles tested, was found 4 in. from the aft edge of the graphite throat insert and was clean, indicating that the crack occurred during quenching. As in previous nozzles, this crack propagated from the point where the aft edge of the steel closure and the asbestos overwrap ends. Erosion of the nozzle entrance section was similar to that of previous nozzles. Prefiring and postfiring weights of the nozzle were 432 and 387 lb, respectively.

Thermocouple locations on the motor are shown in Figure 11. Temperature data are included in Figures 12 through 14.

2. Insulated Chamber

The chamber used for this test was of the same flight-weight configuration as those of motors IIA-2, -3, and -2 (Rehab). Postfiring examination revealed that the insulation maintained its integrity throughout the firing. A prefiring and postfiring insulation contour is shown in Figure 15. Thermocouple data are presented in Figures 16 through 21.

IV, C, Motor Components (cont.)

3. Igniter

The igniter used in this test was the same as those used in motors IIA-2, -3, and -2 (Rehab) except that in this test the igniter had an improved initiator seal. Figure 22 compares the performance of igniters with and without the improved initiator seal. These data show that this modification reduced the ignition delay significantly. Figure 23 illustrates the consistent performance in open-air qualification tests of the igniter with the improved initiator seal.

Despite a 3.7-sec hangfire, igniter transient data show that the igniter performance was consistent with the results obtained in the qualification tests. An investigation was initiated immediately after the firing to find the cause of the hangfire. The investigation covered the specific areas outlined below:

a. Igniter components; compliance to specifications and drawings
   (1) Squibs
   (2) Alclo pellets; igniter charge
   (3) Metal parts
b. Igniter production specifications
c. Igniter acceptance tests
d. Motor components; compliance to specifications and drawings
   (1) Propellant raw materials
   (2) Inert parts
e. Motor processing specifications
   (1) Propellant qualification
   (2) Loaded motor
f. Static-test setup

IV. C, Motor Components (cont.)

g. Comparison of test data with previous tests

h. Comparison of above parameters from tested motor with similar motors produced under this contract

The results of the above investigation indicate that the ignition-system performance was within specification limits. This was the first motor tested that was processed by using a permanent or hard (aluminum) core for casting the grain. All previous Algol IIA motors that have been tested and launched successfully were cast with an interim or soft core: wood with Styrofoam. However, this type of hard core is used in most of the other solid-rocket programs at Aerojet-General Corporation and was used on all Algol I motors.

The following corrective actions were investigated:

a. Increasing the main charge of the igniter. This would increase the total heat transfer to the propellant surface.

b. Providing a rough and more ignitable surface by mechanical abrasion. Propellant ignitability (arc-image furnace) tests had shown that the surface produced by a Styrofoam core was more ignitable than that produced by a smooth core.

c. Using a combination of a and b.

The objective is to increase the rate of heat transfer between the hot igniter gases and particles and the exposed propellant surface. This can be accomplished by increasing the total heat available, by directing the gases more uniformly over the propellant surface, or by providing a surface that is more susceptible to entrapping the igniter exhaust. The mechanical-abrasion procedure presented reproducibility problems, possibly necessitating an extensive tooling and development program to obtain an improved, reproducible grain surface.

IV, C, Motor Components (cont.)

Also, logistic problems associated with the reworking of field motors would be encountered. Therefore, the decision reached by NASA and Aerojet was to follow the corrective action described in a, above. This action will provide the earliest possible solution with minimum cost, schedule, and program changes.

The overpressurization that occurred when the motor did ignite was attributed to the deep preignition heating of the propellant during the 3.7-sec hangfire.

D. JET-VANE PERFORMANCE

For the static firing of Algol IIA-3 (Rehab), two jet vanes were installed. One vane, of tungsten and molybdenum, was positioned at the 0-degree (top) position. The second, of phenolic-Refrasil, was positioned at the 180-degree position. Both vanes were actuated from +20 to -20 degrees, which is the same duty cycle used for both Algol IIA-3 and IIA-2 (Rehab). Postfiring inspection revealed complete erosion on the phenolic-Refrasil vane. Thermocouple, lift, and drag data indicated that this vane lasted for 21 sec. The tungsten-molybdenum vane was only slightly eroded on the leading edges, consistent with results of previous tests. Prefiring and postfiring views of the vanes are shown in Figures 24 through 30. Prefiring and postfiring profiles of the vanes are shown in Figure 31.

Internal vane temperatures were recorded by means of thermocouples installed by NASA. Thermocouple locations are shown in Figures 32 through 34. Temperature data are shown in Figures 35 through 47. Force data from the vanes are shown in Figure 48.

E. FLIGHT-TYPE-TRANSDUCER PERFORMANCE

A Bourns pressure transducer (SN 72517-0-6-752) complete with plumbing was installed on Algol IIA-3 (Rehab). The configuration is identical

to that used to monitor pressure on Algol IIA flight tests except that an Aerojet-furnished Taber pressure transducer was substituted for Switch CVC 23-000-356 in the static test to determine the actual temperature increase of the pressure transducer and the plumbing during motor operation. Ten thermocouples were installed on the plumbing and pressure transducer at the Langley Research Center. Figure 49 shows the thermocouple locations. An additional chromel-alumel thermocouple was added at Aerojet to monitor temperature at the extreme bend in the plumbing.

Thermocouple data presented in Figures 50 through 53 show that the thermocouple installed by Aerojet was subjected to the greater initial temperature rise, reaching 292°F 5 sec after fire switch. Except for the thermocouple mounted on the Bourns transducer, all thermocouples recorded peak values from 60 to 250°F at 5 sec after fire switch. The temperatures recorded on the thermocouple located on the Bourns transducer were ambient until 28 sec after fire switch, and then progressively increased to 576°F at 56 sec. Figure 54 shows pressures measured by both transducers during the test.

F. ACCELEROMETER DATA

High-frequency instrumentation for Algol IIA-3 (Rehab) consisted of eight accelerometers and two microphones. Also, for correlation purposes, one low-frequency chamber-pressure measurement was recorded. Figure 55 shows the location of this instrumentation.

With two exceptions, all data appear valid. Accelerometer channel GCCz-90-10 had serious discontinuities throughout the run, i.e., very rapid shifts in the level of the signal. These occurred in a random manner. The data from GCCz-90-10 should be disregarded. The amplitude of sound-pressure-level measurement from SPL-60-100 exceeded the expected value; the recording

IV, F, Accelerometer Data (cont.)

system clipped the peaks of the signal during most of the firing. Amplitude data was thus lost but predominant frequencies can still be determined.

Data were examined by using the following:

1. Visicorder oscillograph playbacks of all data obtained for the full duration.
2. Visicorder high-speed playbacks of sections of special interest.
3. Plots of the g, rms vs time, for all accelerometers except GCCz-90-10 are shown in Figures 56 through 62. Note that GIGNy was ranged for ignition shock detail.
4. Plots of power spectral density (g^2/cps vs frequency) for all data obtained, except for chamber pressure and that data from GCCz-90-10, GIGNy, and SPL-60-100, are shown in Figures 63 through 69.
5. Filtered playbacks made of each accelerometer to check for presence of 63 cps.

In general, the vibration levels were somewhat lower than expected. The range of the accelerometers on the chamber and aft end of the motor could be reduced to -15 g in future tests. The vibration was steady following ignition disturbances and no large amplitude transients were evident. No 63-cps frequencies were recorded on any of the accelerometers except GIGNy; this channel showed the presence of some 60-cps frequencies prior to firing. Very little energy was found at frequencies below 100 cps on any of the accelerometer channels. The following is a discussion of data derived from each accelerometer.

1. GCF6-0-2 The vibration level was steady through the firing at 0.6 g rms. A pronounced energy peak occurred at approximately 1700 cps (1.6×10^{-4} g^2/cps) with a lesser peak at 400 cps (0.8×10^{-4} g^2/cps).

IV, F, Accelerometer Data (cont.)

2. GCFy-0-20 The vibration level was relatively steady at approximately 0.26 g rms. Maximum energy content was contained in frequencies below 2000 cps, the energy decreasing steadily with increasing frequency to that of the noise level at 5000 cps and above.

3. GCCz-90-304 and GCCz-90-160 The vibration level was steady at 0.4 g rms until t + 40 sec and then increased to 2.5 g rms at t + 55 sec. Energy content showed a pronounced peak between 400 and 500 cps of 2×10^{-4} g^2/cps and then decreased steadily to the noise level at 8000 cps.

4. GCAy-45-20 and GCAy-225-20 Following a slight rise at motor ignition, the vibration level was steady throughout a 1.1 g rms. The vibration energy was found in a very broad frequency spectrum to 10 kc, the limit of analysis. The maximum was reached at approximately 1 kc.

The sound pressure levels were higher than expected. SPL-60-100 was in excess of 150 db instead of the expected 145 db, and SPL-30-200 reached approximately 142 db instead of the expected 137 db. A spectral plot of the energy found in SPL-30-200 revealed that nearly all the energy was below 100 cps with the maximum at about 20 cps. Playback of SPL-60-100 shows predominant frequencies to be about 100 cps although spectral analysis was not possible because of the clipping of the data. The results of this test will enable a closer estimate of sound pressure level on future motors of similar configuration.

The ignition phase of the motor was unusual in that a 3.7-sec delay occurred between igniter and grain ignition. The igniter shock sensed by GIGNy reached a maximum of 950 g at approximately 7600 cps and then decayed rapidly to a very low vibration level. The time for the igniter shock to reach each of the accelerometers is tabulated below; time listed is time from fire switch to first significant shock:

IV, F, Accelerometer Data (cont.)

Accelerometer	Time, millisec
GIGNy	6.2
GCFy-0-2	6.2
GCFy-0-20	6.7
GCCZ-90-304	12.2
GCCz-90-160	19.5
GCCz-90-10	26.8
GCAy-45-20	27.8
GCAy-225-20	27.8

V. FUTURE WORK

Processing of motors for delivery will be suspended following motor IIA-20 until the modification to the igniter proves to be effective in eliminating hangfires.

Algol IIA-18 is scheduled to be statically fired at +50°F on 25 April 1963. This will be a straight ballistic firing to qualify the modified igniter. No jet vanes will be installed.

ALGOL II A

NAS-1-1330

MOTOR PRODUCTION/DELIVERY SCHEDULE

SCHEDULE REVISION "E" NOV 1962
LETTER CONTRACT RECEIVED 7 JUNE 1961

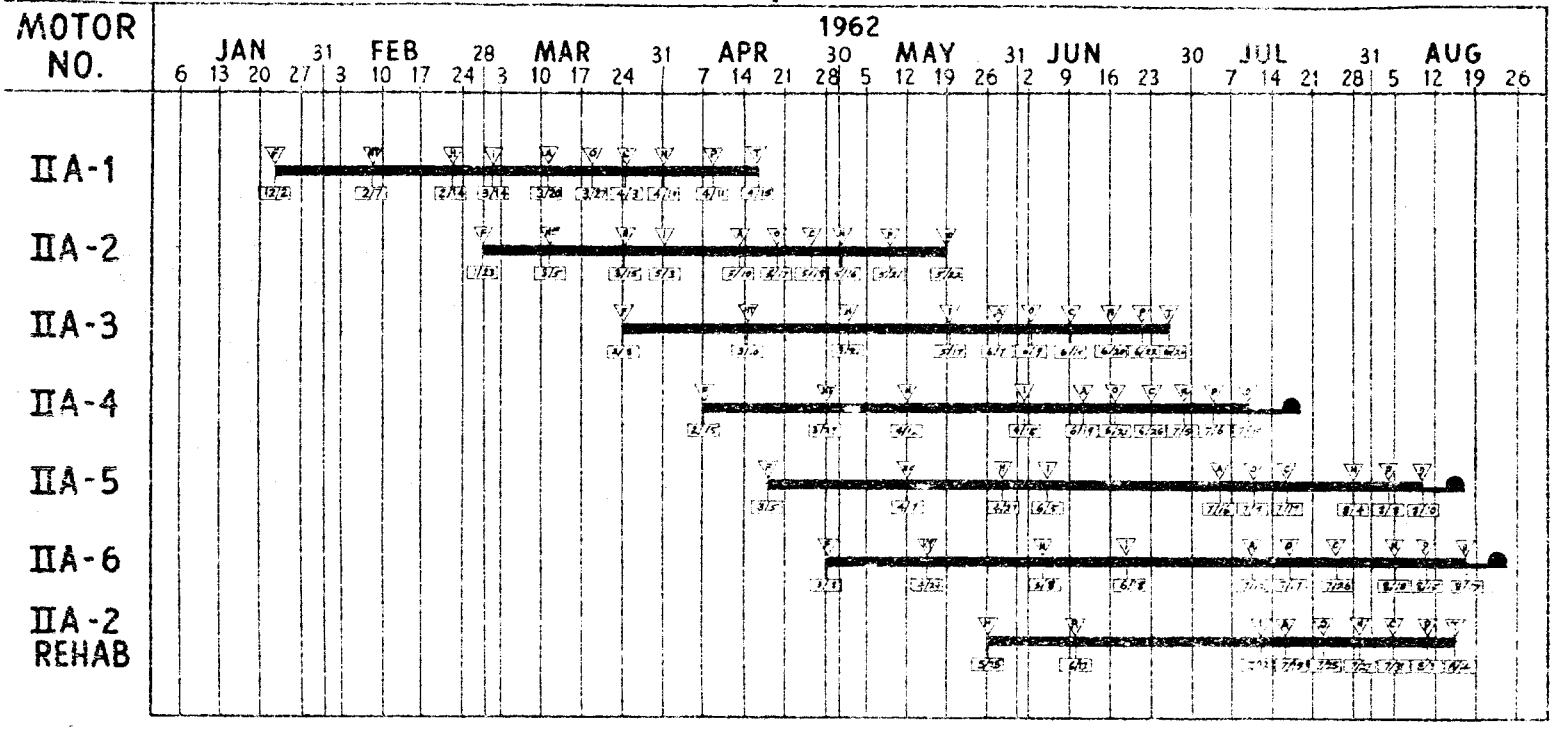

F START FABRICATION CHAMBER
HT HEAT TREAT
H HYDROTEST
R REHABILITATE CHAMBER
I INSULATE CHAMBER

A RECEIVE, ABRADE AND LINE
O CAST PROPELLANT
C CURE PROPELLANT
N RECEIVE NOZZLE
P FINAL ASSEMBLY

D FINAL INSPECTION AND SHIPMENT, F.O.B. NIMBUS, CALIF.
T TEST FIRE (A.G.C. SACRAMENTO)
▽ SCHEDULED TASK COMPLETION DATE
[DATE] ACTUAL DATE TASK COMPLETED
---- REVIEW DATE- ● FLOWN(SUCCESS)

PAGE 1 OF 4

AEROJET GENERAL

TP 7415
4 JAN 63

Figure 1, Sheet 1 of 4

Report 0498-01M-2.2

Program Schedule

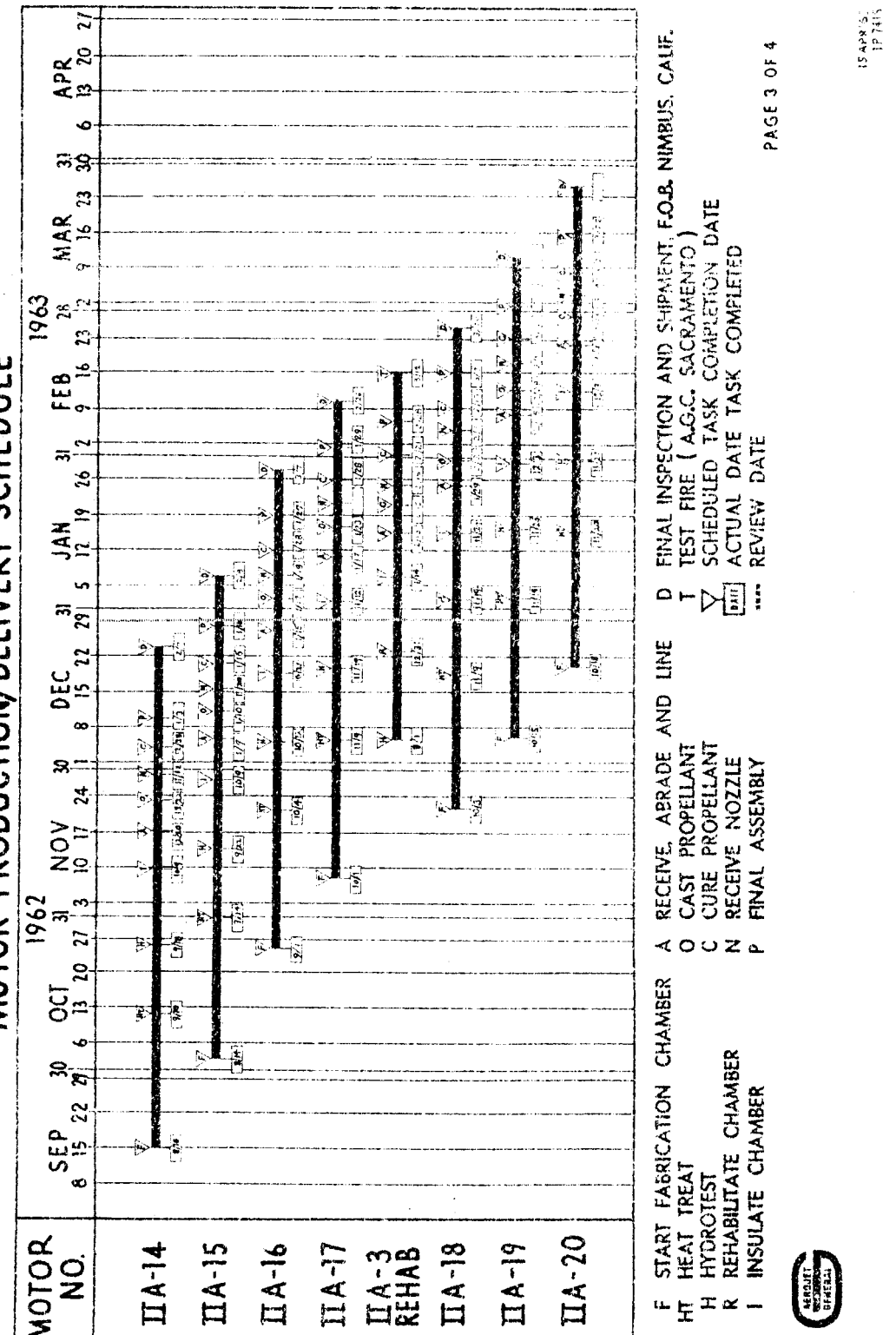

Program Schedule

Figure 1, Sheet 3 of 4

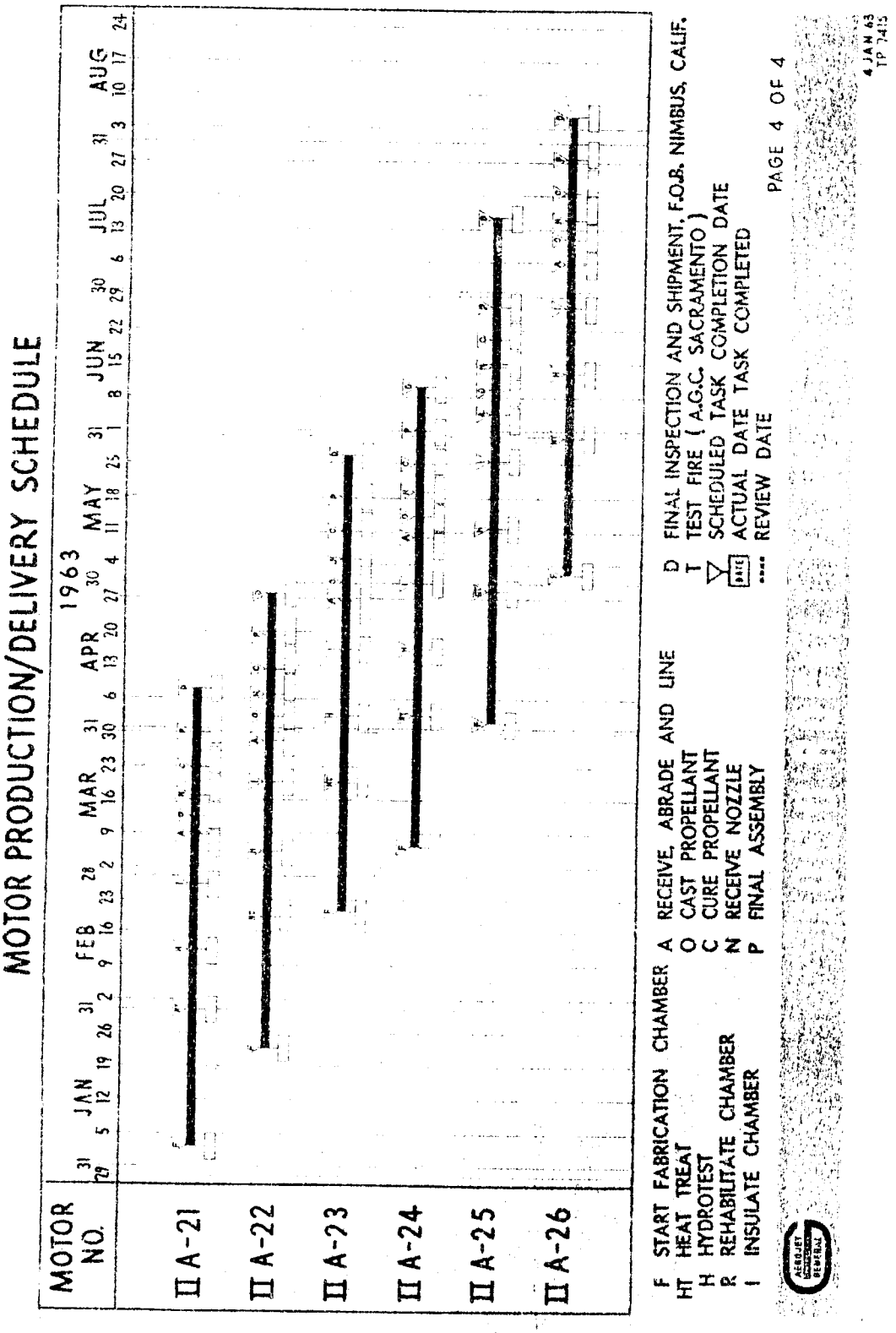

Program Schedule

Figure 1, Sheet 4 of 4

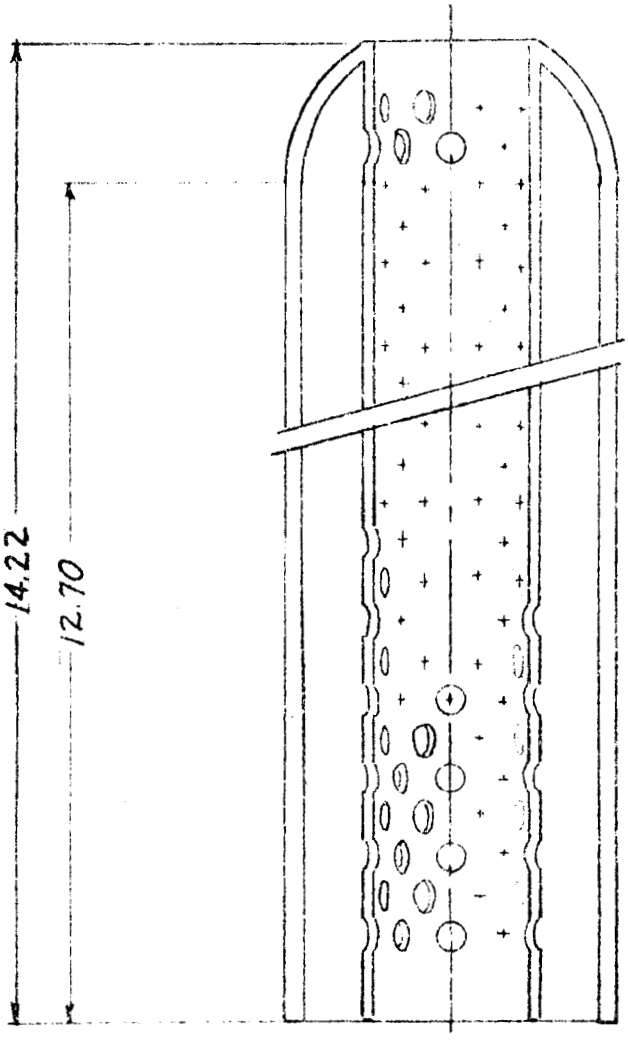

Algol IIA-3 (Rehab) Igniter Chamber

Figure 2

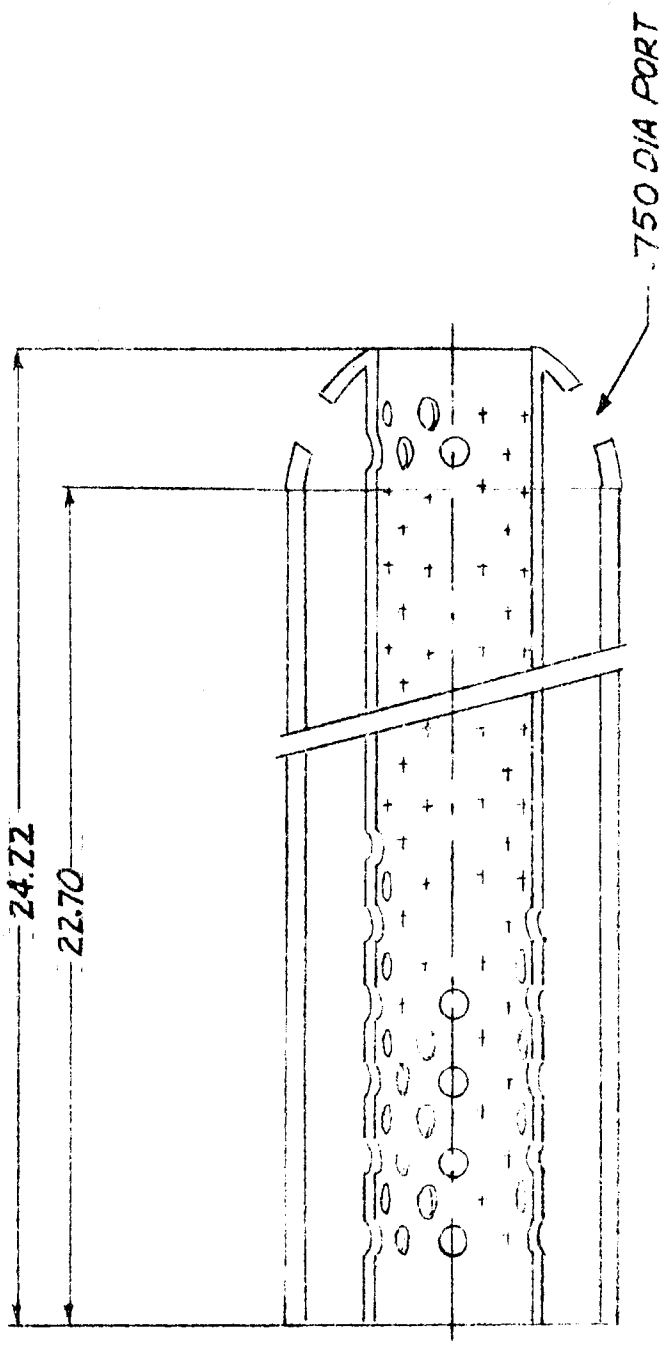

Modified Igniter Chamber

Figure 3

TOOLING SCHEDULE-ALGOL II A MOTOR

CONTRACT NAS1-1330

ITEM NO.	TOOL NO.	DESCRIPTION	QTY.
1.	T-422132	SOFT CORE ASSEMBLY	2
2.	T-422152	CASTING EQUIPMENT	2
3.	T-422163	HANDLING CART CORE	2
4.	T-422188	CURING STAND-TWO MOTORS	1
5.	T-422263	INSTALLATION TOOL-IGNITER	3
6.	T-404262	HORIZONTAL LIFTING BEAM	1
7.	T-420378	BELL EXTENSION	1
8.	T-421737	HANDLING RINGS	3
9.	T-422306	TRANSPORT CART-ALUMINUM CORE	3
10.	T-422305	CORE ASSEMBLY-ALUMINUM	3
11.	E-300044	HORIZONTAL TRAILER	1
12.	T-416147	CORE ASSEMBLY BRACKET	3
13.	T-416148	BREAKAWAY FIXTURE CORE	1
14.	T-422131	PAINT FIXTURE	1

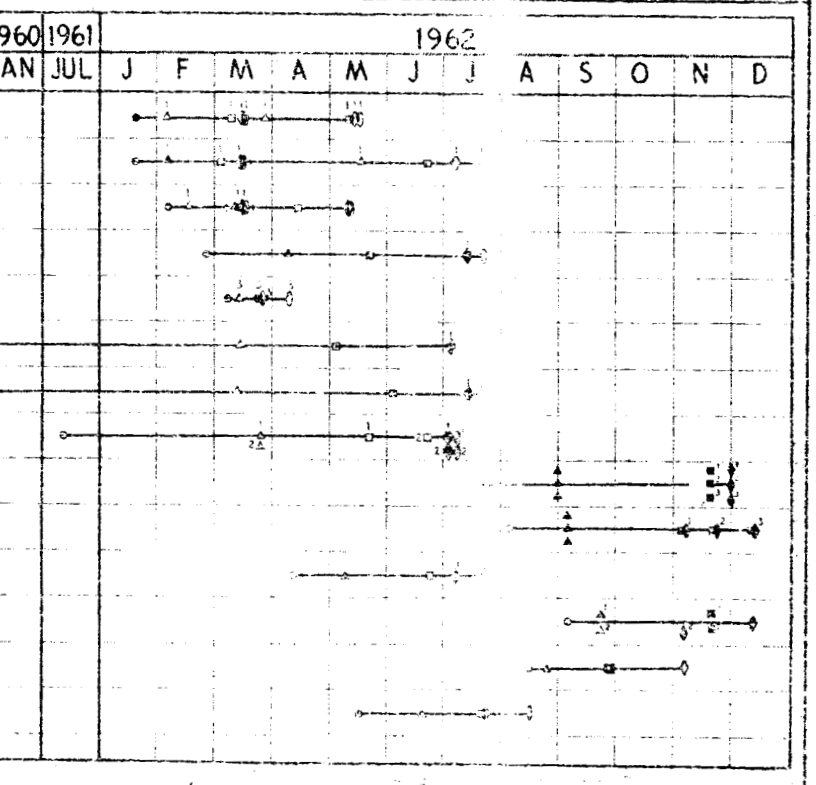

○ DESIGN COMP DATE △ IN FABRICATION □ DATE TO BE INSPECTED ♦ DRY RUN ◊ DATE REQUIRED

CHART NO. TP 8334
DATE 28 JUN '62

Aerojet-General

Figure 4

Tooling Schedule

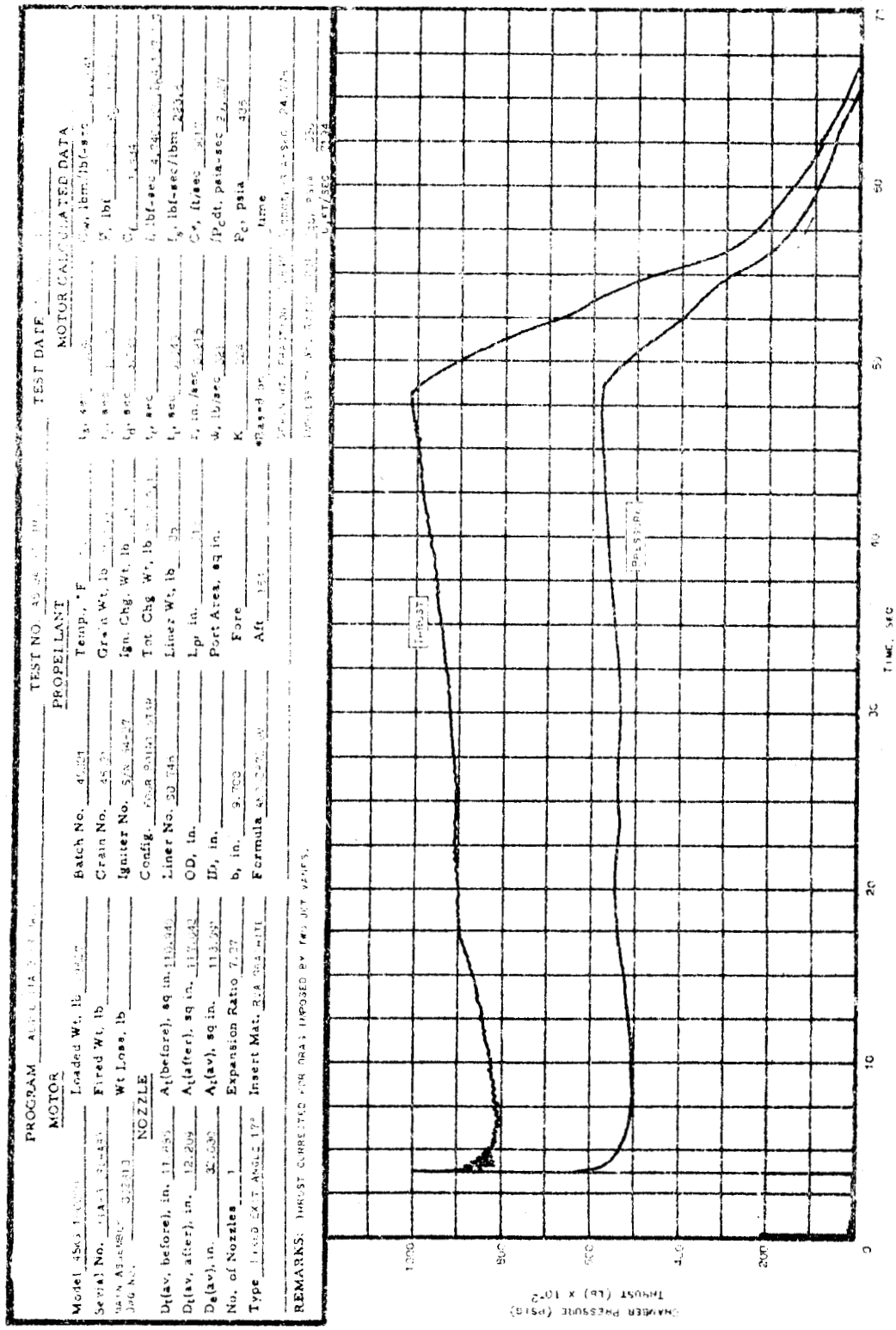

Curves of Algol IIA-3 (Rehab) Pressure and Thrust vs Time

Figure 5

General Motor Characteristics

Loaded motor weight, lbm	23,627
Propellant weight, lbm	21,199
Total inert parts weight, lbm	2428
Expended motor weight, lbm	2201
Nozzle weight, lbm	432
Chamber weight, lbm	1650
Insulation weight, lbm	288
Liner weight, lbm	35
Igniter weight, lbm	23
Weight loss, lbm	21,426
Igniter charge weight, lbm	3.1
Characteristics velocity (C*), ft/sec	5017
C_w (total burning time), lbm/lbf-sec	0.00641
Web thickness, in.	9.700
Nozzle exit cone half angle, degrees	17
Maximum thrust misalignment (calculated), degrees	0.2008
Motor overall length, in.	357.6
Chamber dia., in.	40.0
Operating temperature limits, ^{o}F	-70 to -90
Storage temperature limits, ^{o}F	-70 to -70
Initial throat area, sq in.	110.940
Final throat area, sq in.	117.042
Throat area increase, %	5.50

Algol IIA-3 (Rehab) Data

General Motor Characteristics (cont)

Initial exit area, sq in.	806.010
Final exit area, sq in.	804.800
Nozzle expansion ratio	7.27
Propellant mass fraction	0.897
[illegible]	1.64
Initial burning surface area, sq in.	24,800
Free volume, cubic in.	41,800
Grain configuration	4 point star

Motor Ballistic Characteristics

Average thrust (web), lbf	91,119
Average thrust (total), lbf	71,270
Maximum thrust, lbf at 3.807 sec	112,440
Impulse (web), lbf-sec	4,107,181
Impulse (total), lbf-sec	4,740,000
Specific Impulse (total), lbf-sec/lbm	223.6
Average pressure (web), psia	550
Average pressure (total), psia	436
Maximum pressure, psia at 3.819 sec	681.6
Grain temperature, ^{C}F	74
Ignition delay, sec	3.725
Ignition interval, sec	0.040
Burning rate, in./sec	0.215
Web burning time, sec	45,075
Total burning time, sec	66.50

Algol IIA-3 (Rehab) Data

Motor Ballistic Characteristics (cont)

Weight flow rate, lbm/sec	321
C_f (total burning time)	1.44
Impulse to weight ratio, lbf-sec/lbm	201
Center of gravity loaded (calculated) inches aft of forward thrust flange	
Center of gravity expended (measured) inches aft of forward thrust flange	191.82

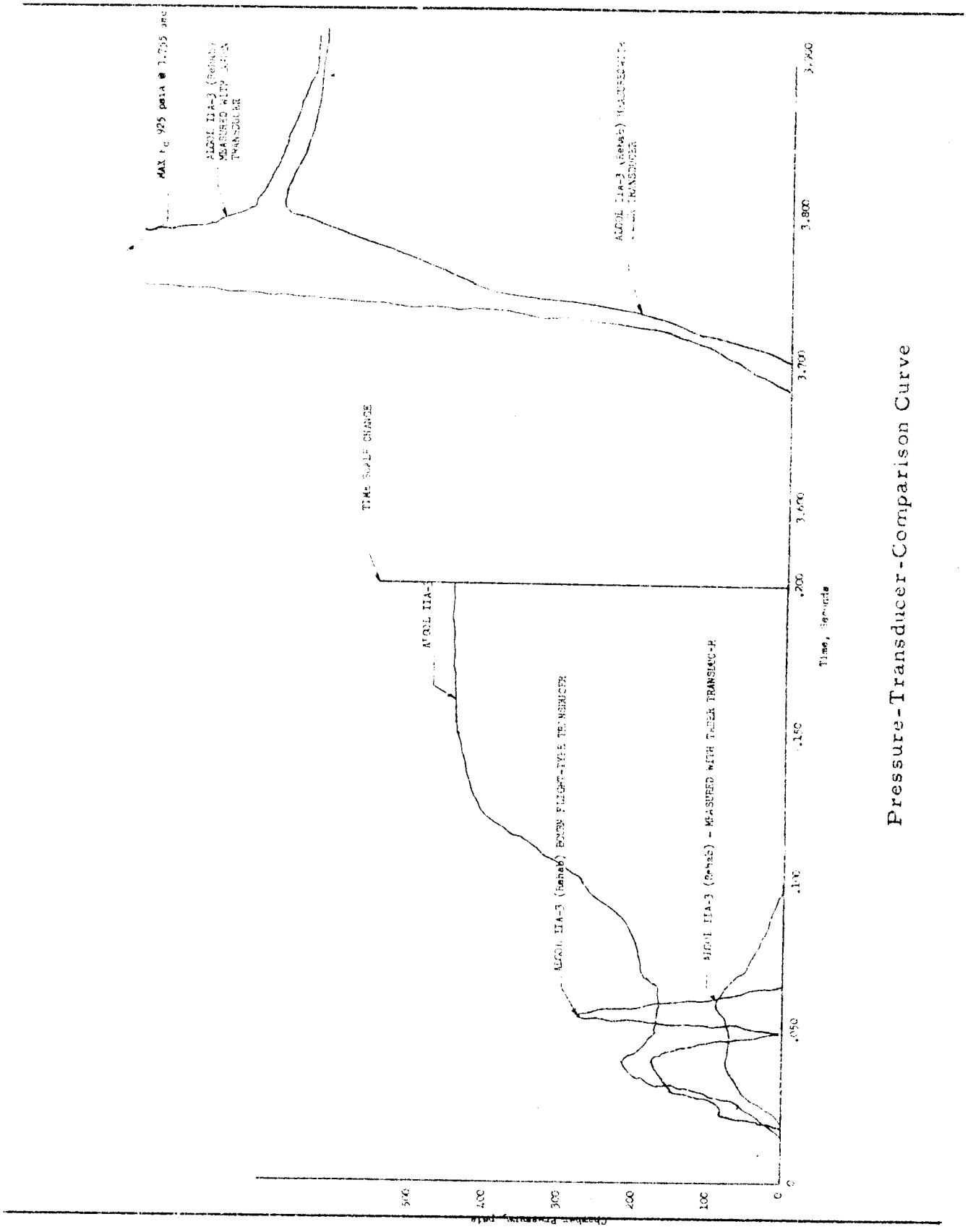
Pressure-Transducer-Comparison Curve
Time, seconds
Chamber Pressure, psia
0
100
200
300
400
500
.050
.100
.150
.200
3,600
3,700
3,800
TIME SCALE CHANGE
MAX t_d 925 psia @ 3.705 sec
AGOL IIA-3 (female) MEASURED WITH STRAIN TRANSDUCER
AGOL IIA-3 (female) MEASURED WITH STRAIN TRANSDUCER
AGOL IIA-3 (female) FROM FLIGHT-TYPE TRANSDUCER
AGOL IIA-3 (female) - MEASURED WITH TUBE TRANSDUCER

Figure 7

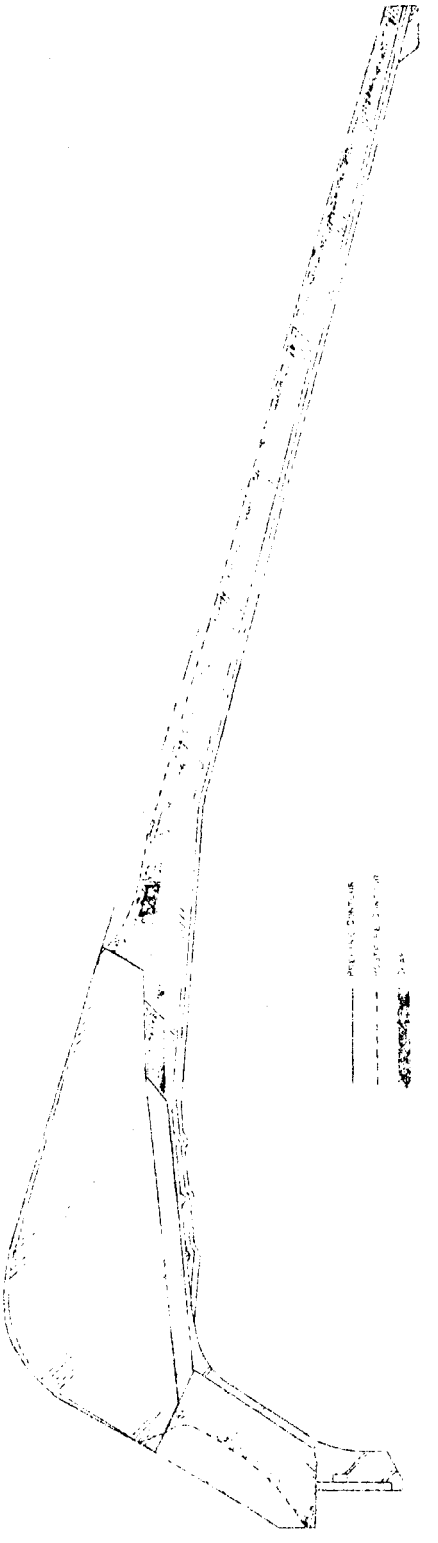

Prefiring and Postfiring Nozzle Contours

Figure 8

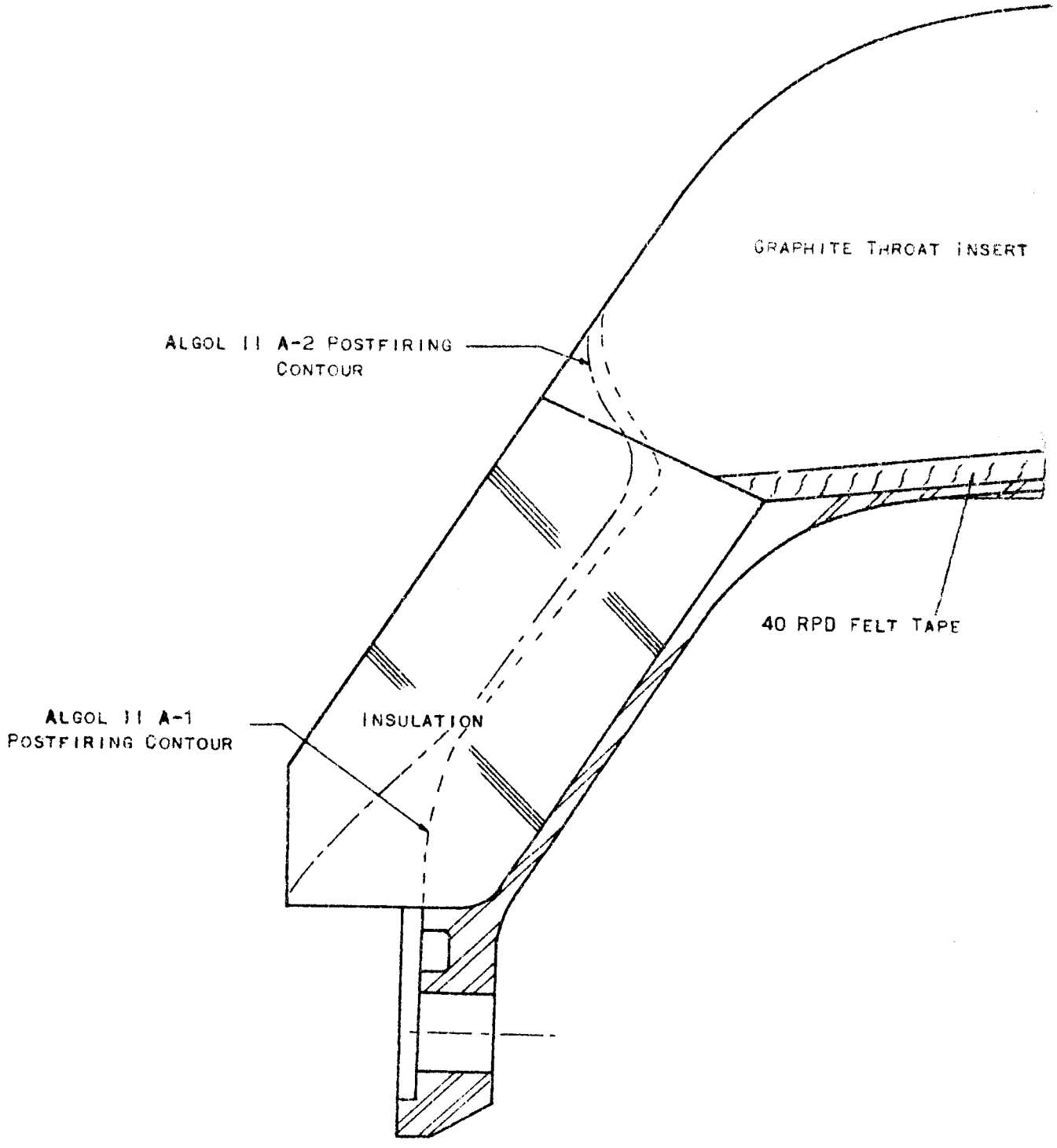

Contours of Algol IIA-1 and IIA-2 Nozzle Entrance Erosion

Figure 9

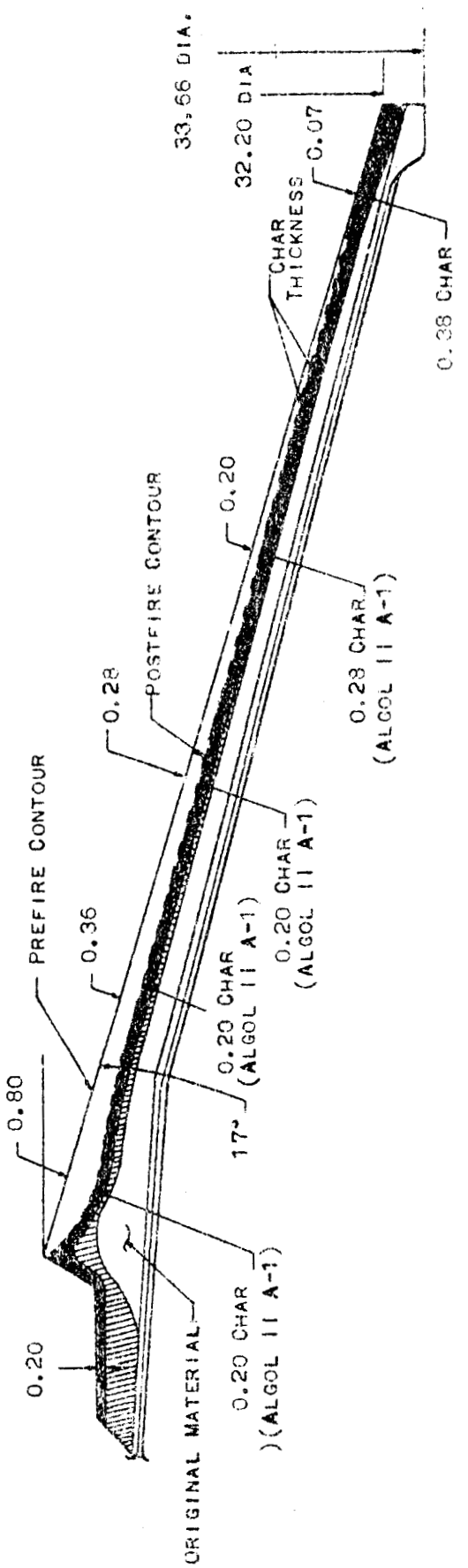

Prefiring vs Postfiring Contour, Algol IIA-1 and IIA-2 Exit Cones

Figure 10

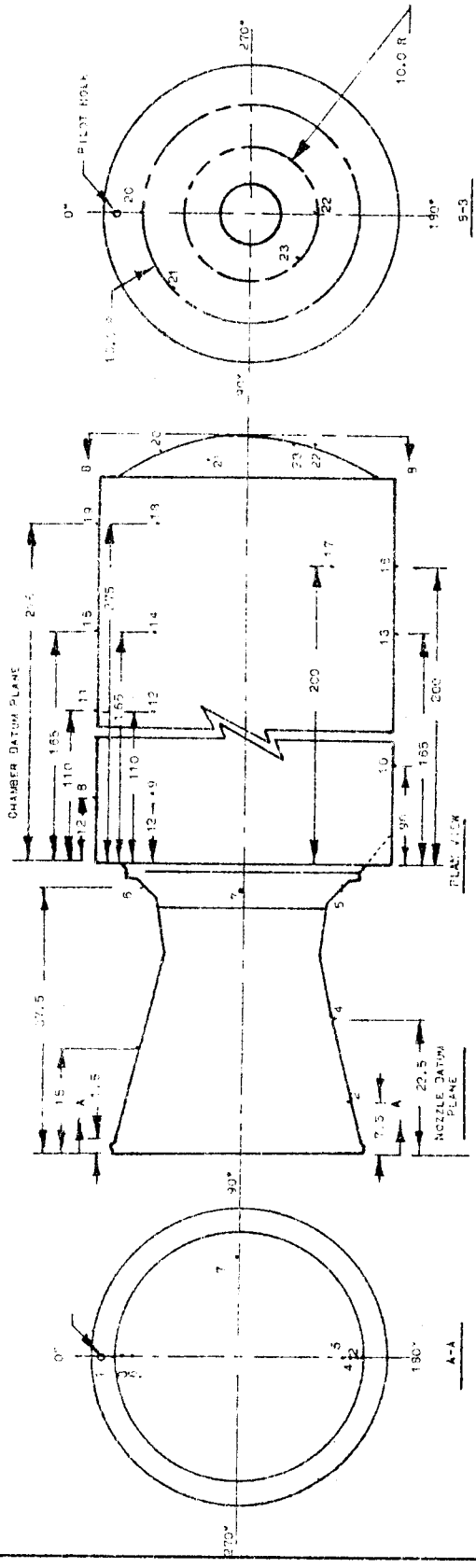

Algol IIA-3 Thermocouple Locations

Figure 11

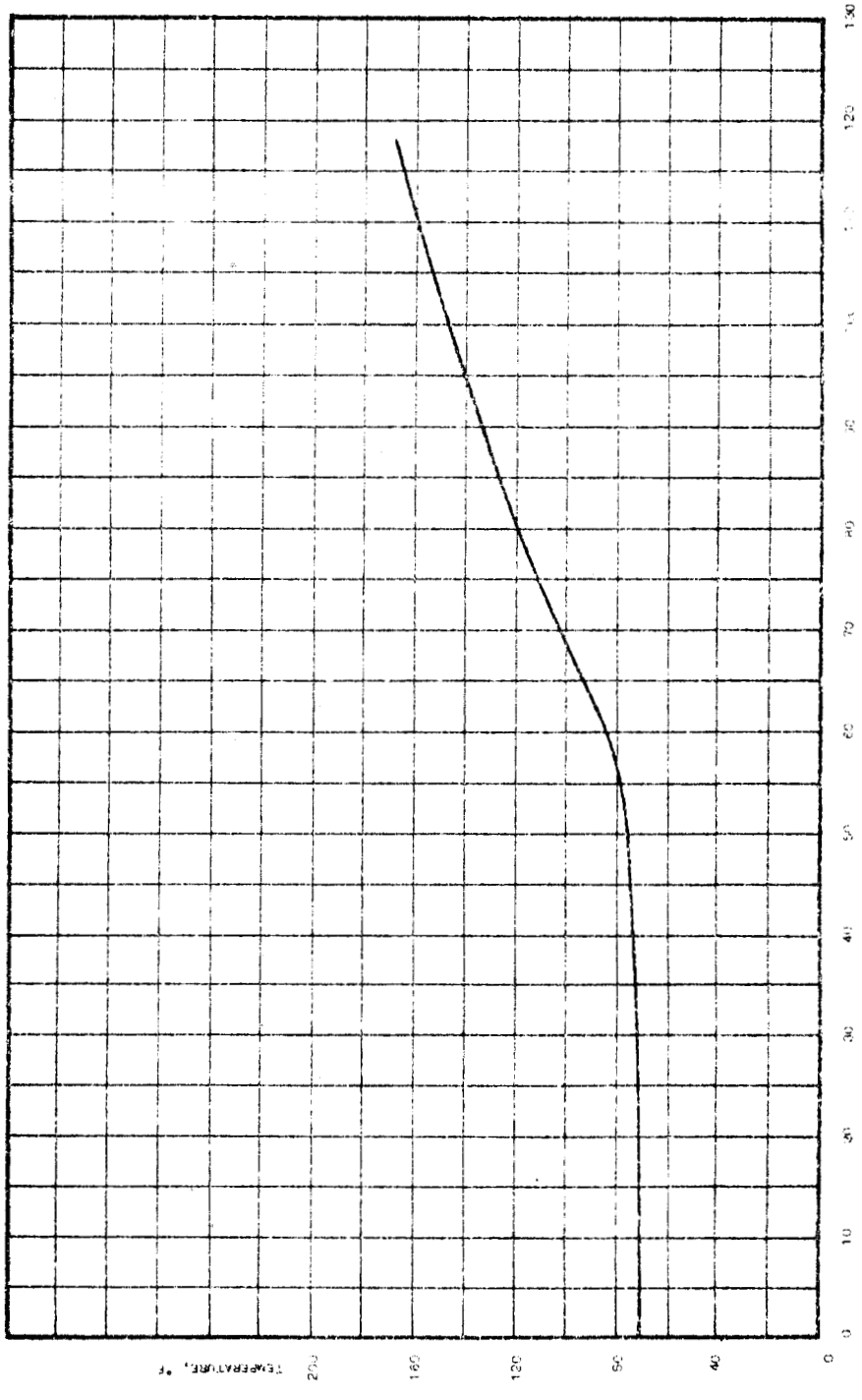

Nozzle Temperature, Thermocouple TN-090-37.5

Figure 12

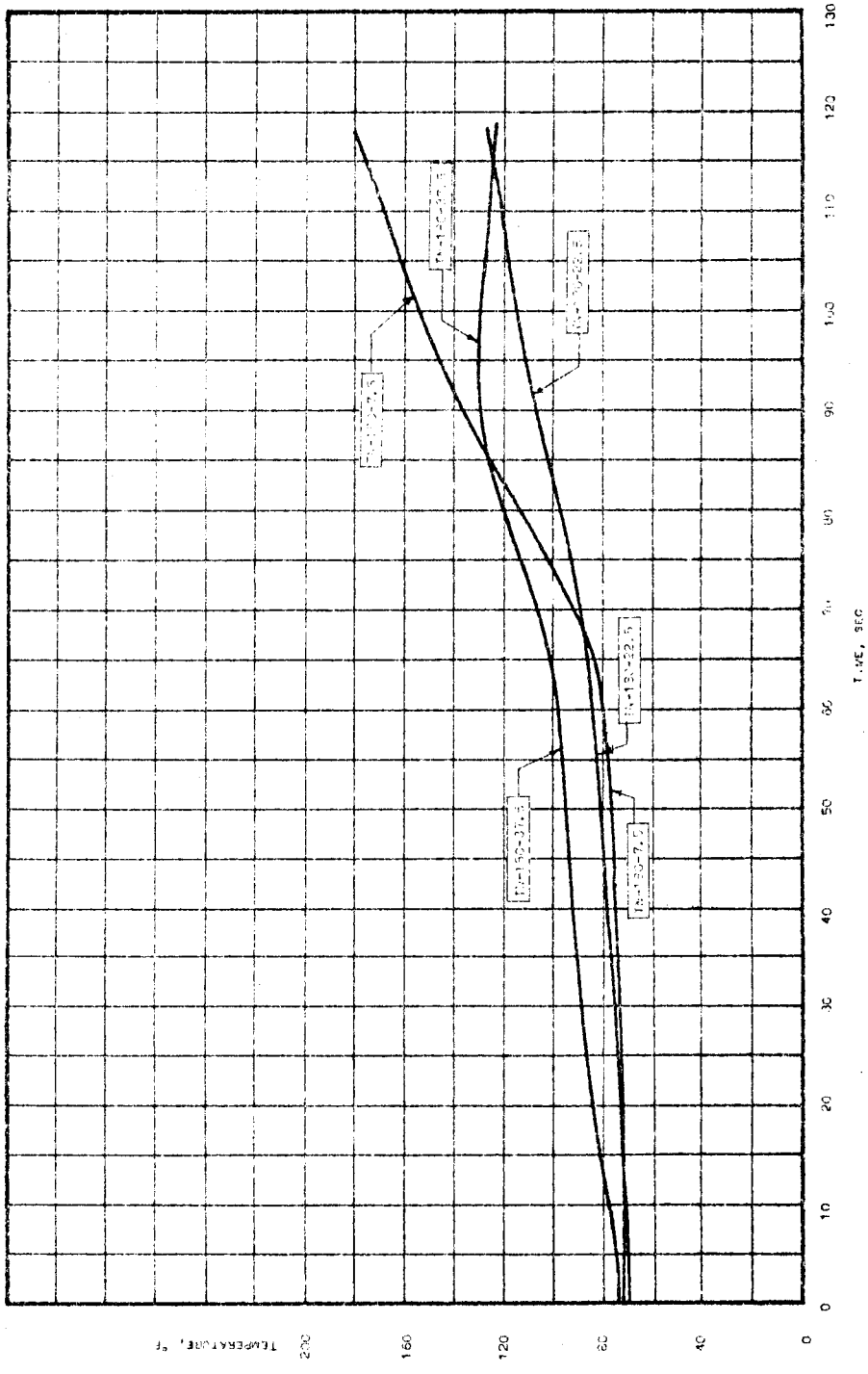

Nozzle Temperature, Thermocouples TN-180-7.5, -22.5, -37.5

Figure 13

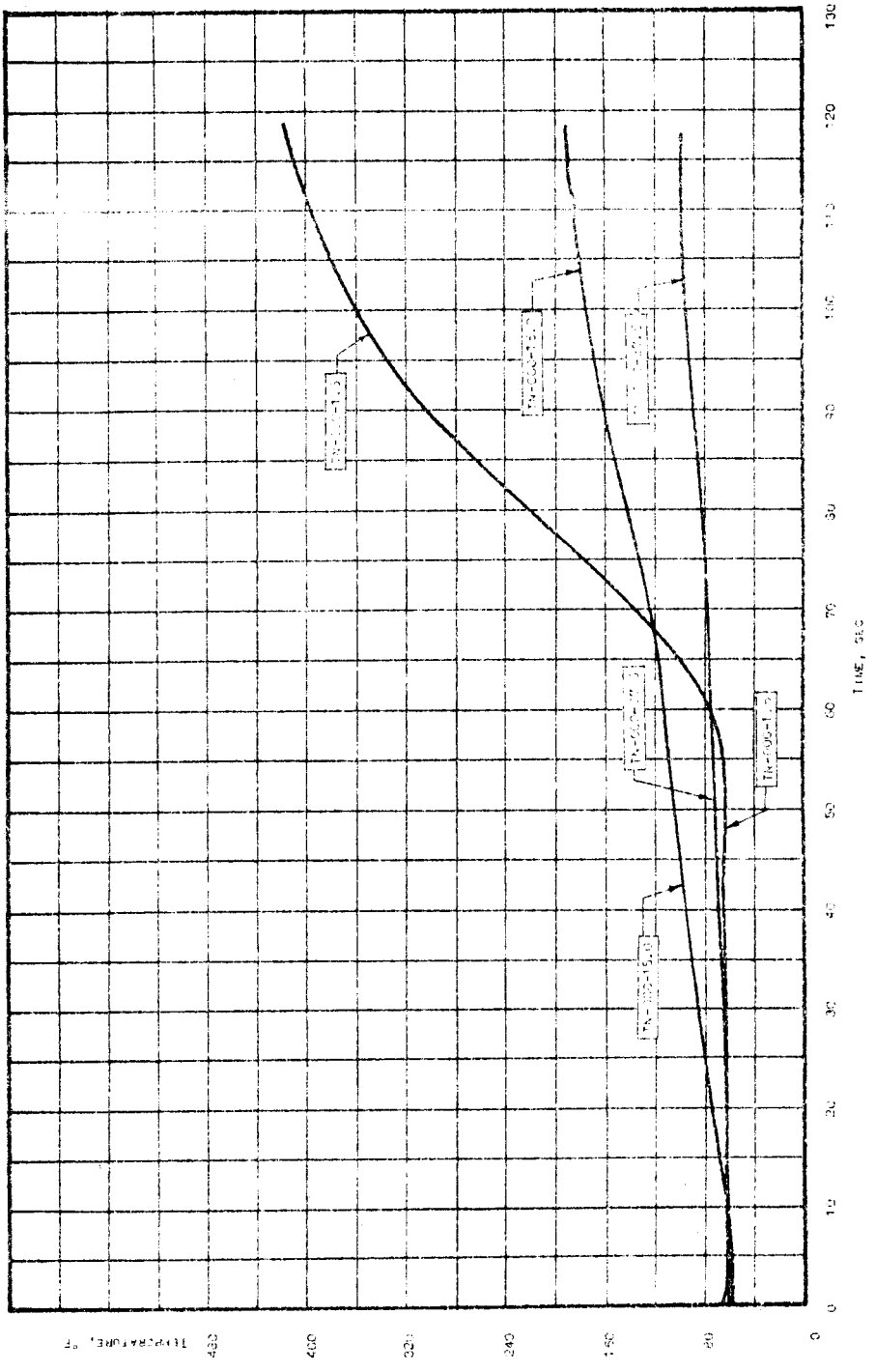

Nozzle Temperature, Thermocouples TN-000-1.5, -15.0, -37.5

Figure 14

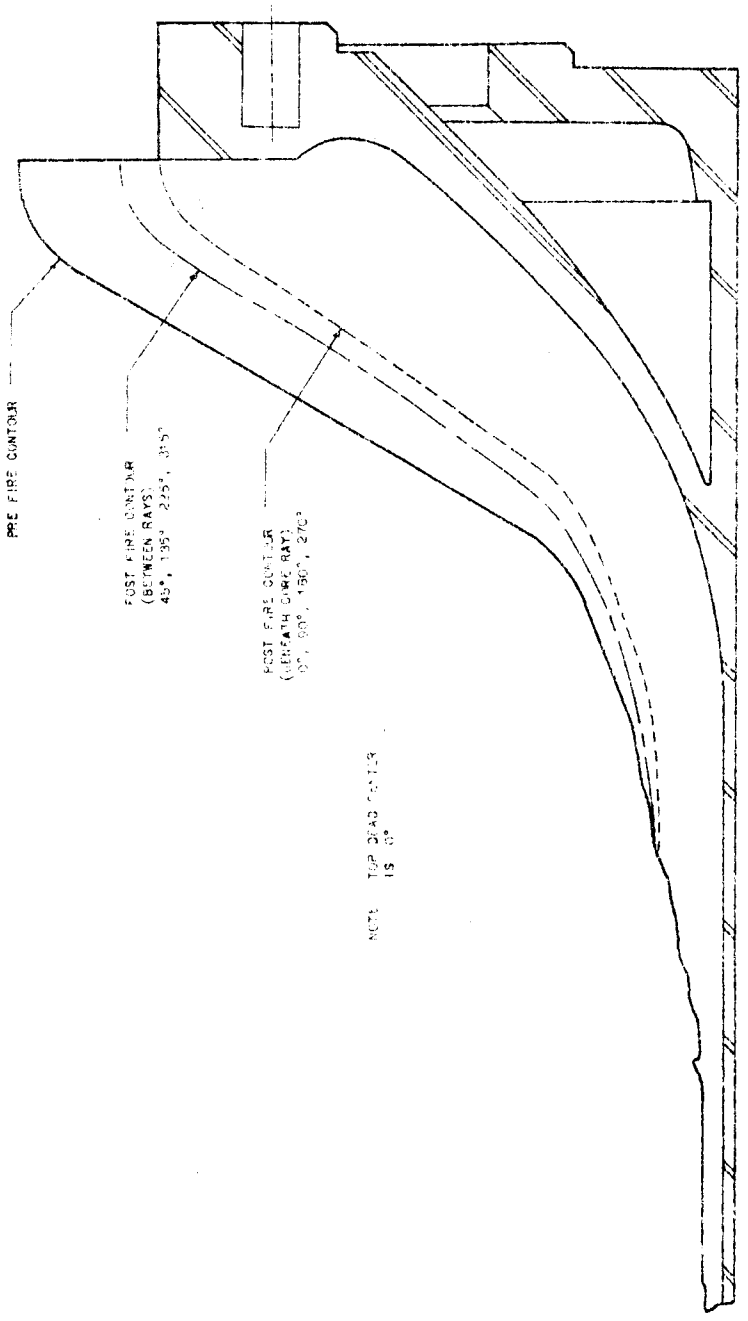

Prefiring and Postfiring Insulation Contour

Figure 15

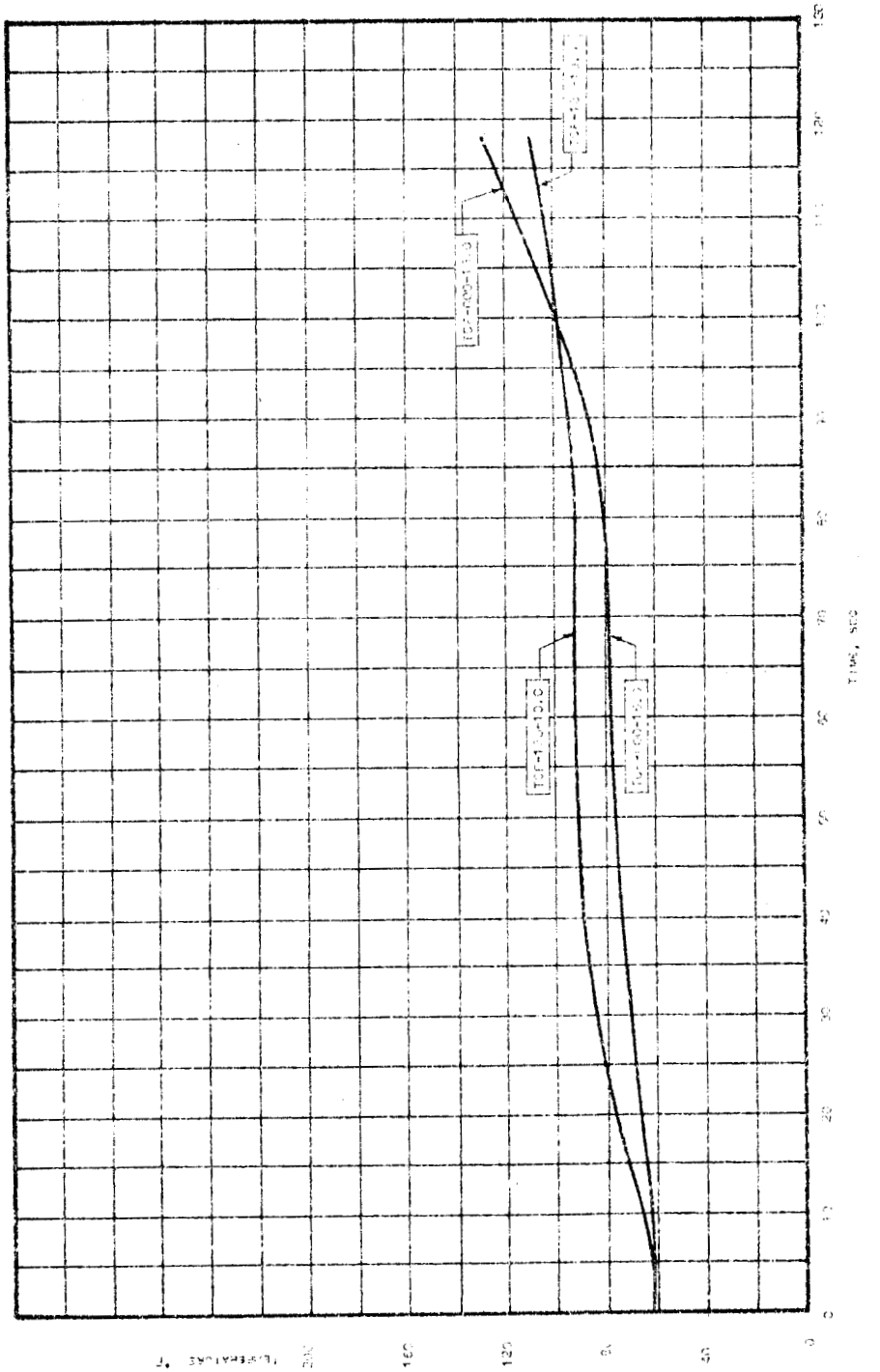

Chamber Temperature, Thermocouples TCF-135-10.0, -16.0

Figure 16

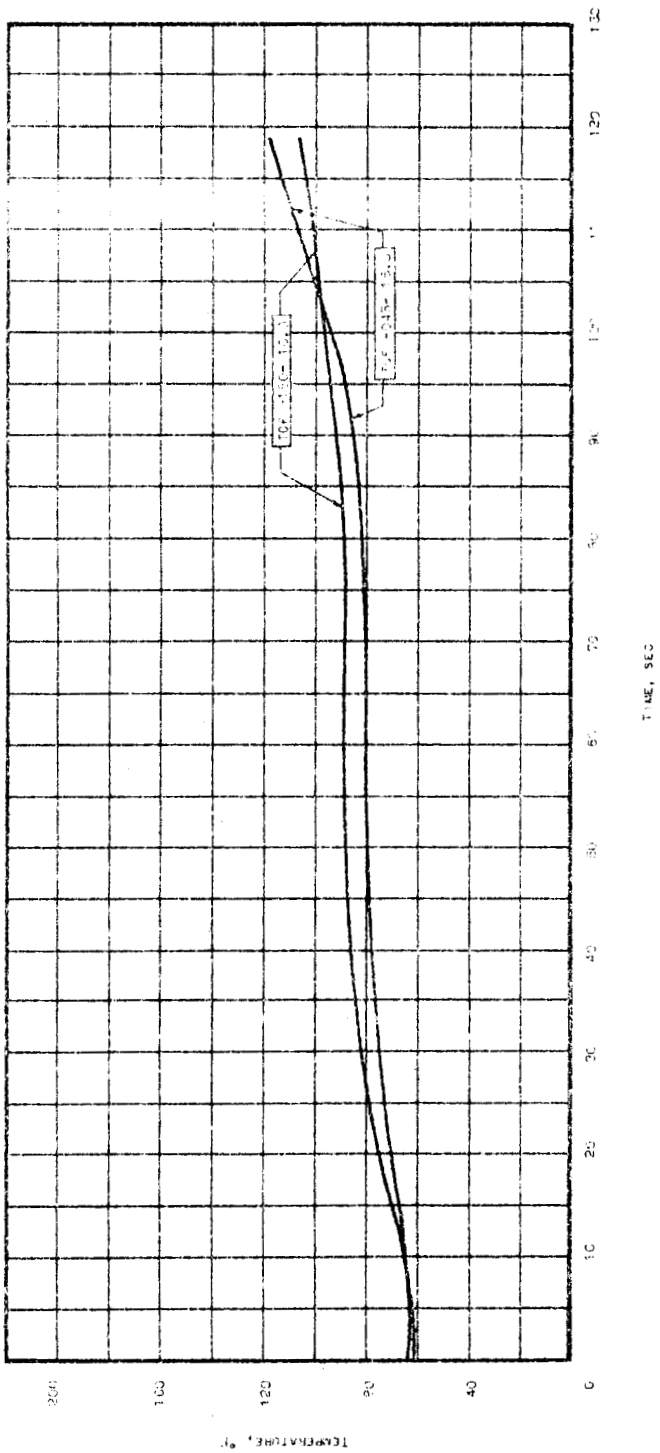

Chamber Temperature, Thermocouples TCF-180-10.0, -16.0

Figure 17

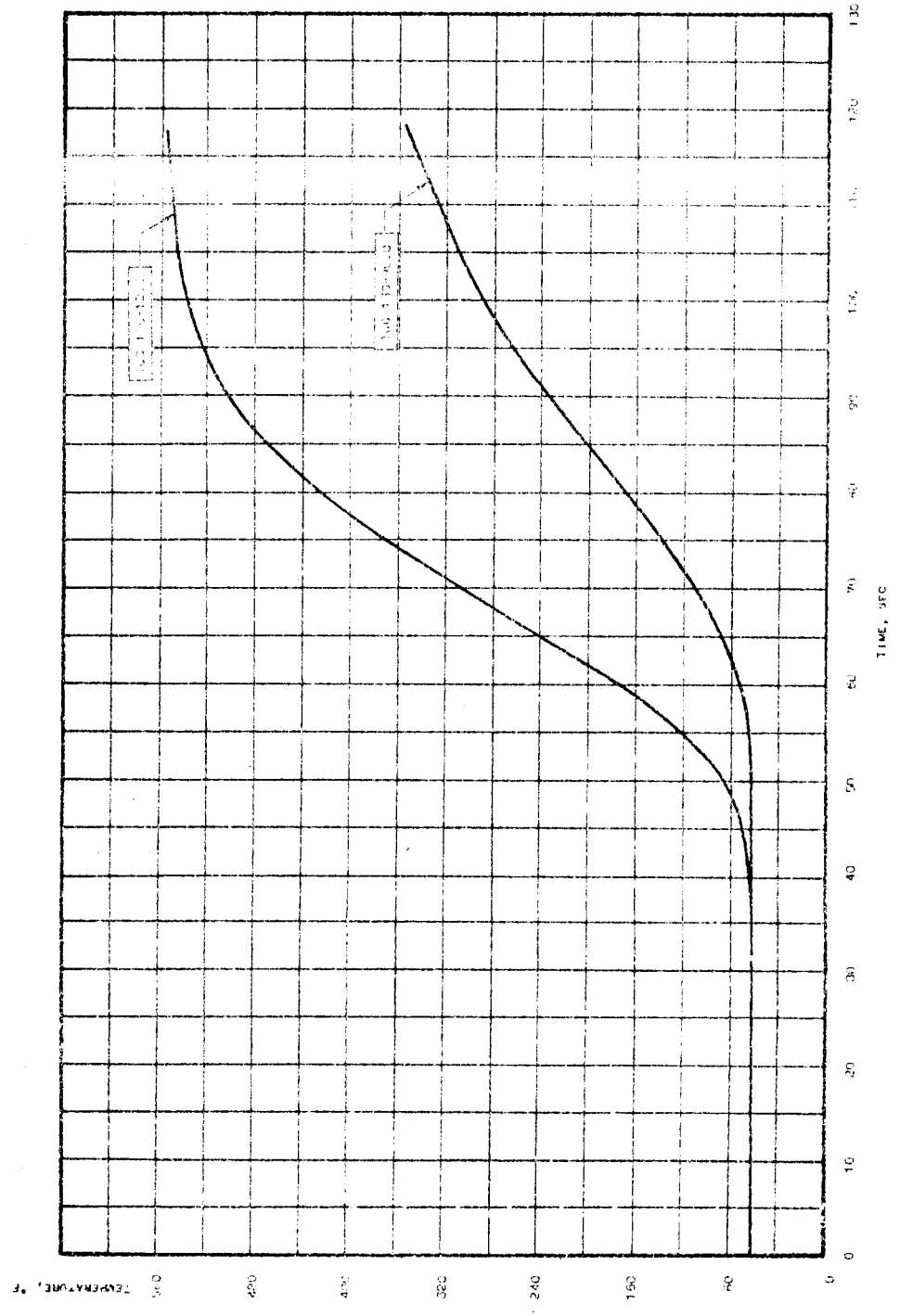

Chamber Temperature, Thermocouples TCC-130-12.0, -90.0

Figure 18

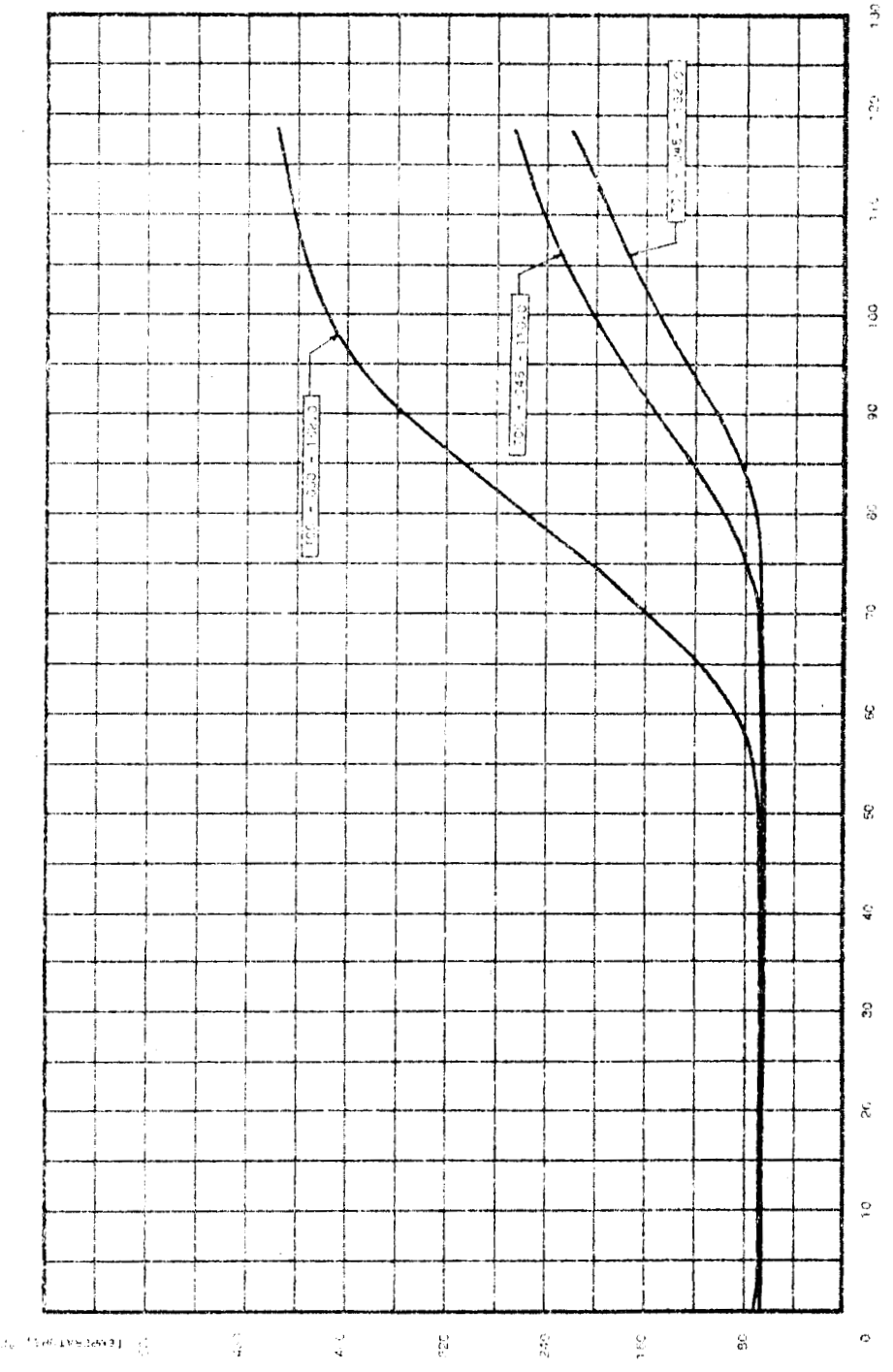

Chamber Temperature, Thermocouples TCC-000-162.0, TCC-045-110.0, TCC-045-162.0

Figure 19

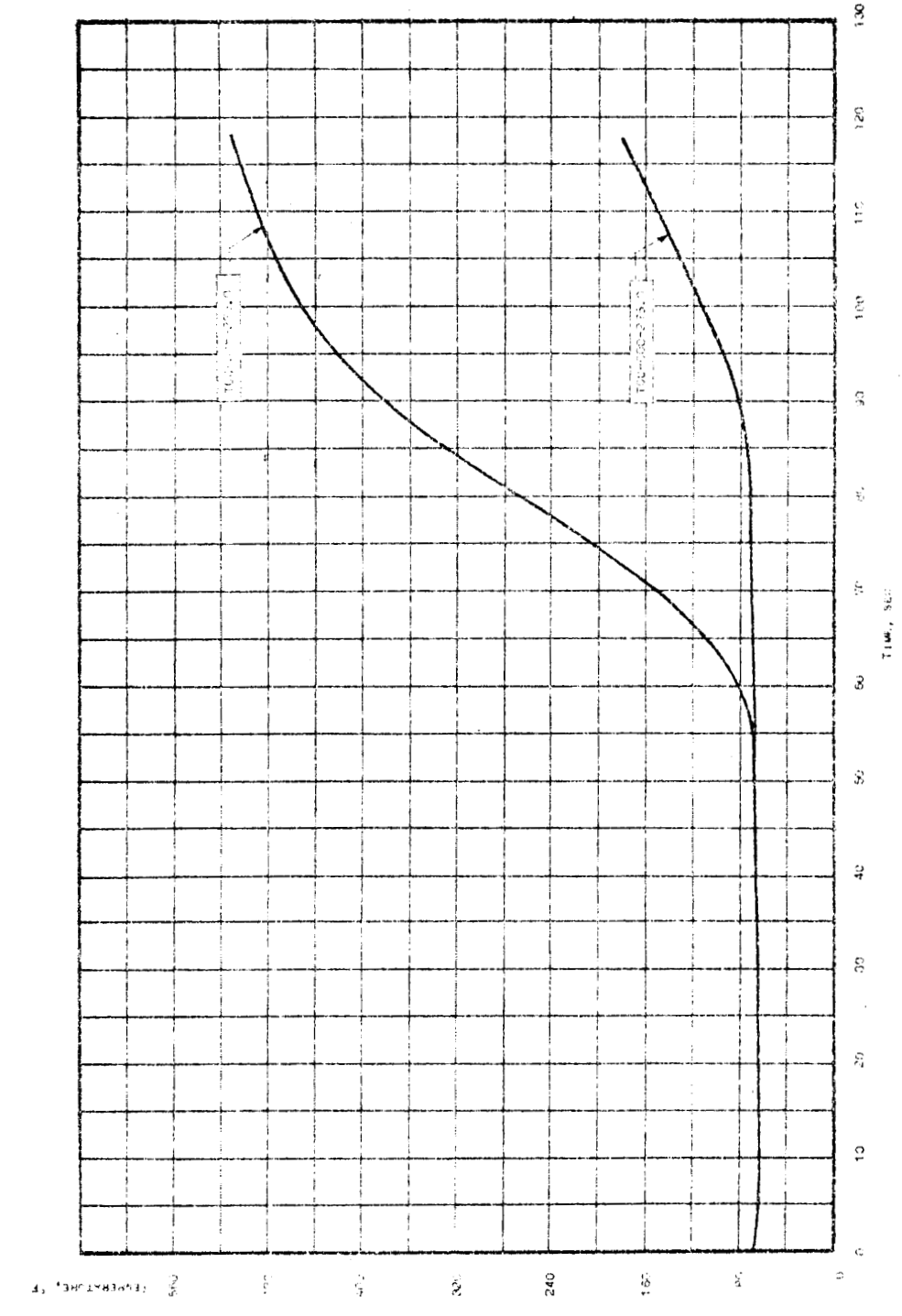

Chamber Temperature, Thermocouples TCC-000-275.0, TCC-045-275.0

Figure 20

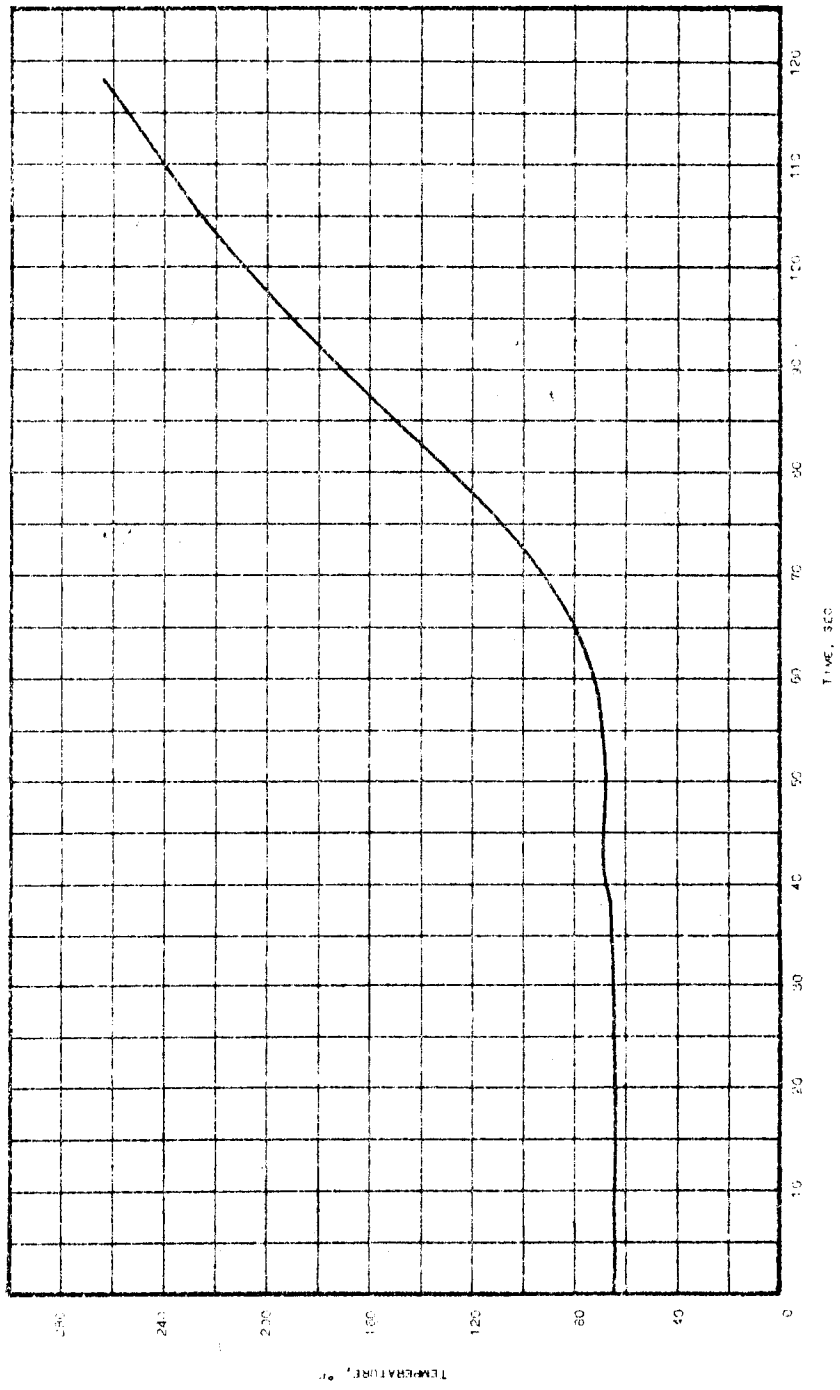

Chamber Temperature, Thermocouple TCC-270-12.0

Figure 21

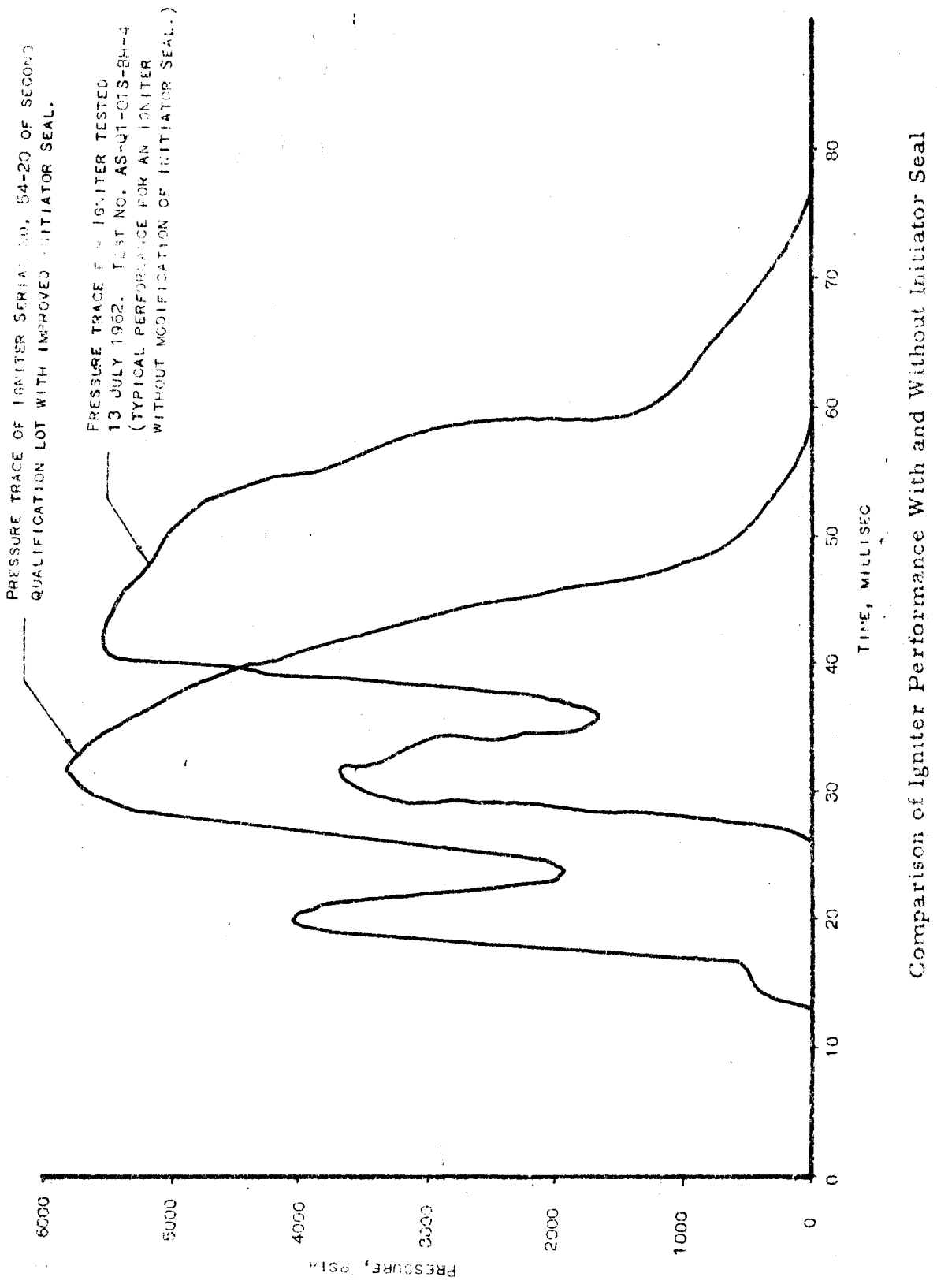

Comparison of Igniter Performance With and Without Initiator Seal

Figure 22

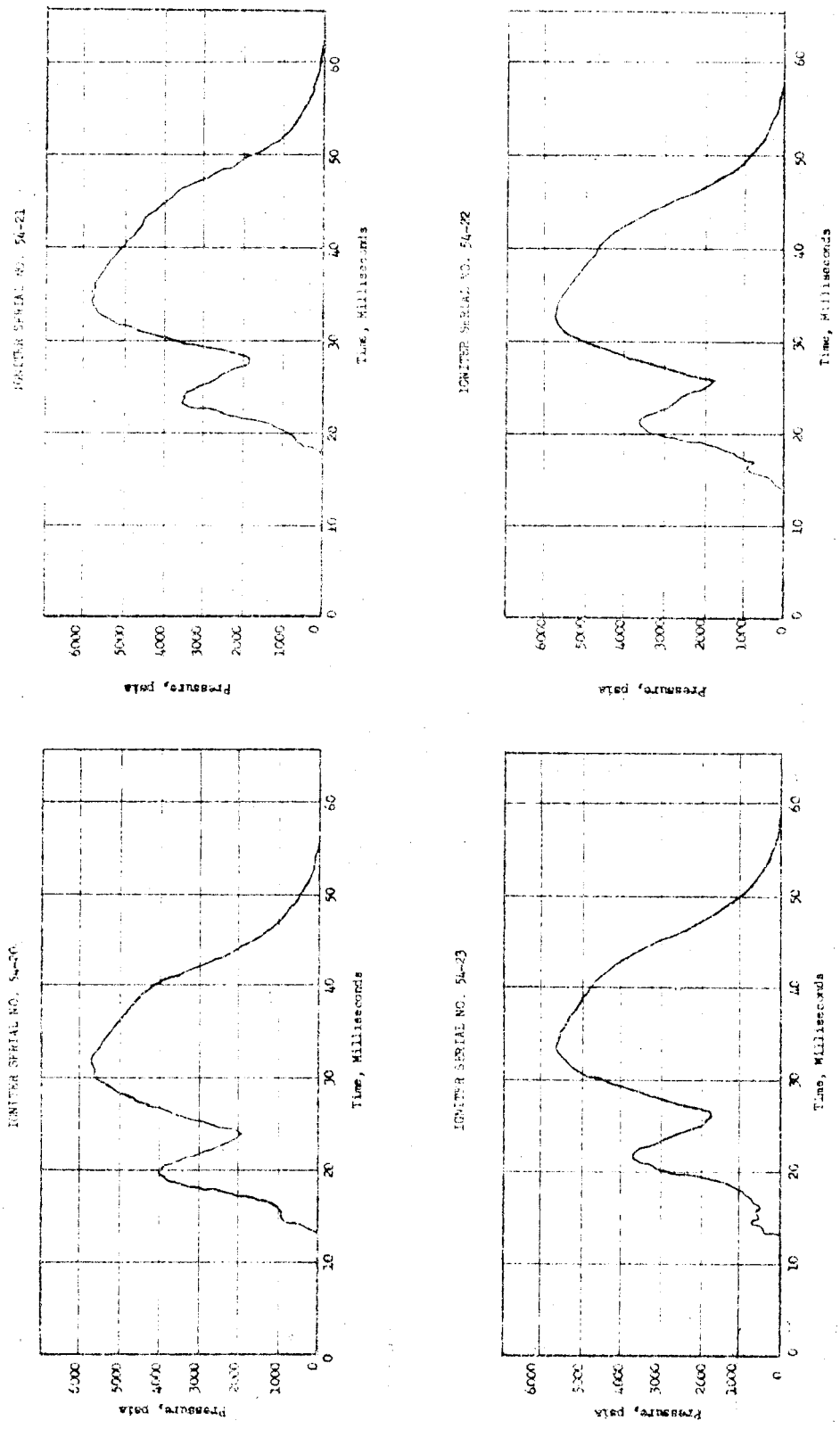

Performance of Igniters With Initiator Seal

Figure 23

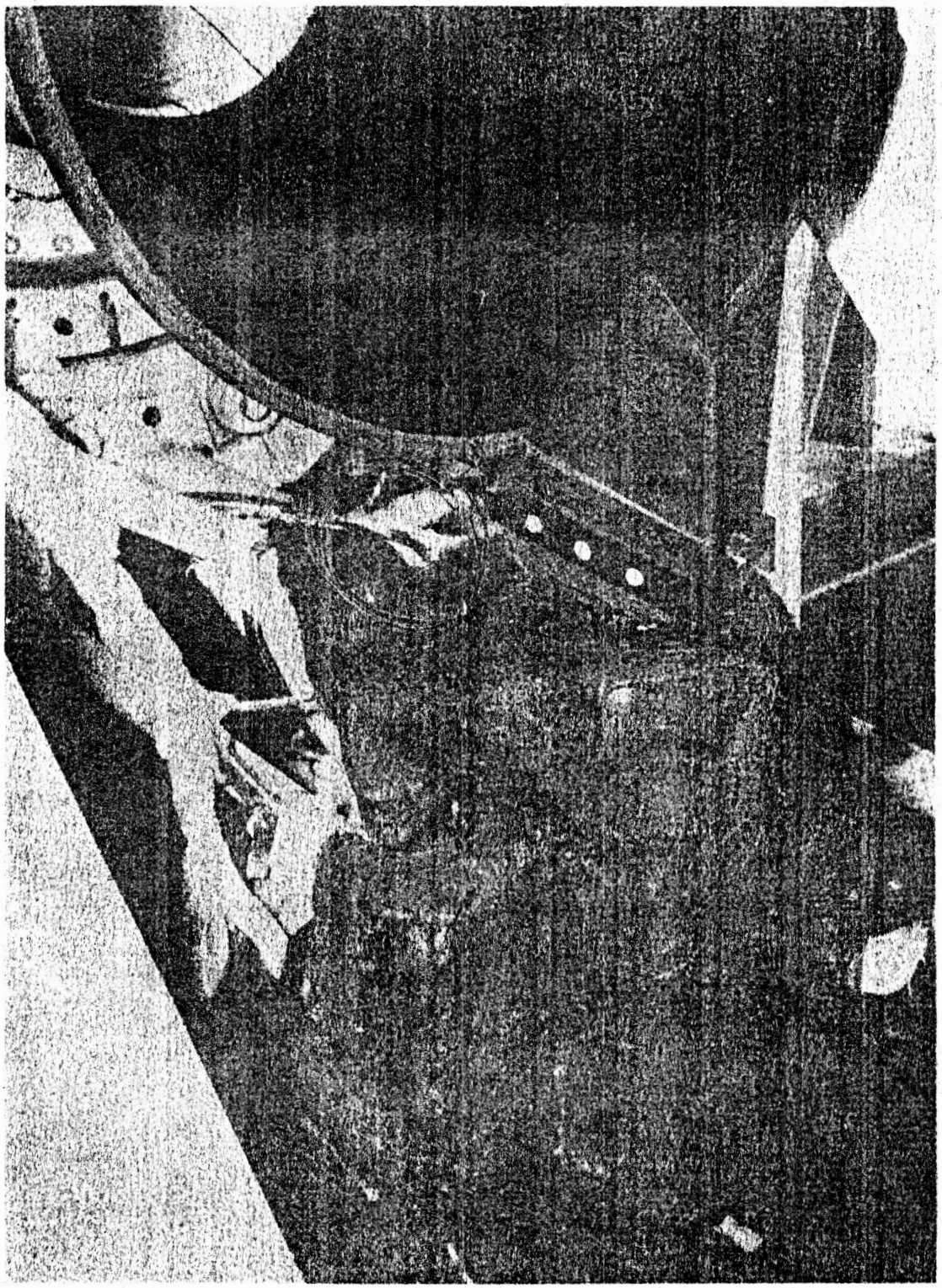

Prefiring View of Phenolic-Refrasil Jet Vane (Photo 3-63S-05255)

Figure 24

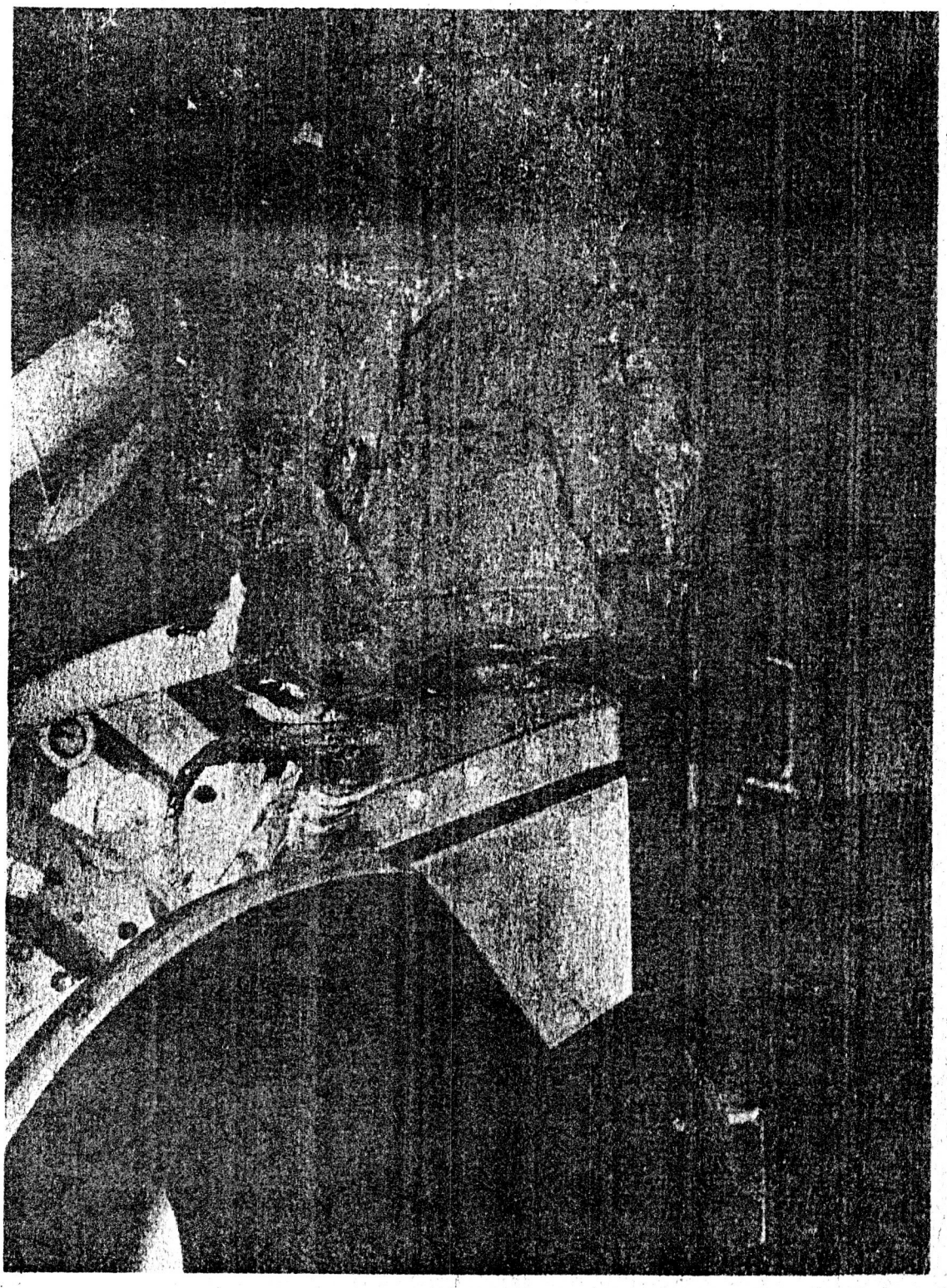

Prefiring View of Tungsten-Molybdenum Jet Vane (Photo 3-63S-05256)

Figure 25

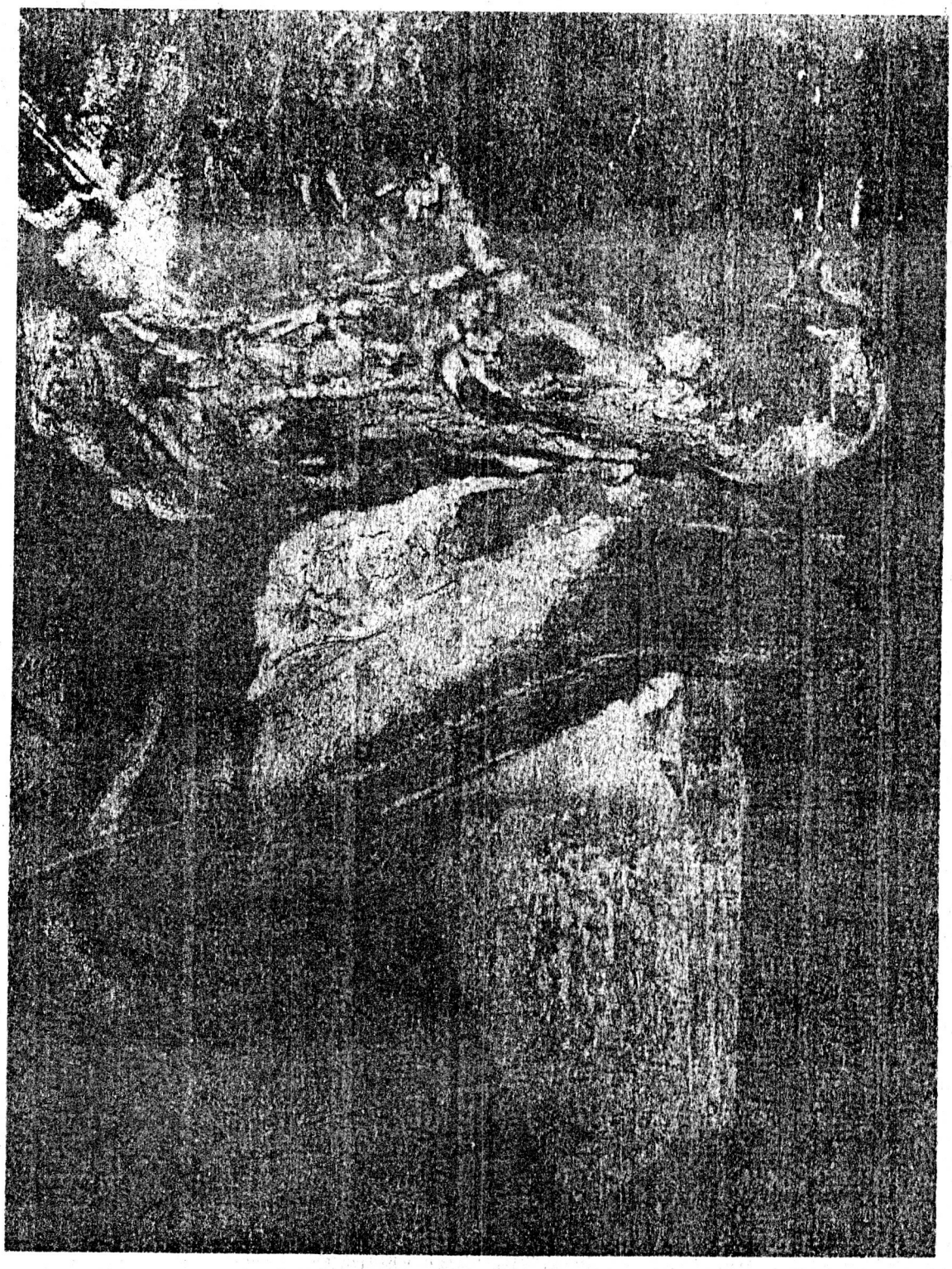

Postfiring View of Tungsten-Molybdenum Jet Vane (Photo 3-63S-05261)

Figure 26

Postfiring View of Tungsten-Molybdenum Jet Vane (Photo 3-63S-05266)

Figure 27

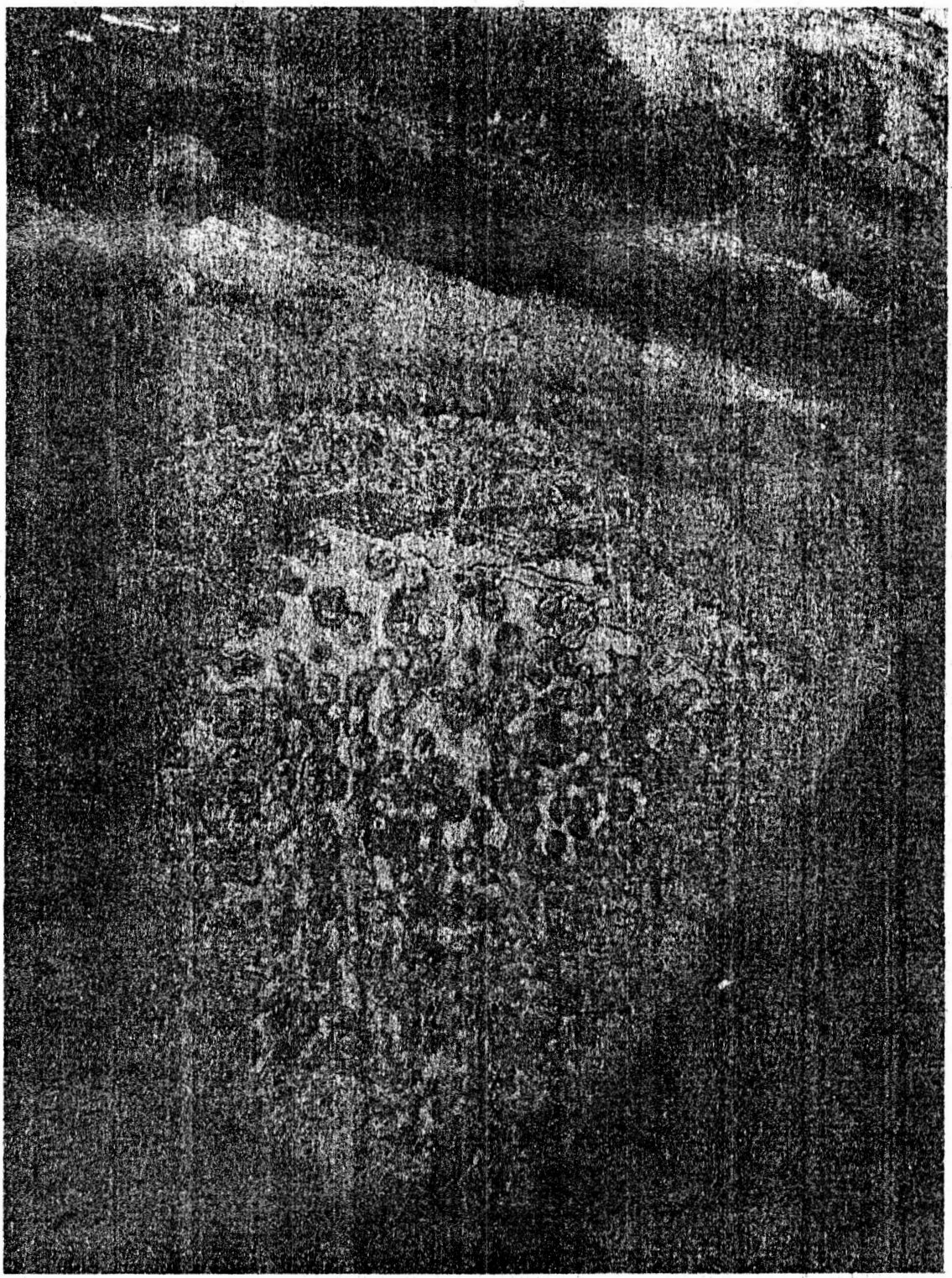

Postfiring View of Tungsten-Molybdenum Jet Vane (Photo 3-63S-05268)

Figure 28

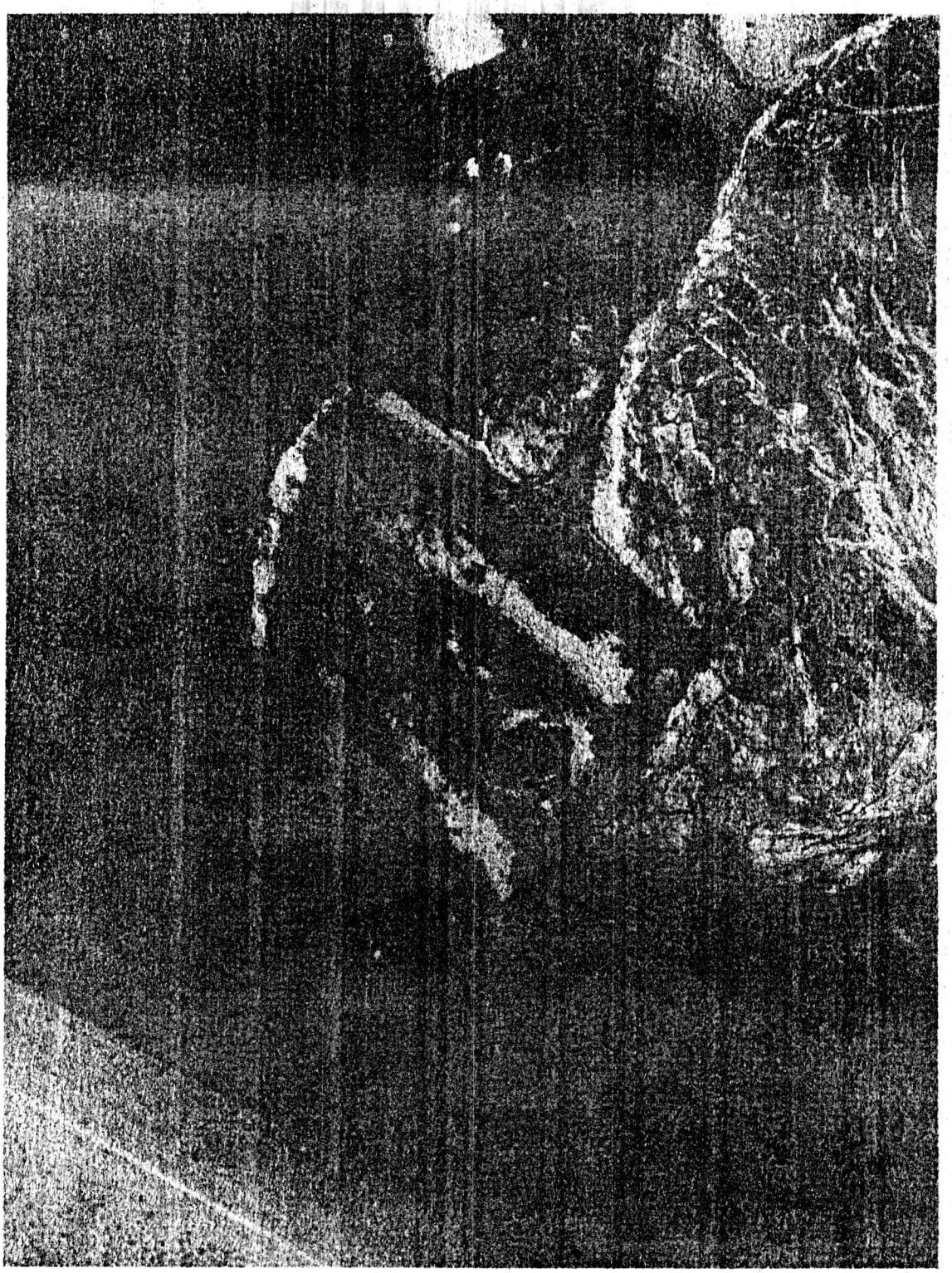

Postfiring View of Phenolic-Refrasil Jet Vane (Photo 3-63S-05270)

Figure 29

Postfiring View of Phenolic-Refrasil Jet Vane (Photo 3-63S-05271)

Figure 30

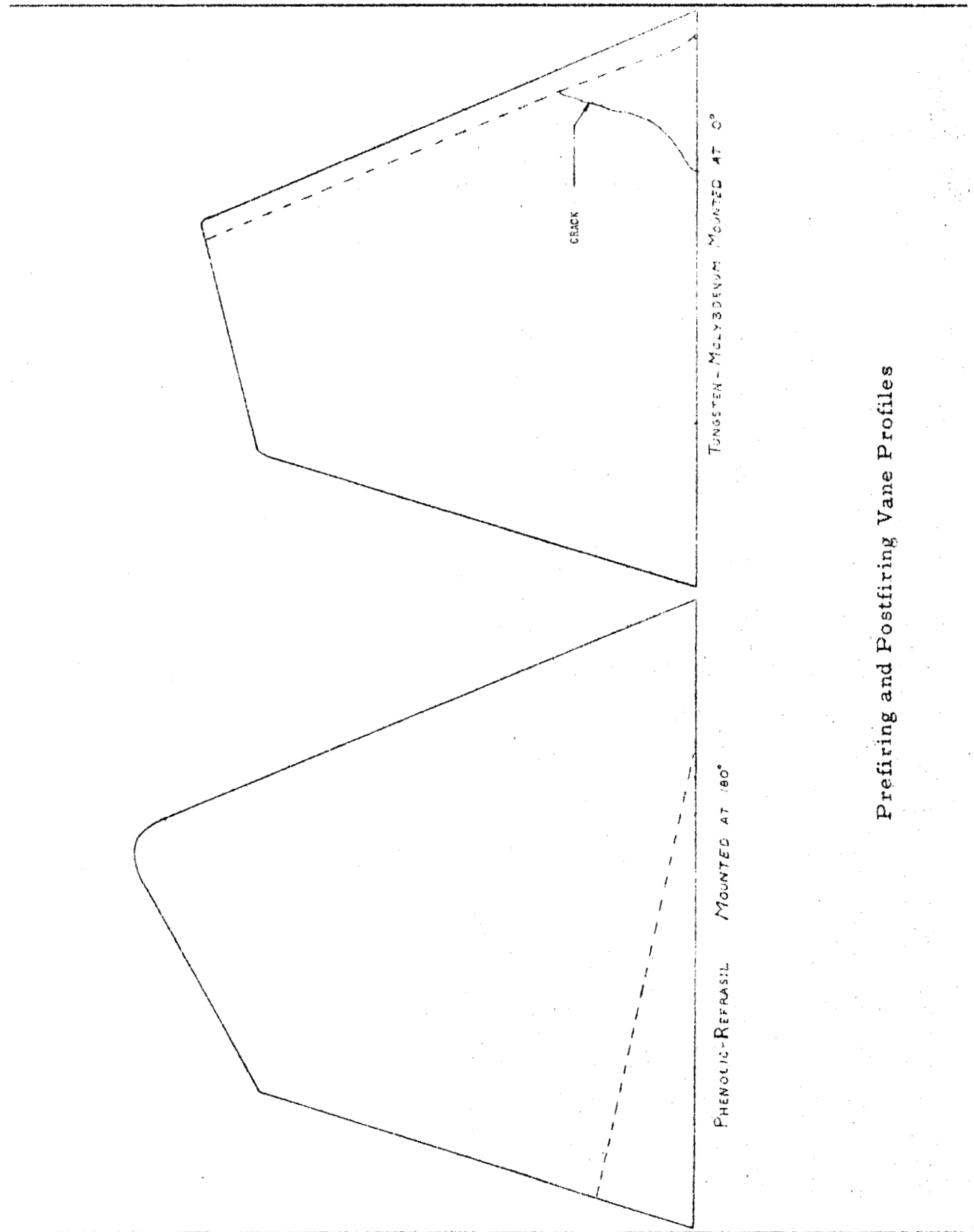
CRACK
TUNGSTEN-MOLYBDENUM MOUNTED AT 0°
PHENOLIC-REFRASIL MOUNTED AT 180°
Prefiring and Postfiring Vane Profiles

Figure 31

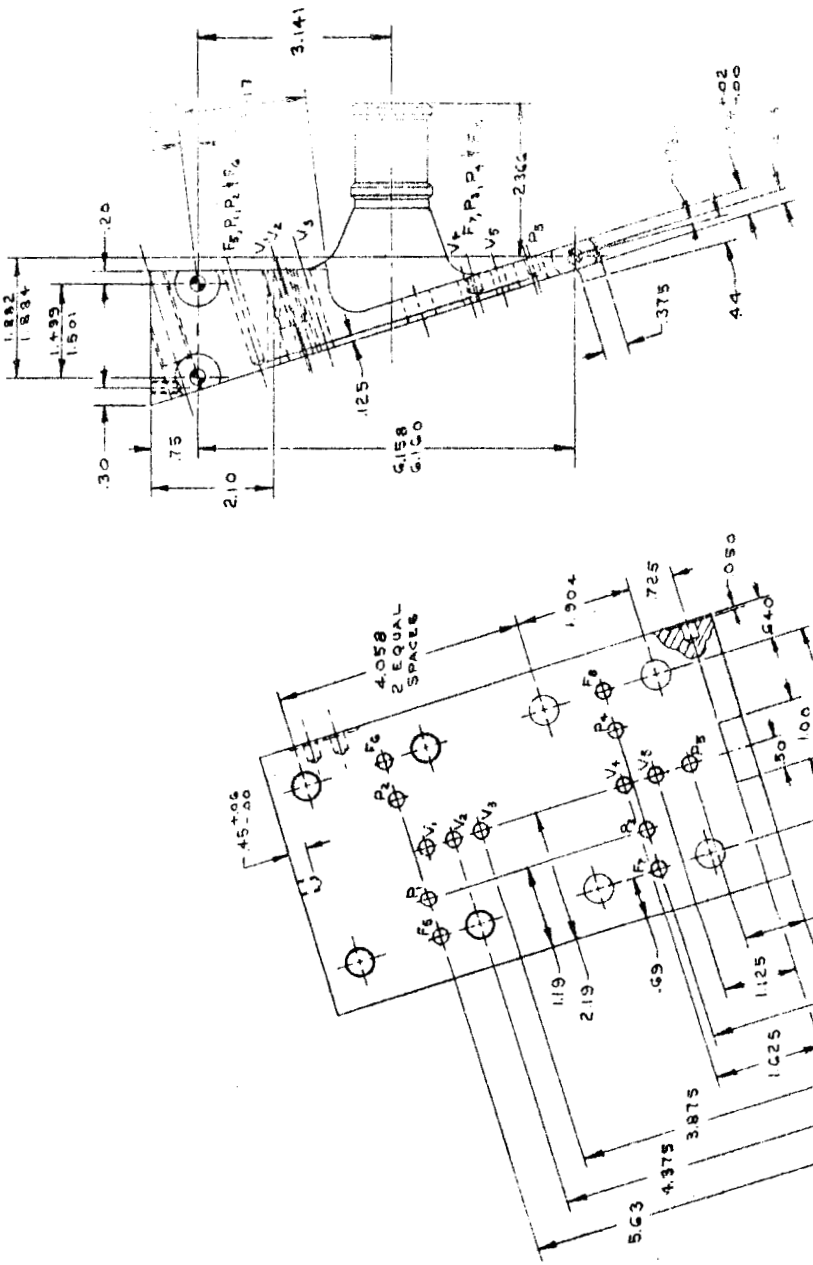
THERMOCOUPLE LOCATIONS, VANES
Jet-Vane Thermocouple Locations
3.141
4.058
2 EQUAL
SPACES
1.904
.725
.050
.640
.350
.100
.050
1.00
1.719
1.125
1.625
3.875
4.375
5.63
.69
1.19
2.19
.375
.44
.125
.30
.75
2.10
6.158
6.150
.25
.17
2.362

Figure 32

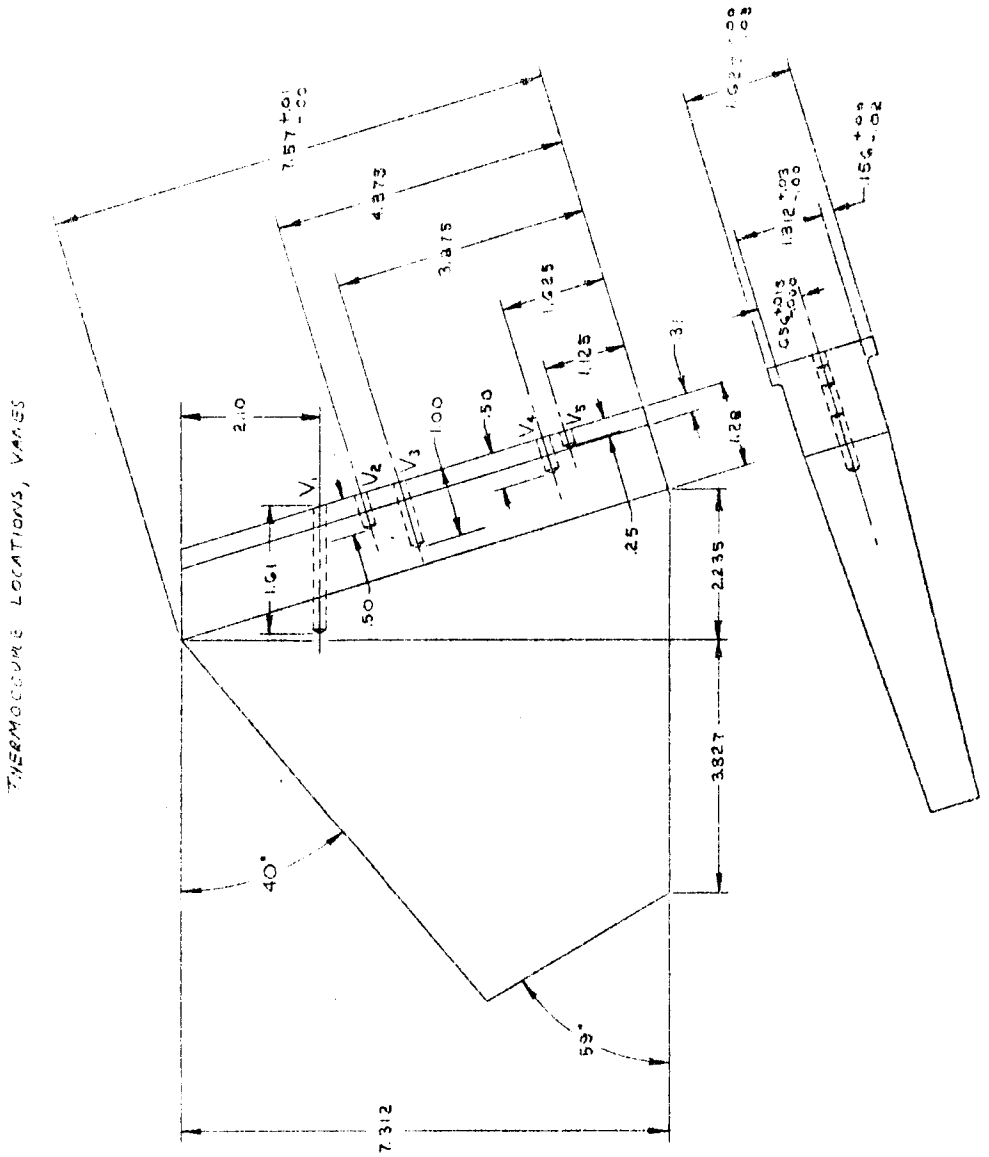

Jet-Vane Thermocouple Locations

Figure 33

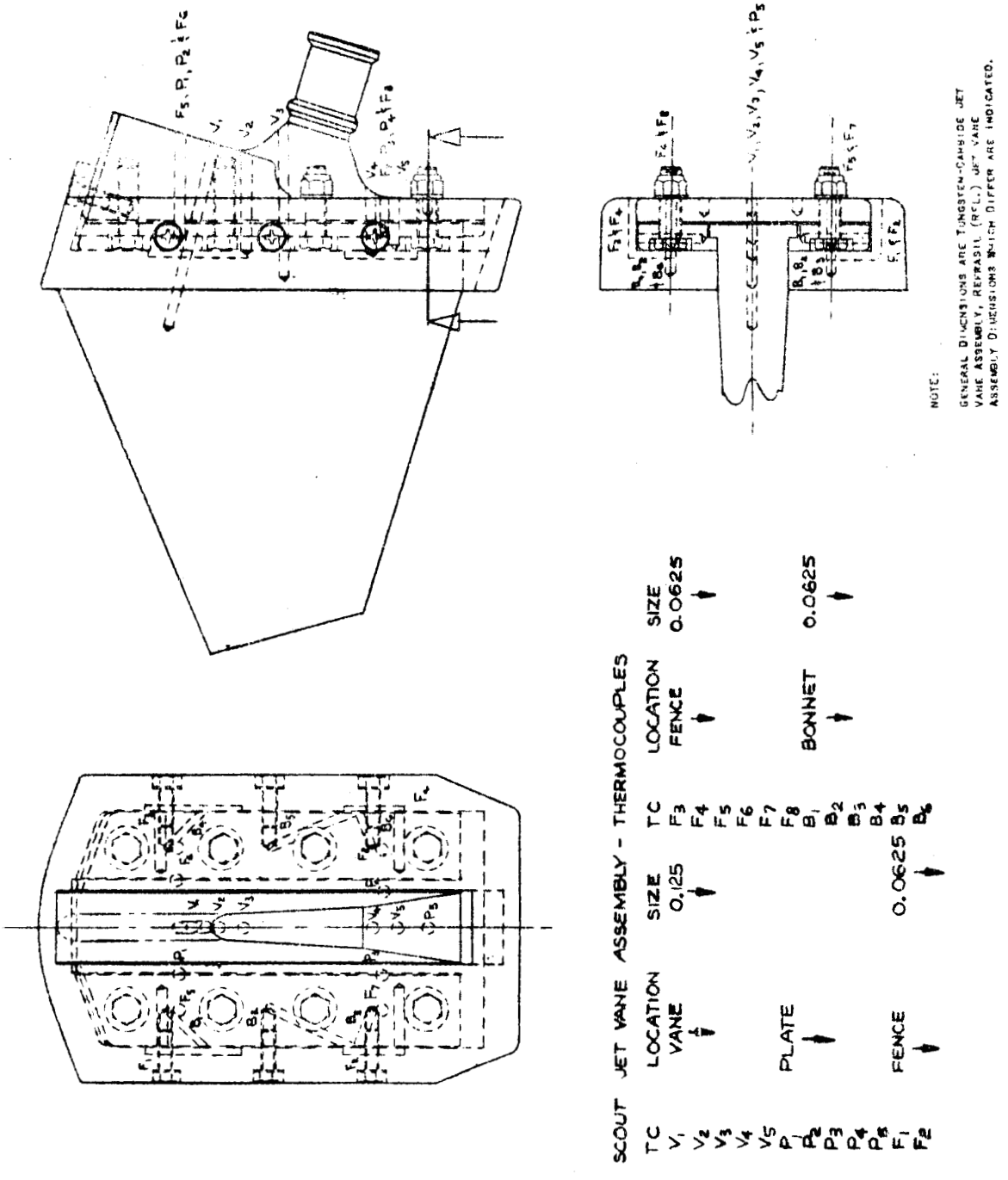

Jet-Vane Thermocouple Locations

Figure 34

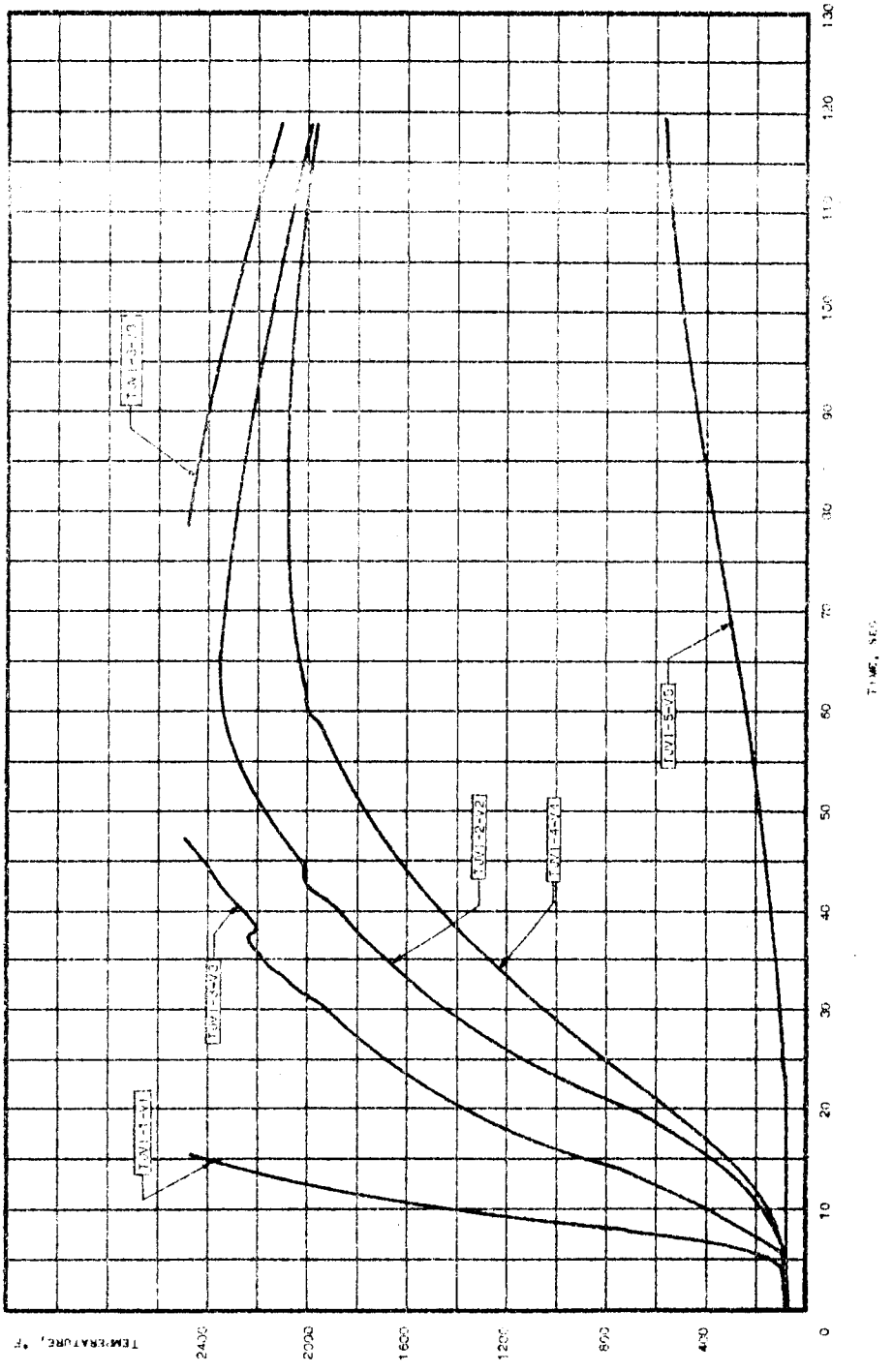

Jet-Vane Temperature, Thermocouples TJV1-1-V1, -2-V2, -3-V3, -4-V4, and -5-V5

Figure 35

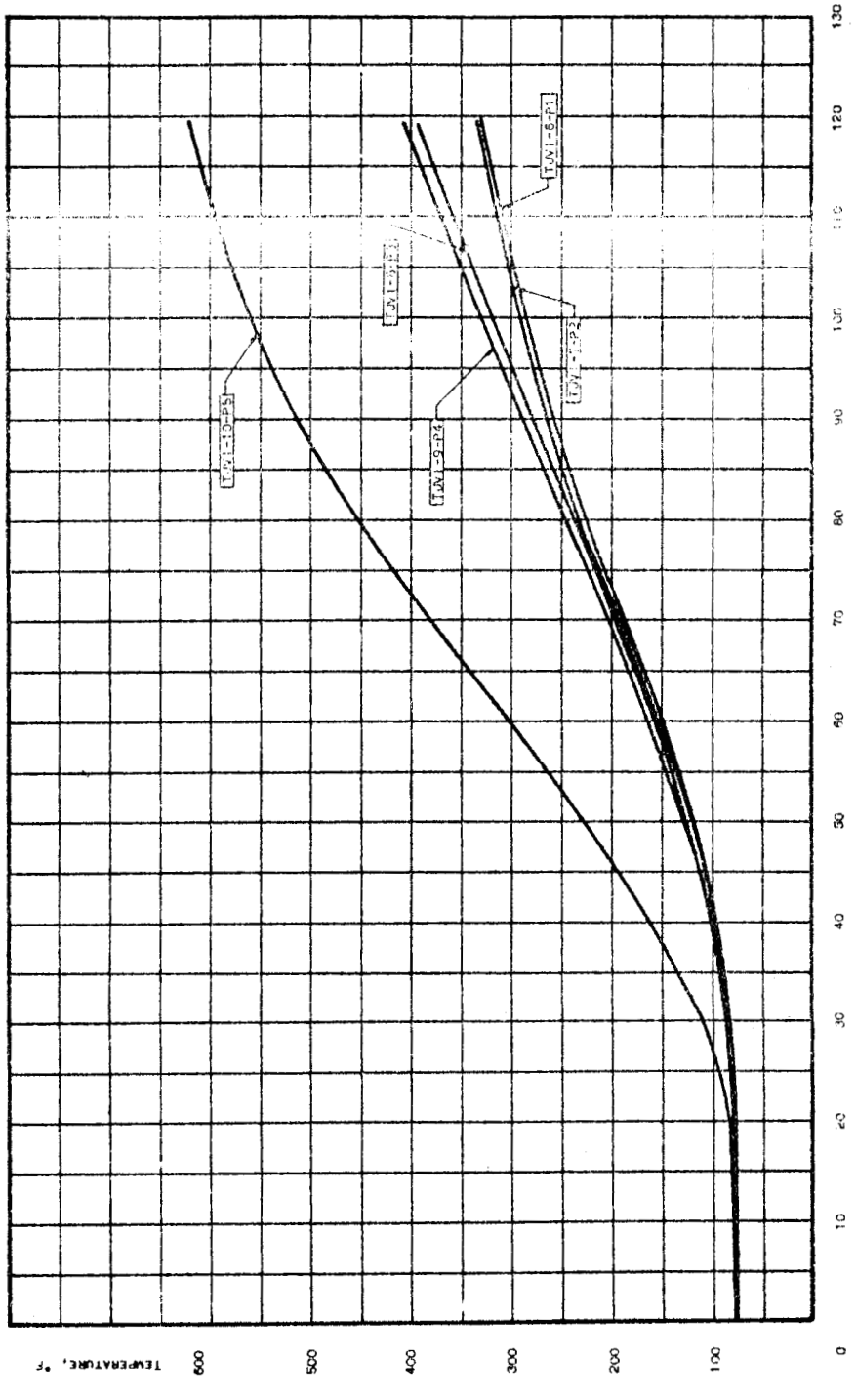

Jet-Vane Temperature, Thermocouples TJV1-6-P1, -7-P2, -8-P3, -9-P4, and -10-P5

Figure 36

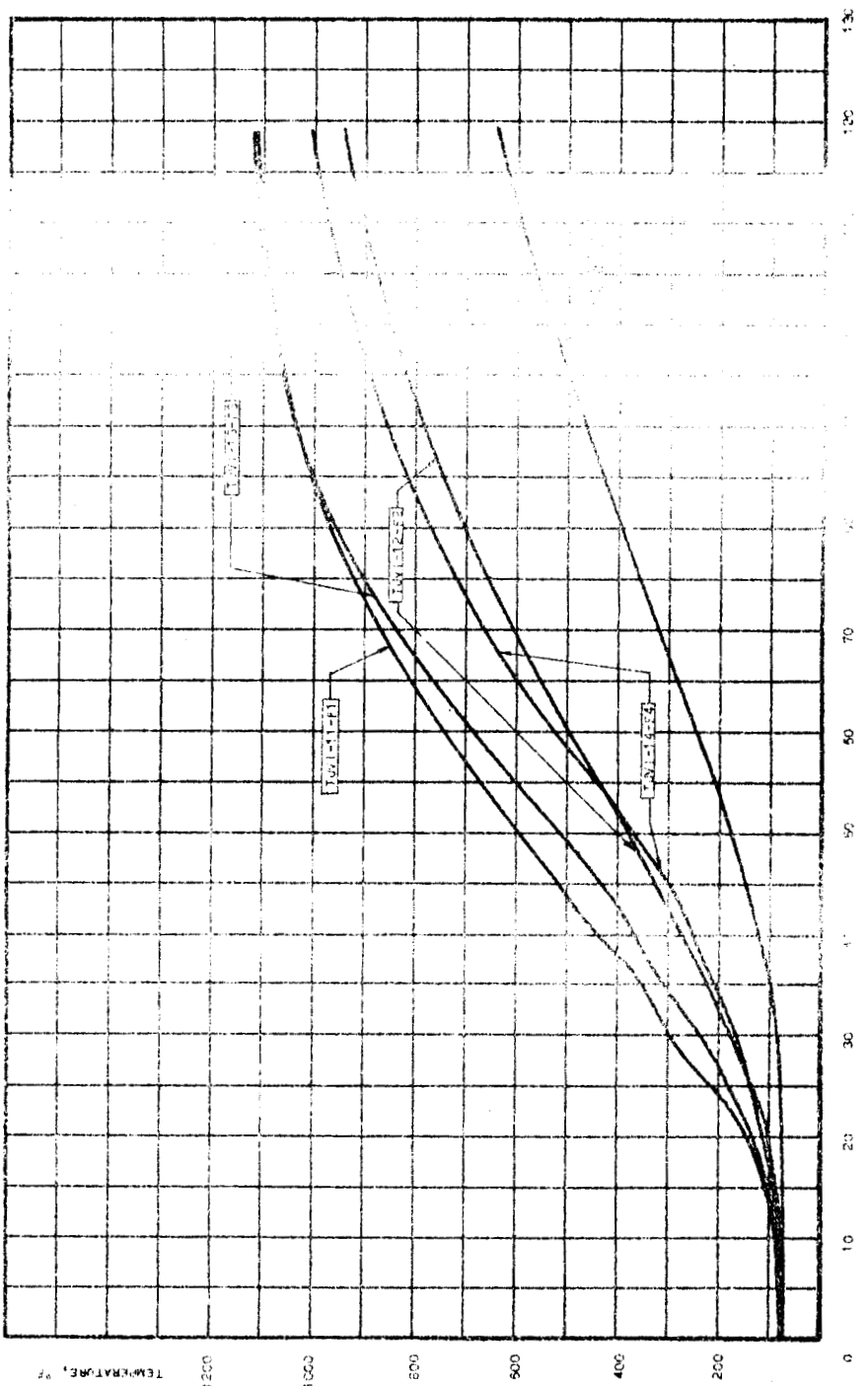

Jet-Vane Temperature Thermocouples TJV1-11, -12, -13, -14-F4, and -15

Figure 37

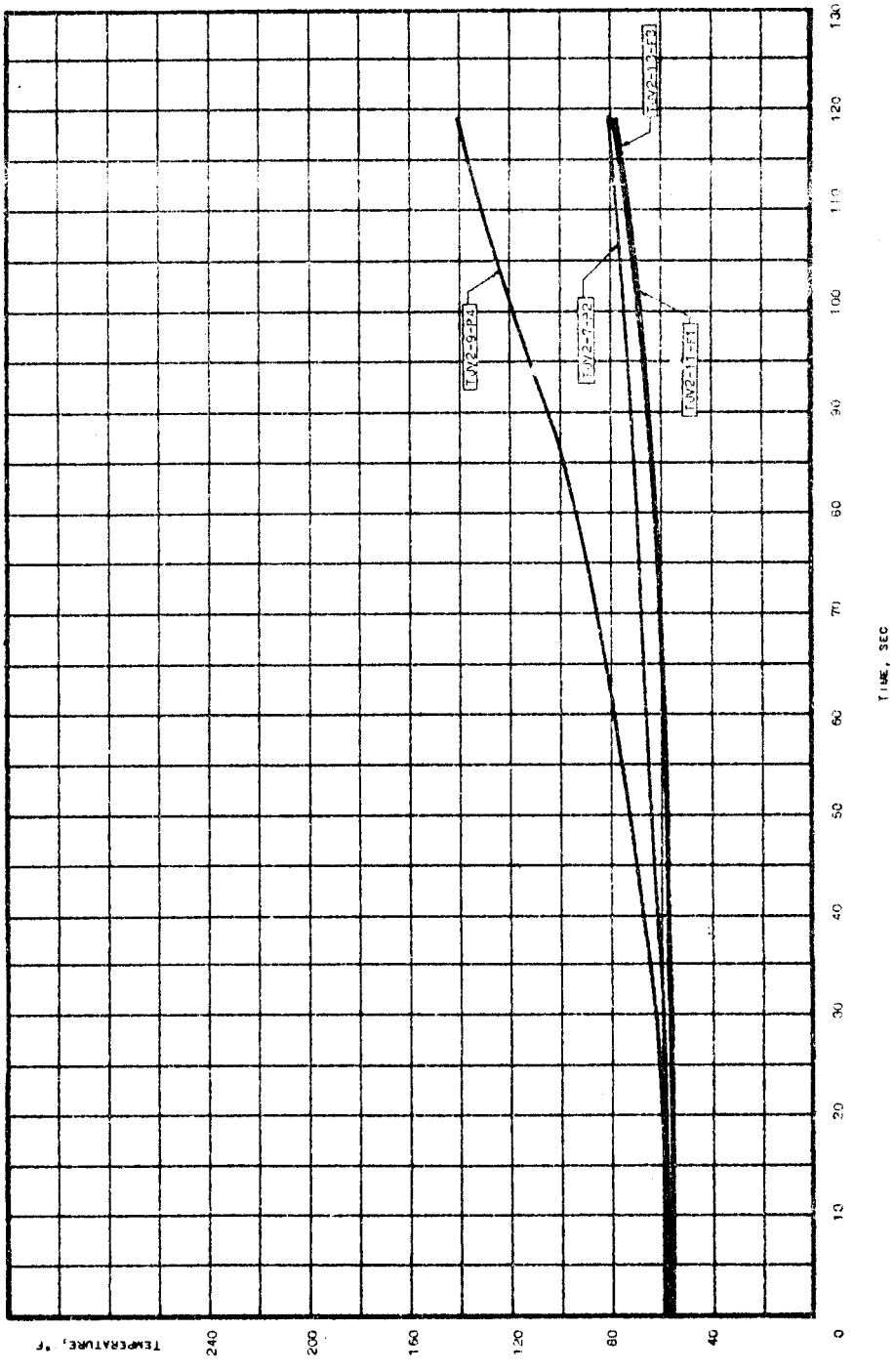

Jet-Vane Temperature, Thermocouples TJV2-7-P2, -9-P4, -11-F1, -13-F3

Figure 38

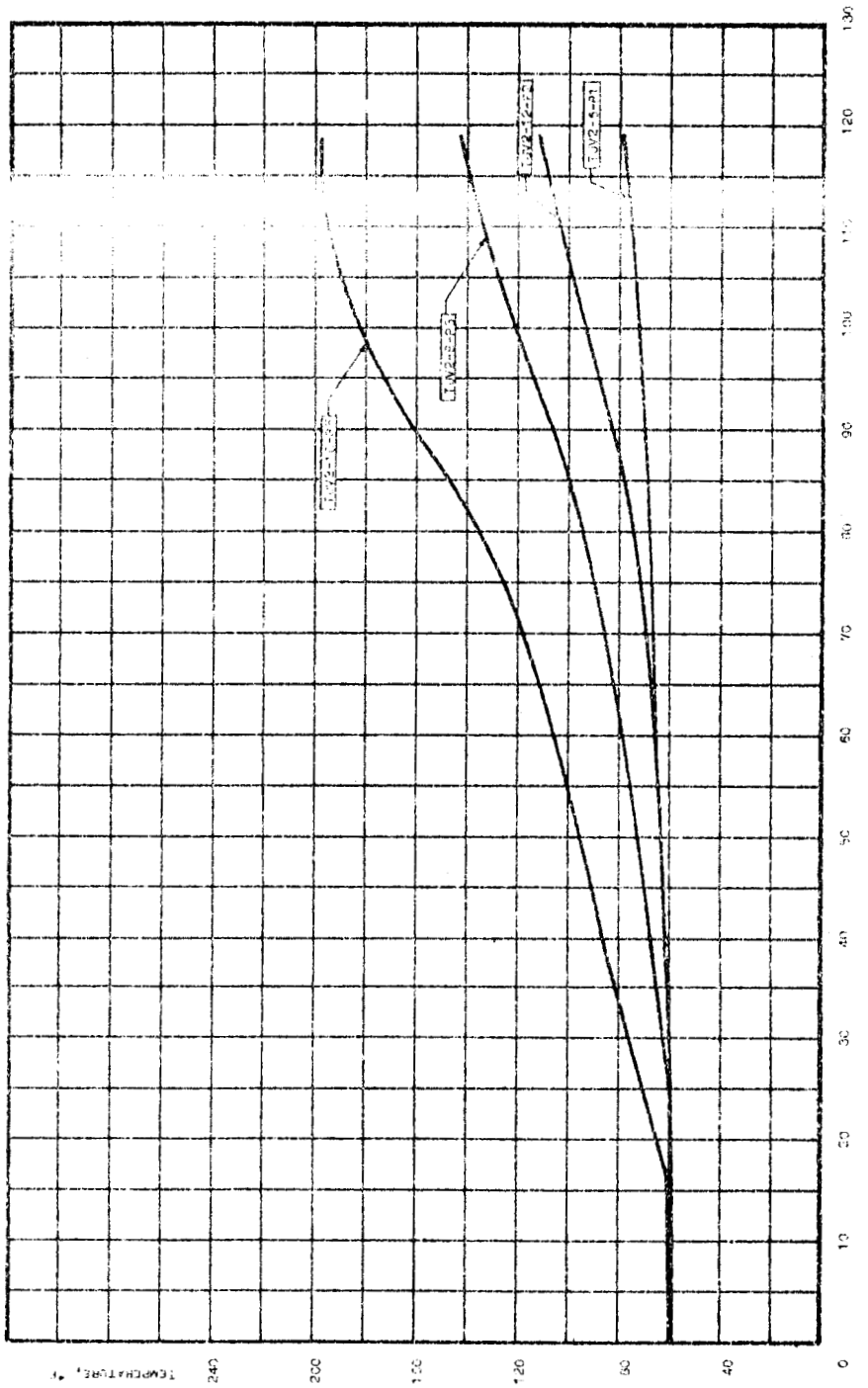

Jet-Vane Temperature, Thermocouples TJV2-6-P1, -8-P3, -10-P5, and -12-F2

Figure 39

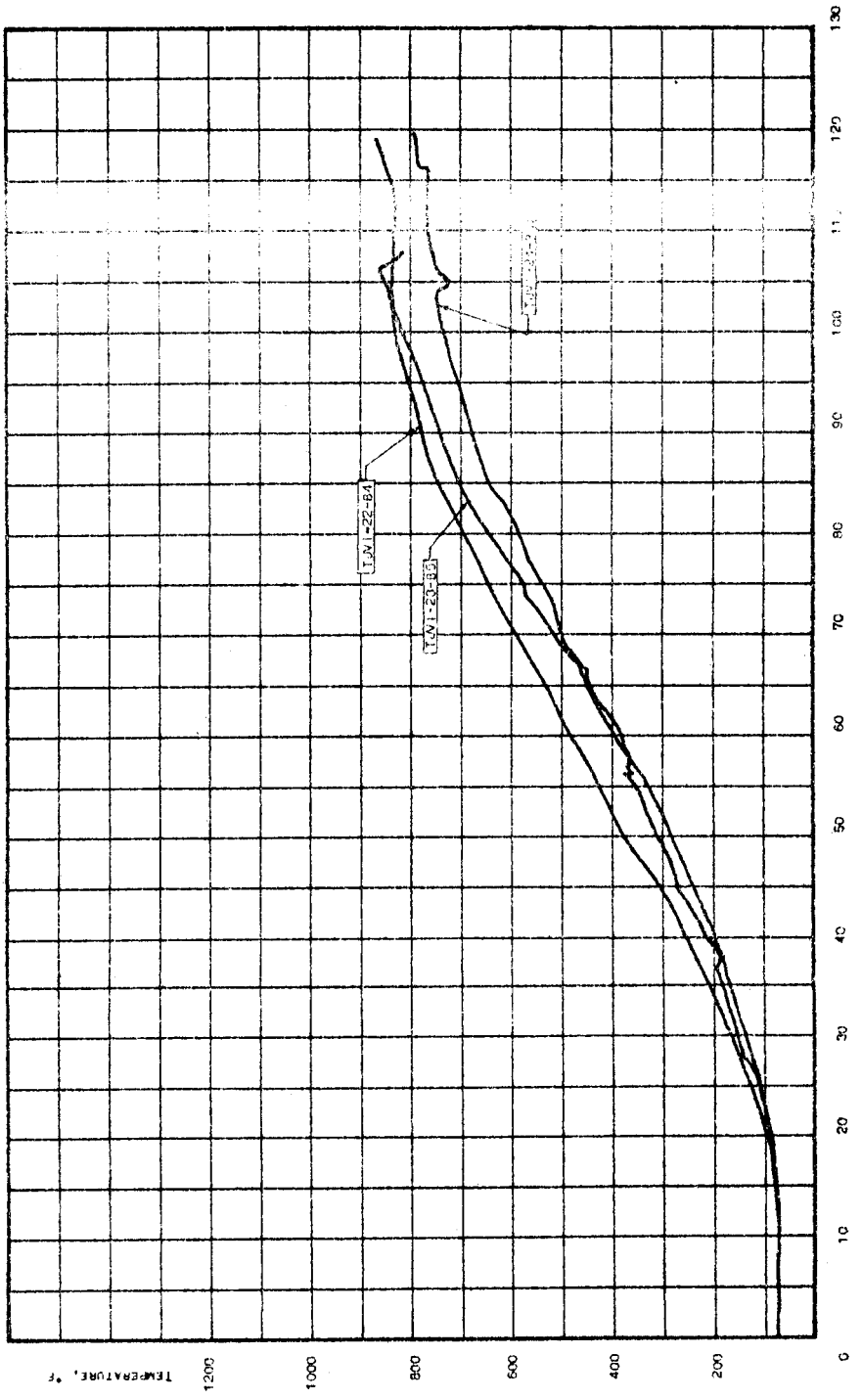

Jet-Vane Temperature, Thermocouples TJV1-22-B4, -23-B5, and -24-B6

Figure 40

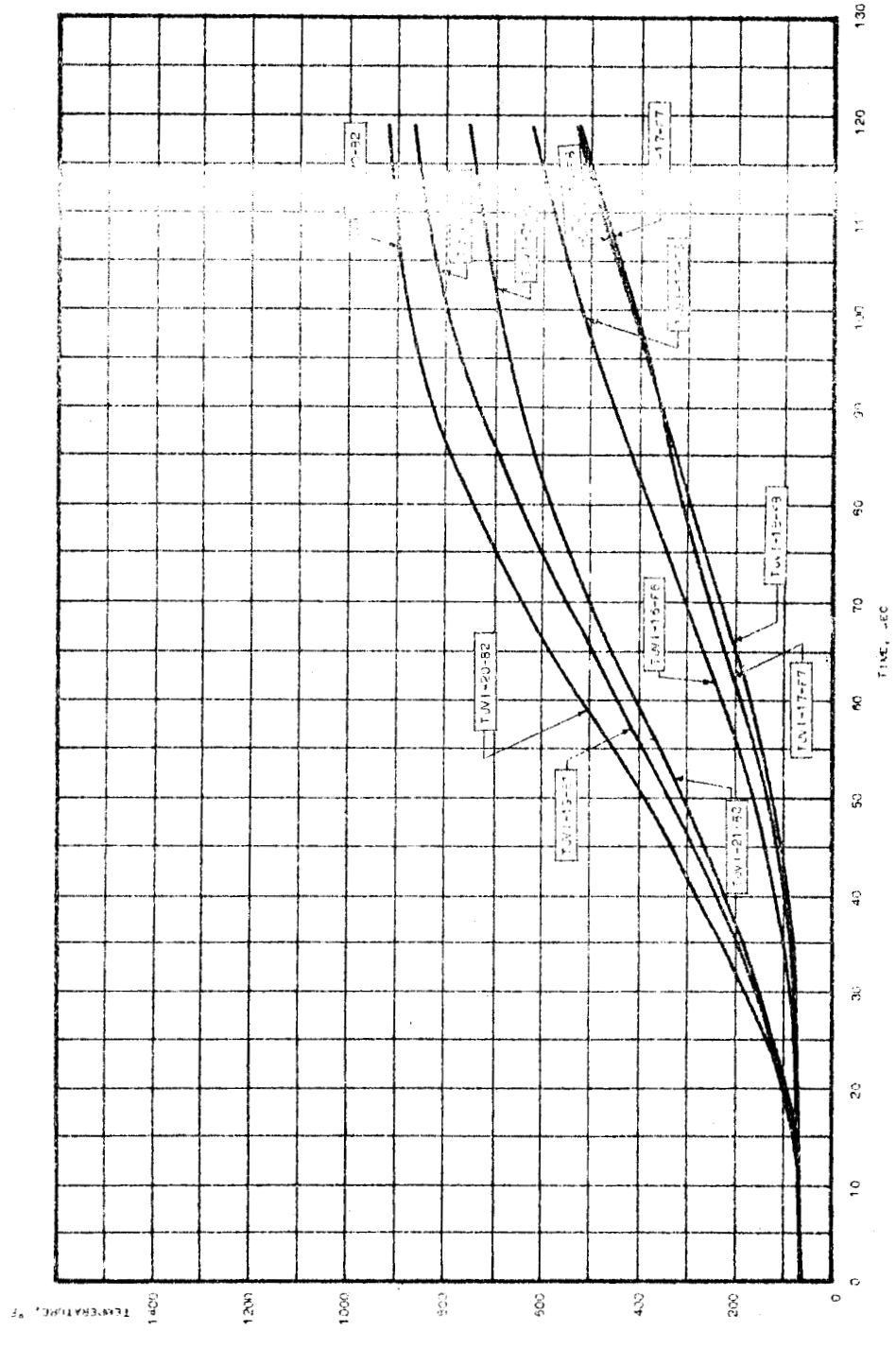

Jet-Vane Temperature, Thermocouples TJV1-16-F6, -17-F7, -[illegible]-F8, -19-B1, -20-B2, and -21-B3

Figure 41

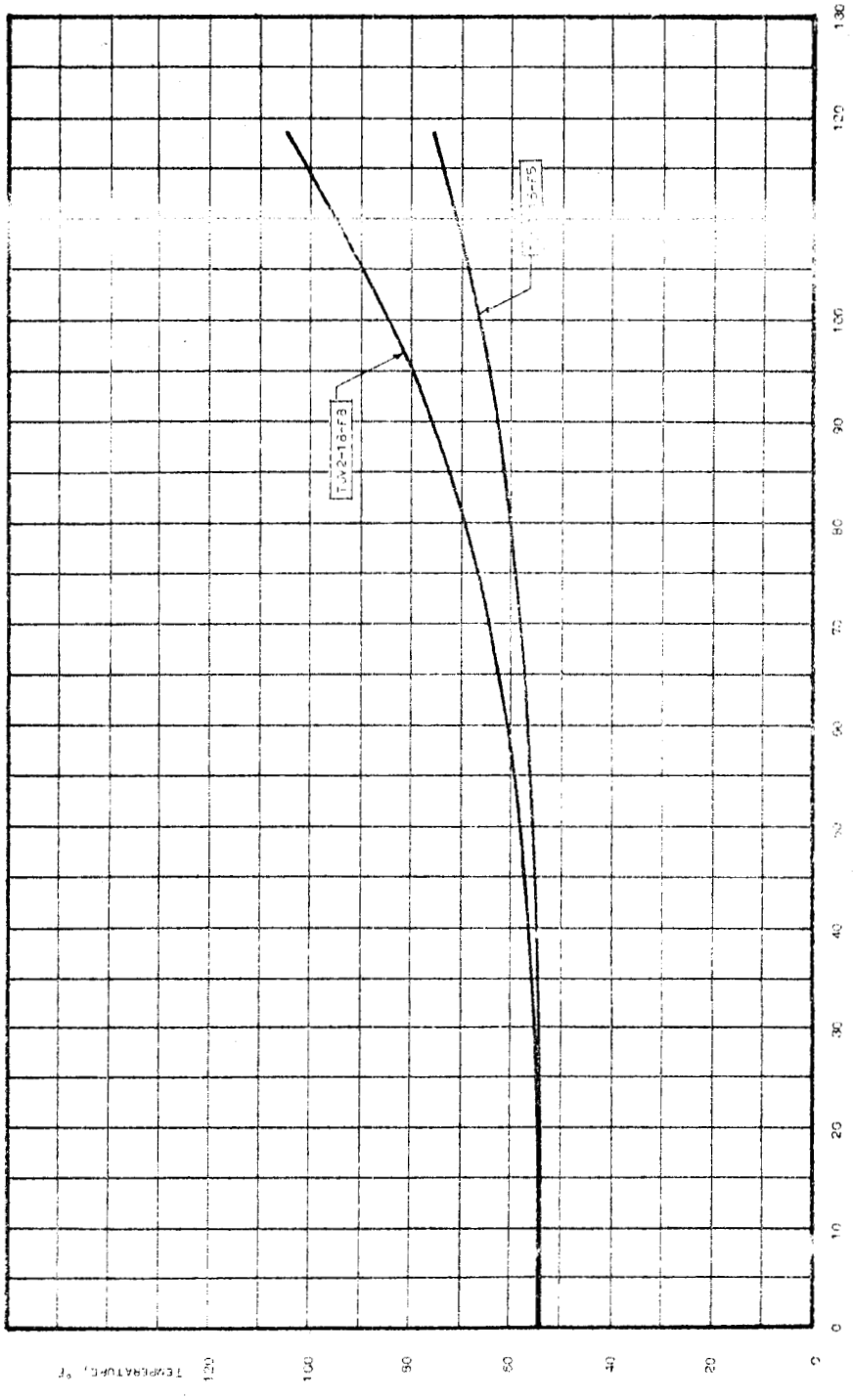

Jet-Vane Temperature, Thermocouples TJV2-18-F8 and -15-

Figure 42

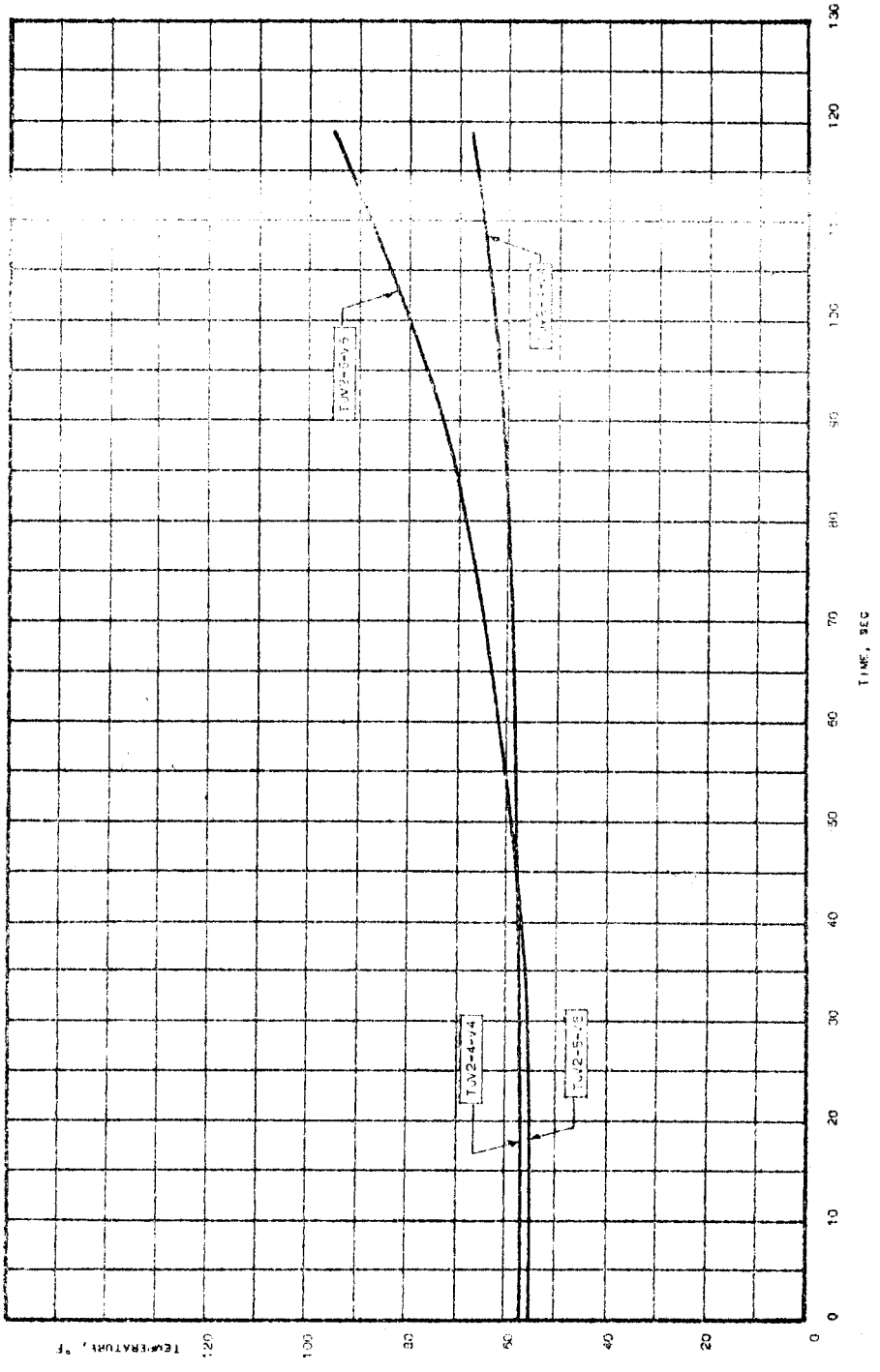

Jet-Vane Temperatures, Thermocouples TJV2-4-V4 and TJV2-5-V5

Figure 43

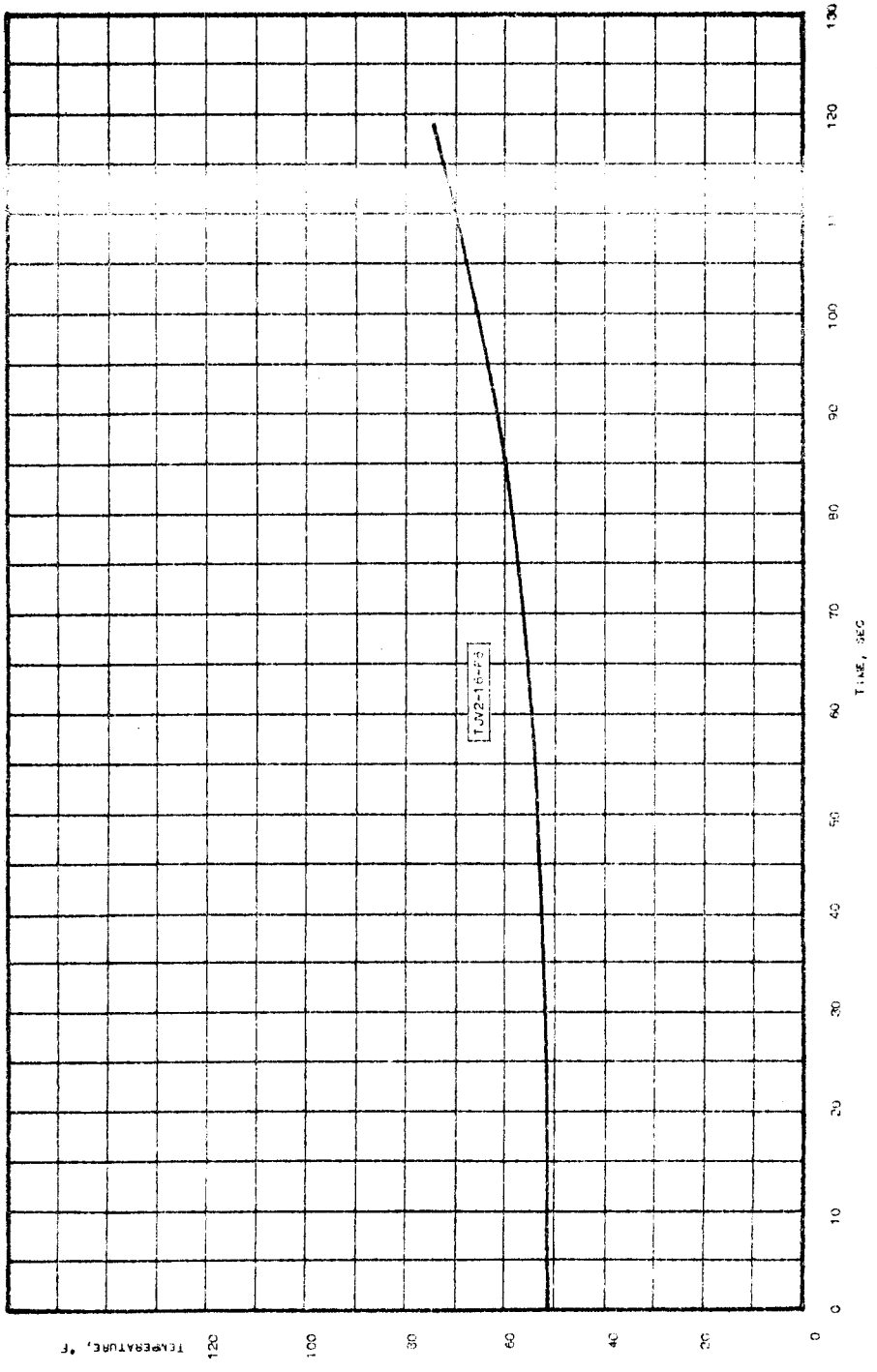

Jet-Vane Temperature, Thermocouple TJV2-16-F6

Figure 44

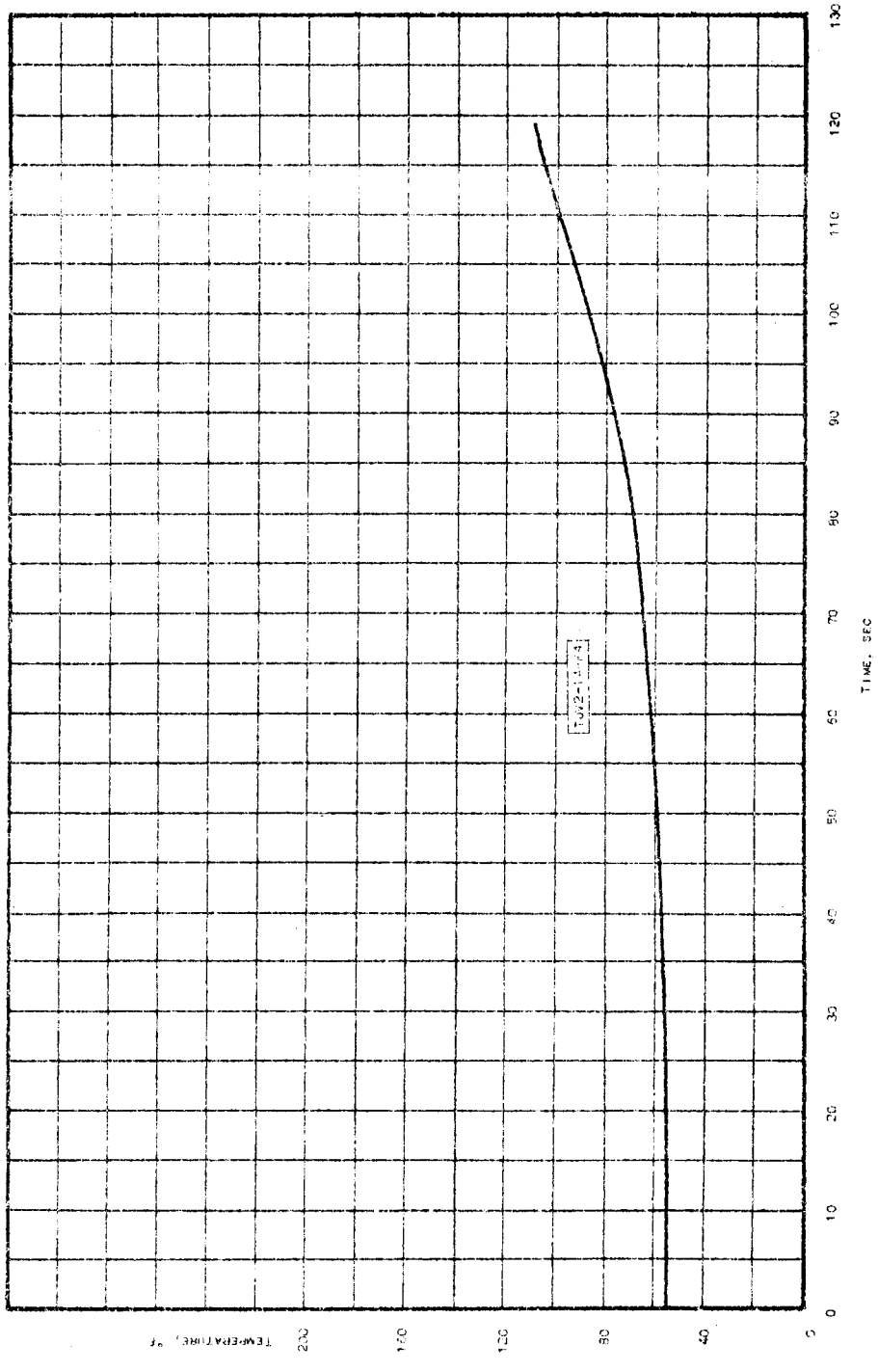

Jet-Vane Temperature, Thermocouple TJV2-14-F4

Figure 45

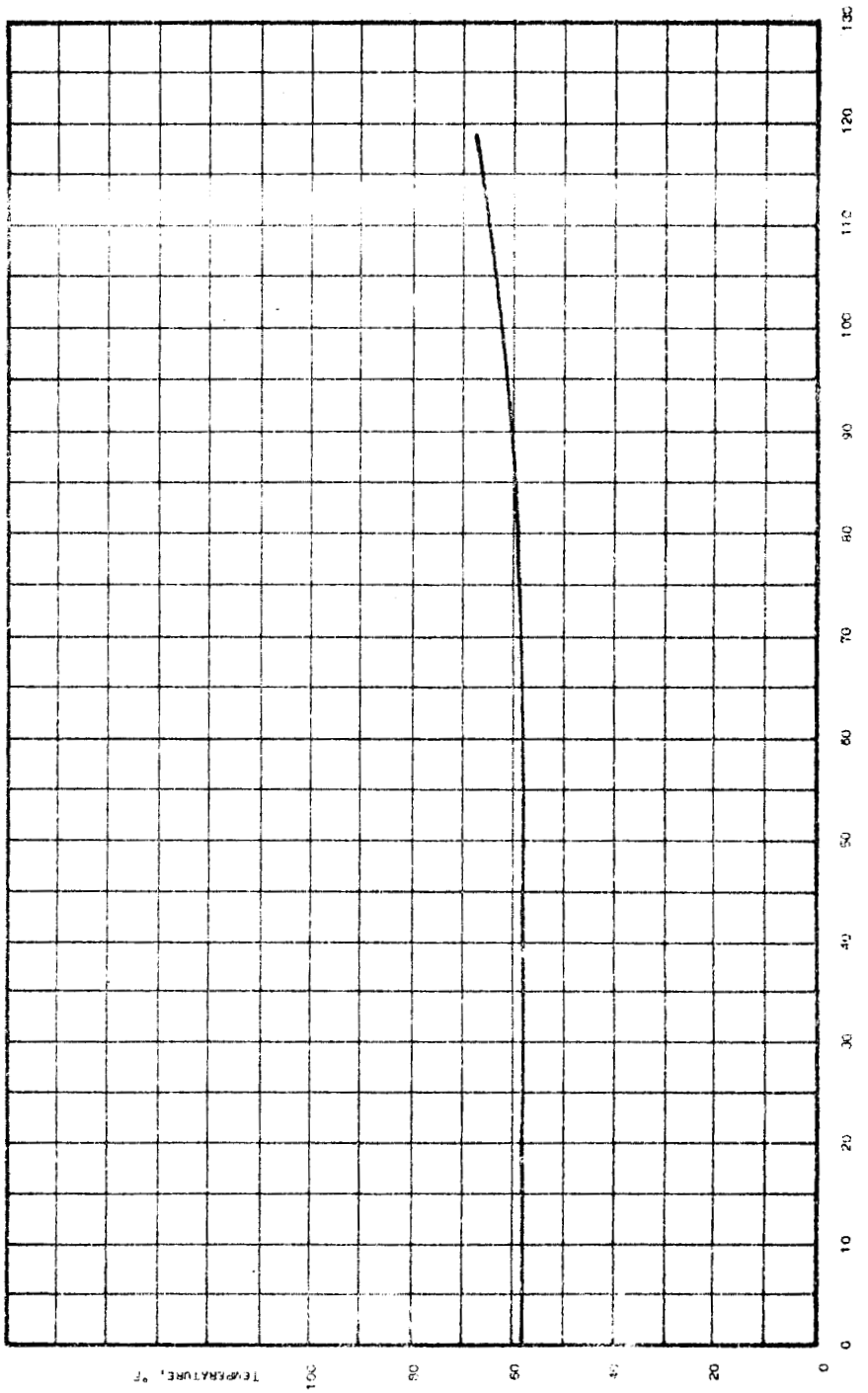

Jet-Vane Temperature, Thermocouple TJV2-2-V2

Figure 46

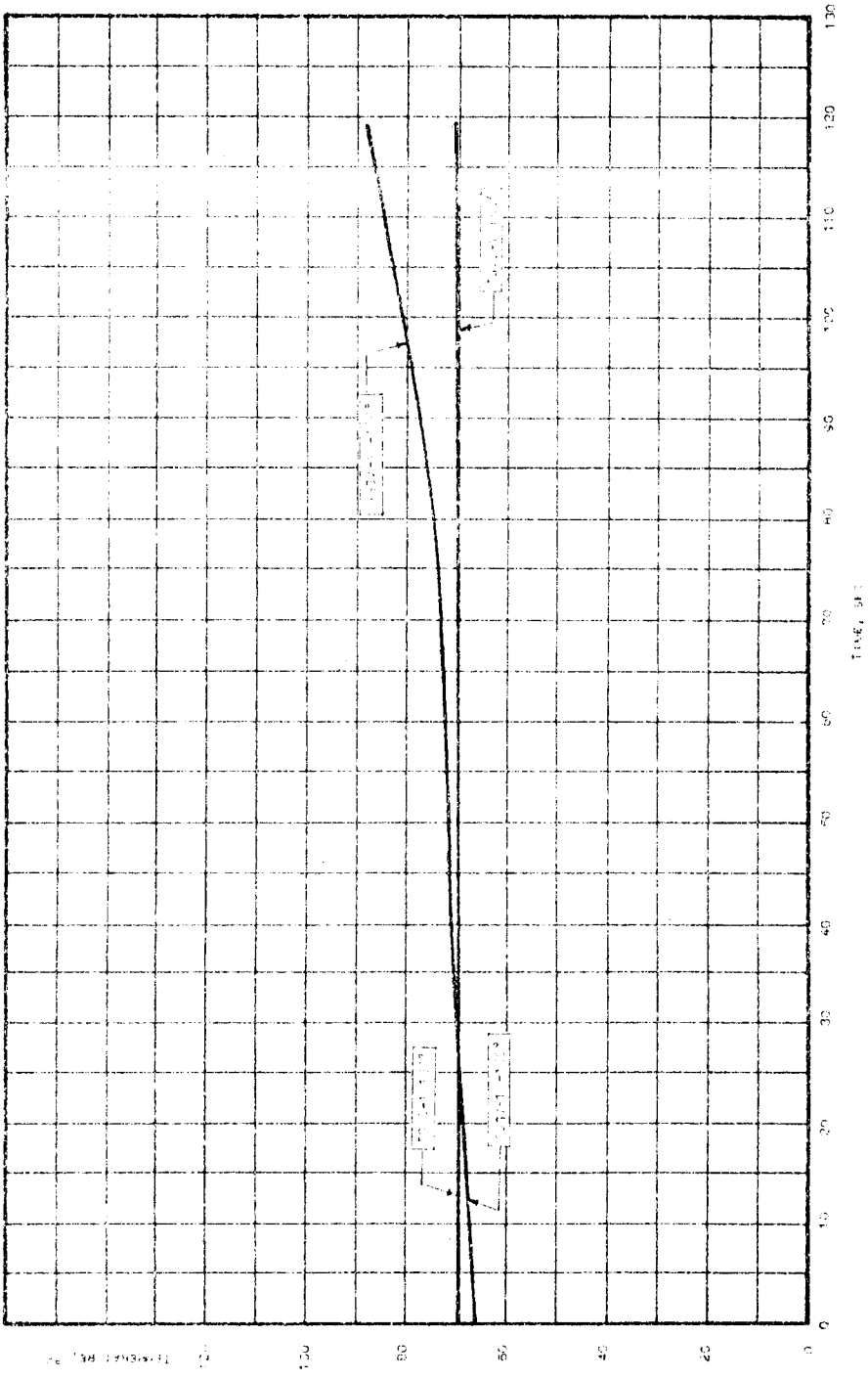

Jet-Vane Temperature, Thermocouples TSCV-1 and TSSV-1

Figure 47

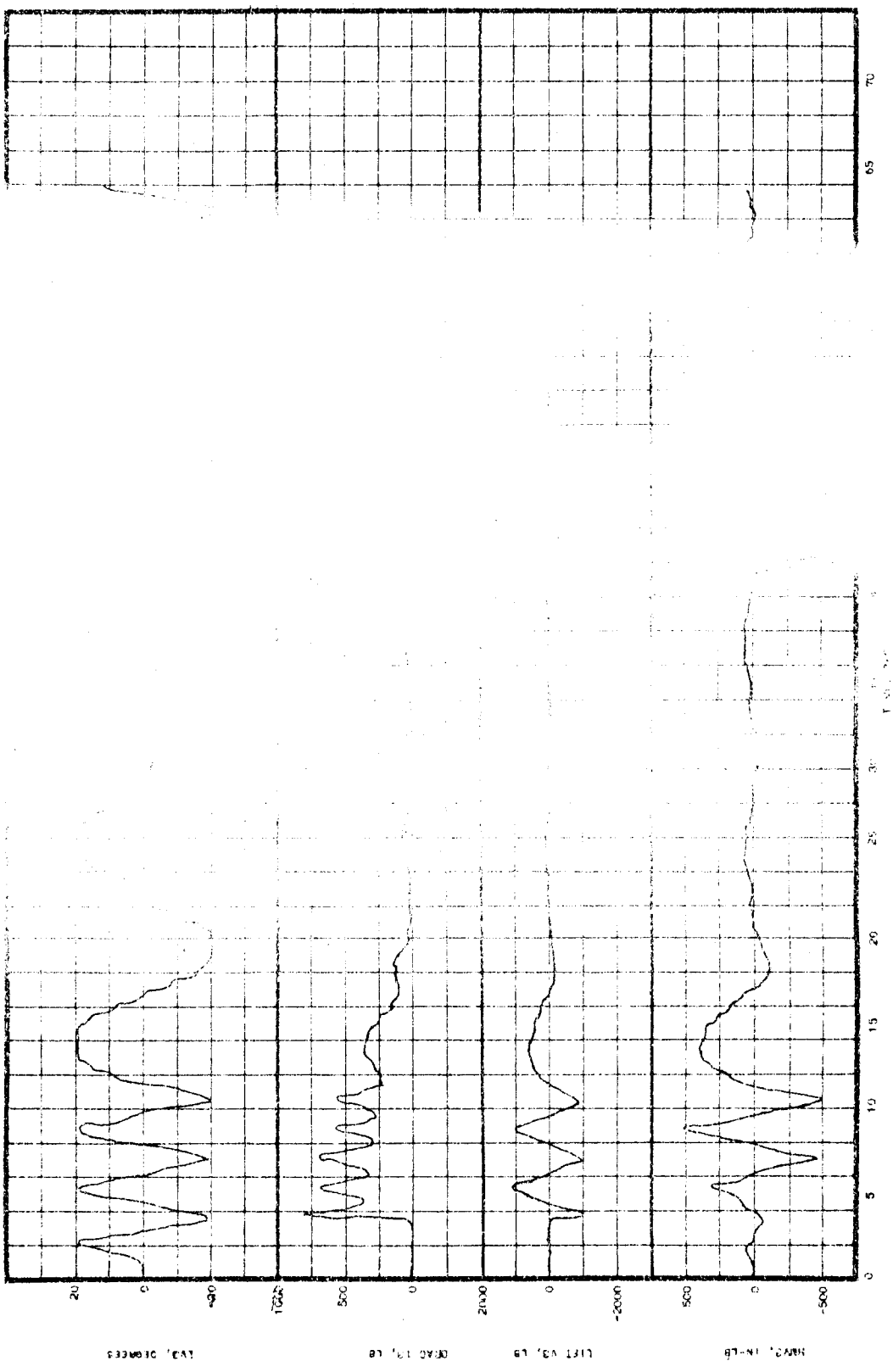
Jet-Vane Force D
70
65
25
20
15
10
5
0
20
0
-500
1000
500
0
2000
0
-2000
500
0
-500

Figure 48

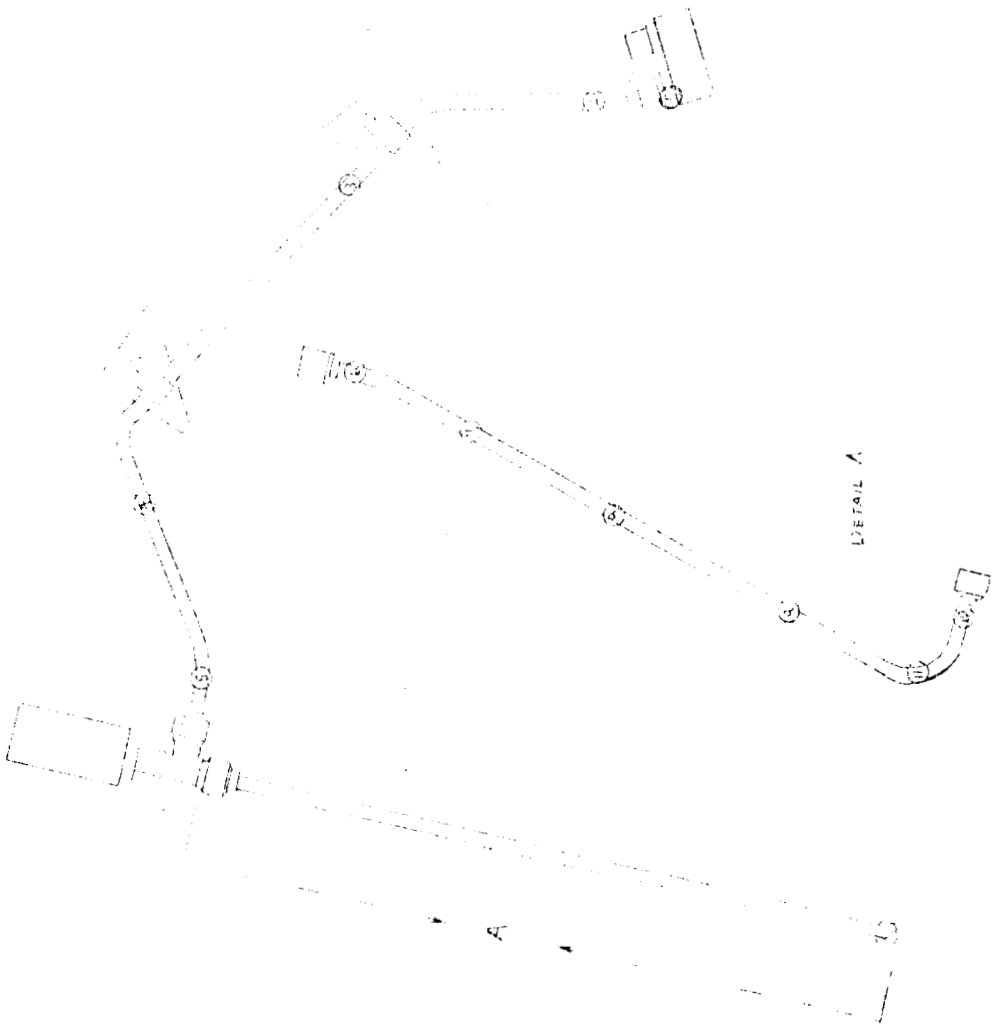

Thermocouple Locations, Bourns Transducer Plumbing

Figure 49

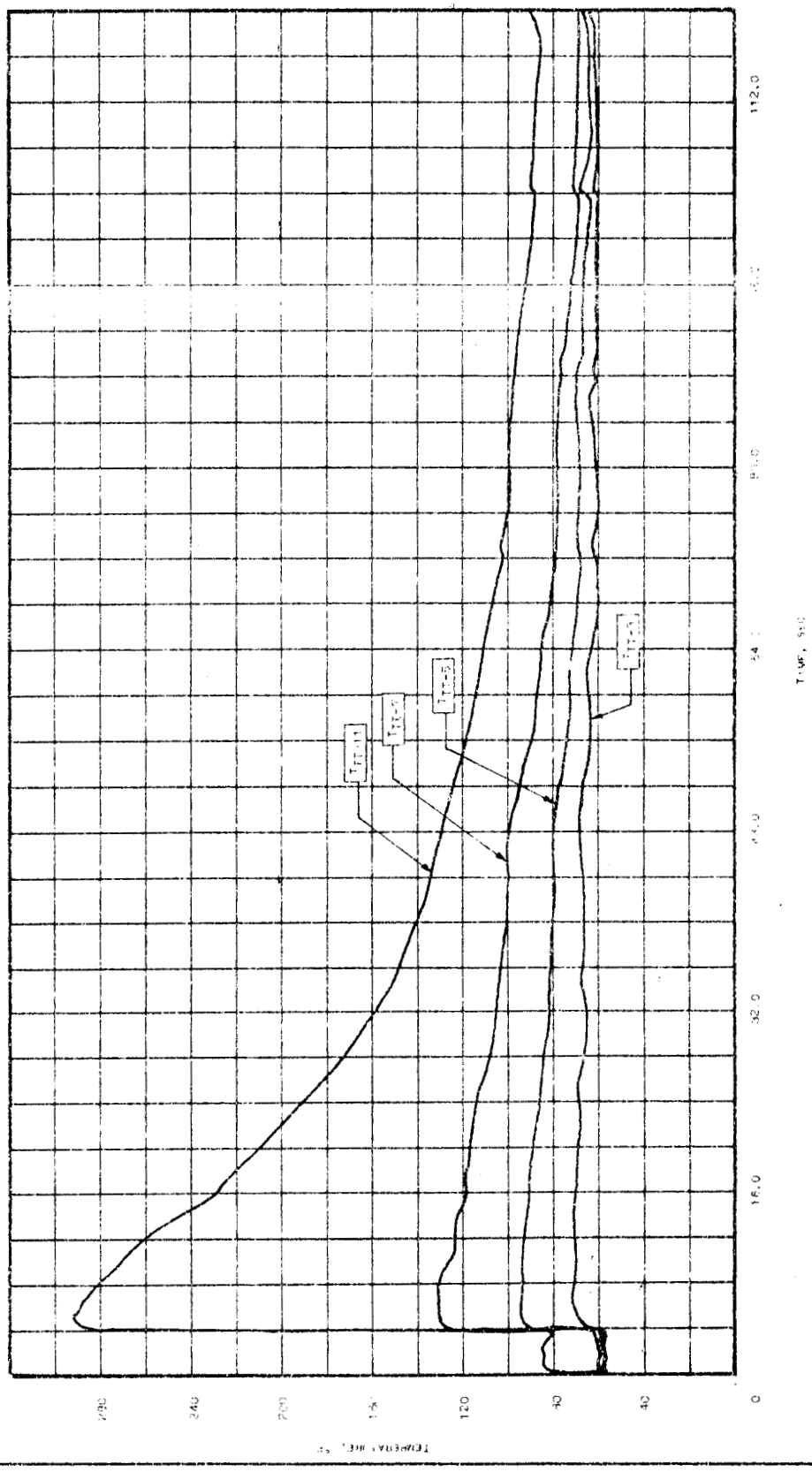

Transducer Temperature, Thermocouples T_{TF}-3, -5, -7 and -11

Figure 50

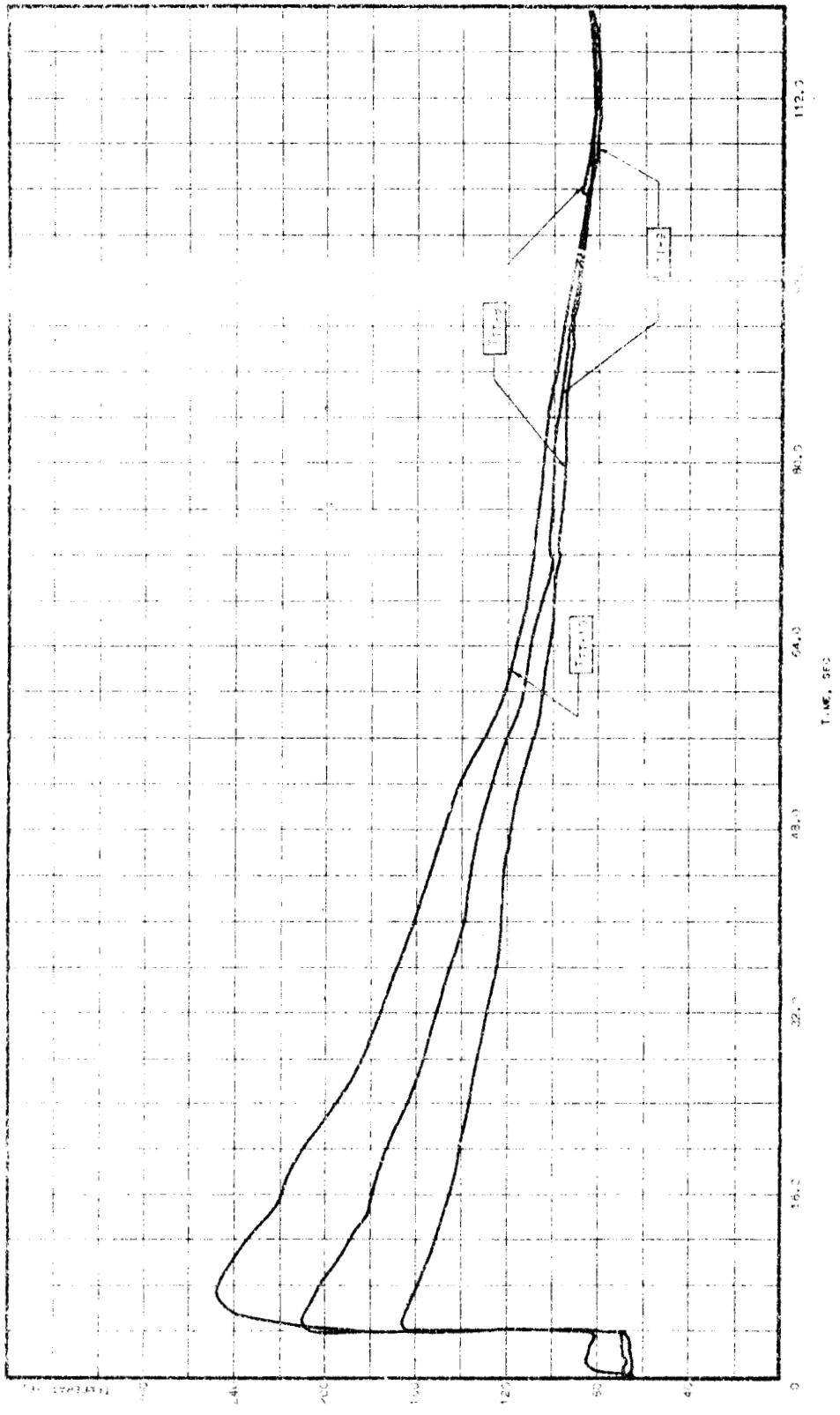

Transducer Temperature, Thermocouples T_{T}-8, -9, and -11

Figure 51

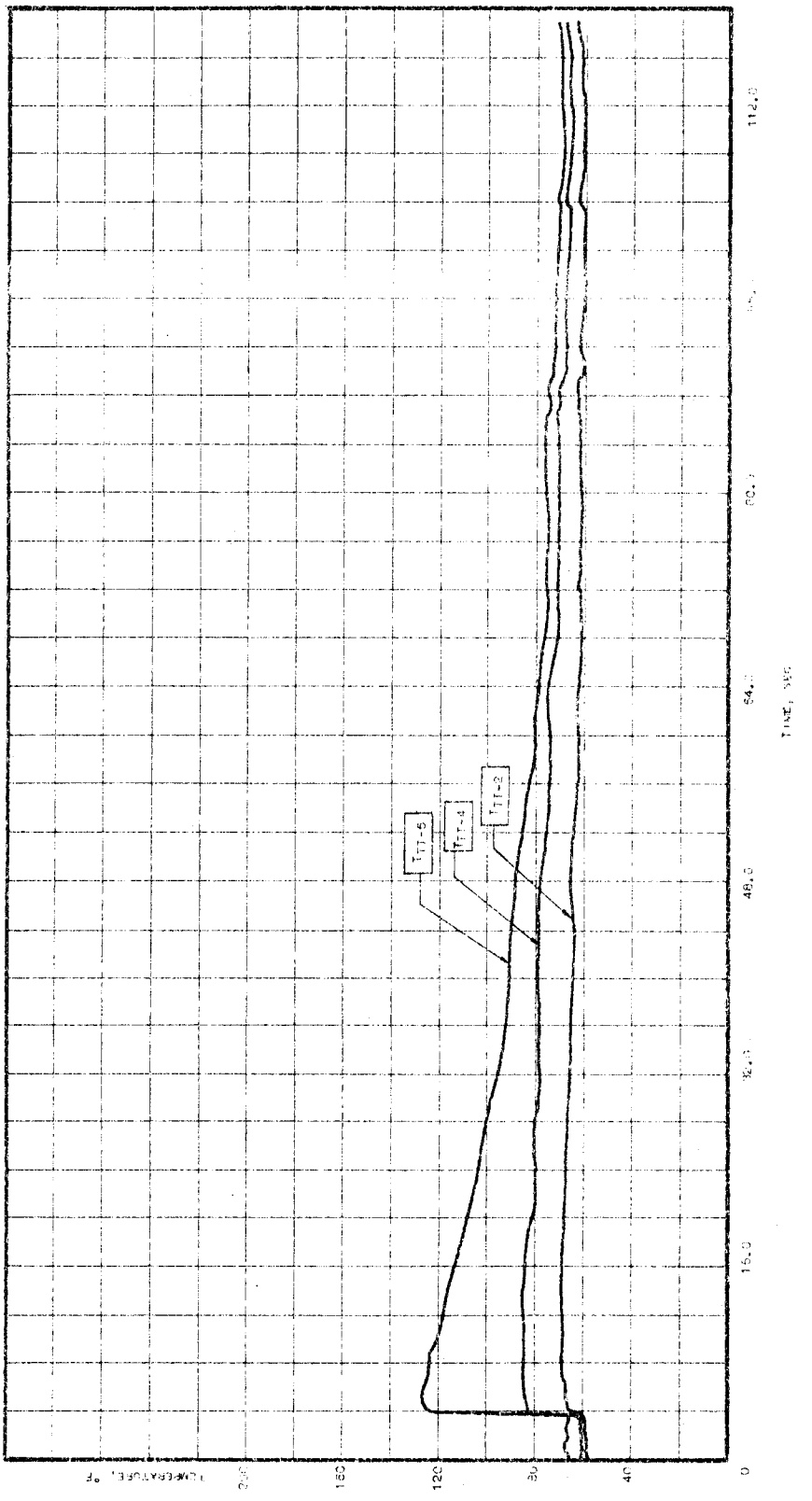

Transducer Temperature, Thermocouples T_{TT}-2, -4, and -6

Figure 52

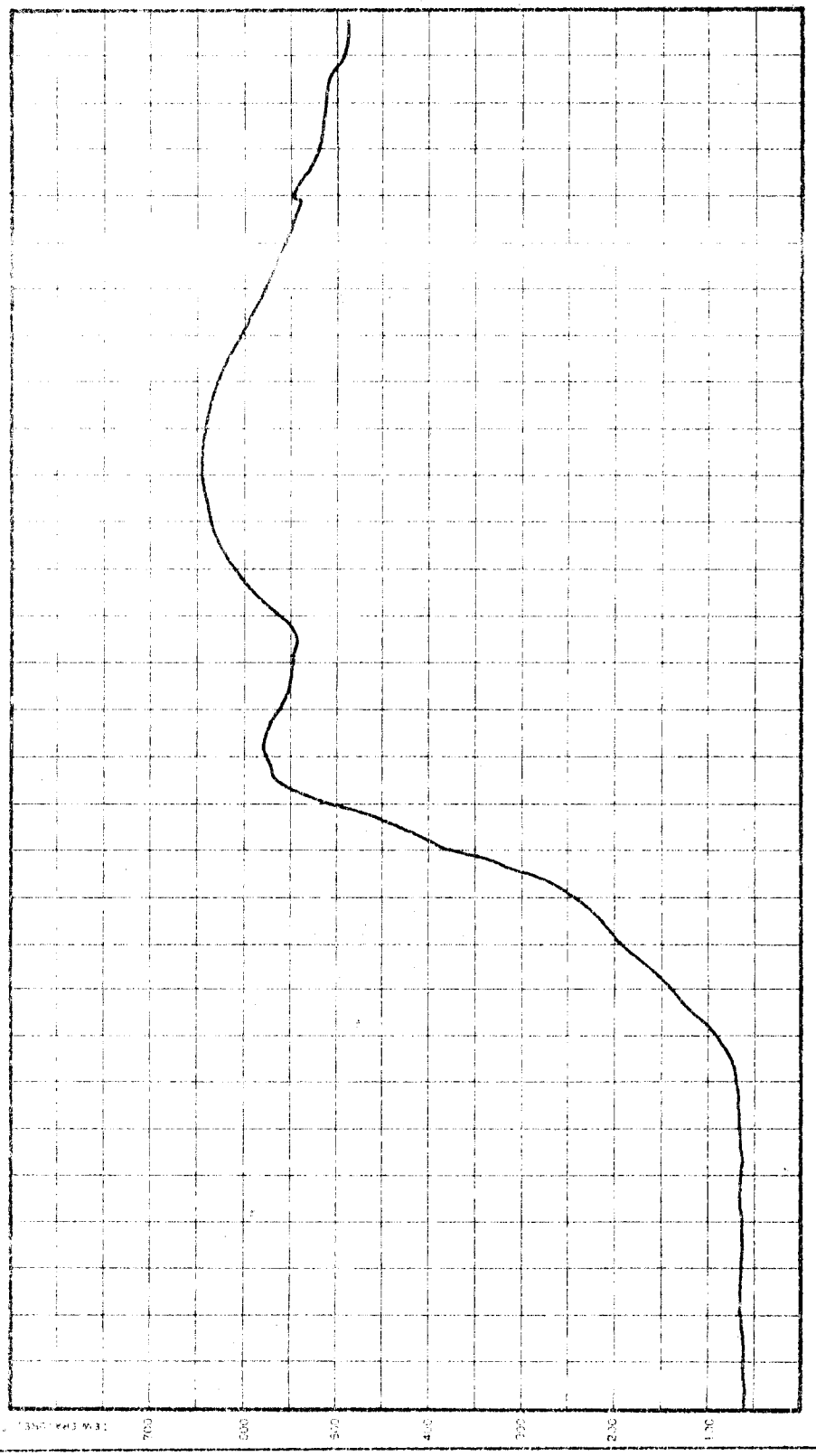

Transducer Temperature, Thermocouple T_{TT}-1

Figure 53

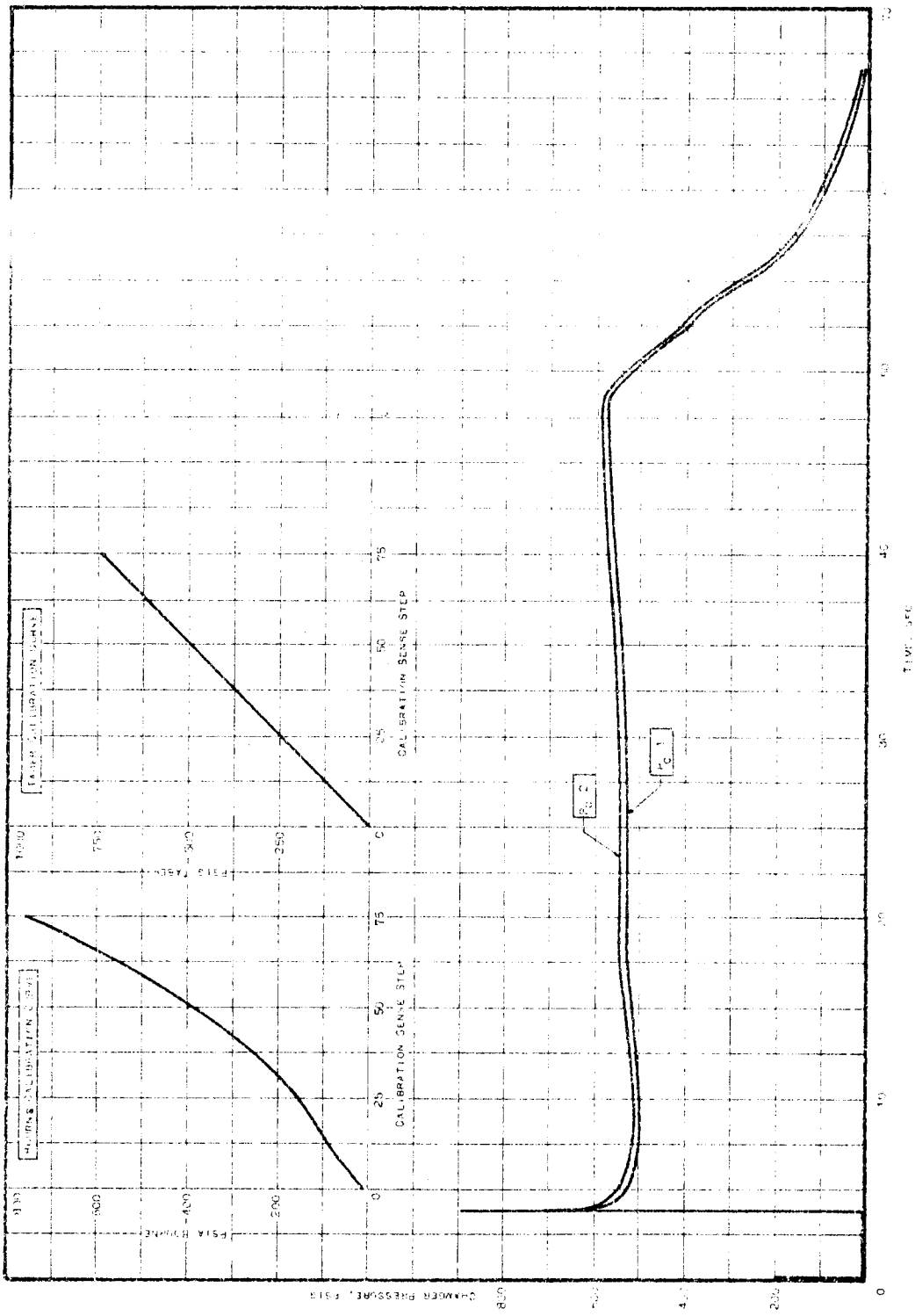

Comparison of Bourns and Taber Transducer Pressure Recordings

Figure 54

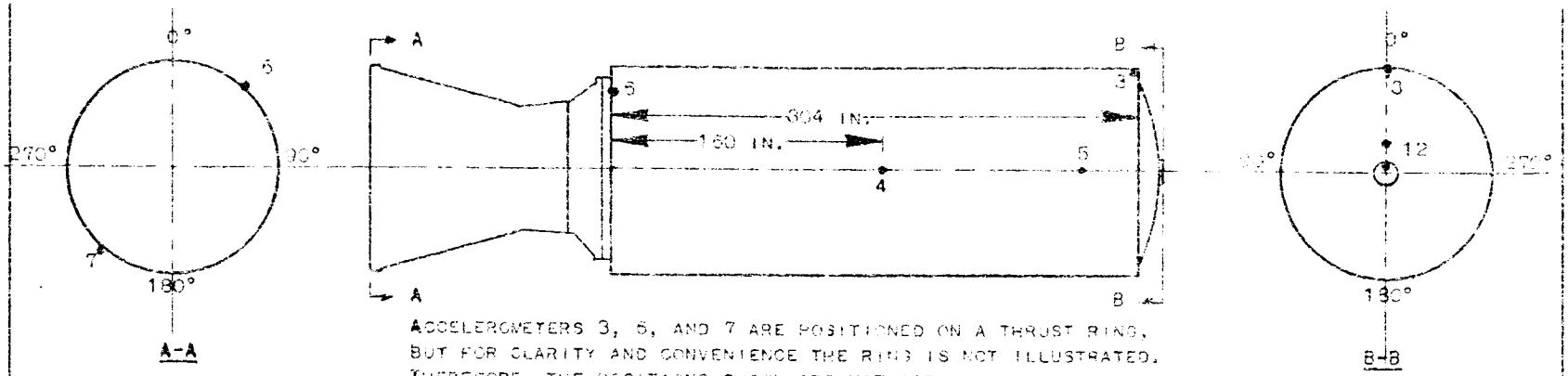

ACCELEROMETERS 3, 5, AND 7 ARE POSITIONED ON A THRUST RING, BUT FOR CLARITY AND CONVENIENCE THE RING IS NOT ILLUSTRATED. THEREFORE, THE POSITIONS SHOWN ARE NOT ACTUAL.

ACCELEROMETER NOTATION EXPLANATION

GIGN - ACCELEROMETER ON FACE OF IGNITER BOSS
GOF - ACCELEROMETER ON FORWARD THRUST RING
GOC - ACCELEROMETER ON CHAMBER
GOA - ACCELEROMETER ON AFT THRUST RING

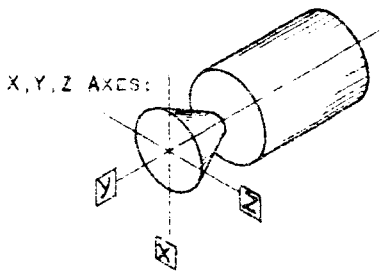

ACCELEROMETER NUMBER, LOCATION & SUGGESTED RANGING

NO.	DESIGNATION	
1	GIGN - Y	± 250G
2	GOFY - 0 - 2.0	± 15 G
3	GOFY - 0 - 20	± 15 G
4	GOCZ -90 - 160	± 25 G
5	GOCZ -90 - 304	± 25 G
6	GOAY -45 - 20	± 50 G
7	GOAY -225- 20	± 50 G

EXAMPLE

GOFY - 0 - 20

GOFY - GIVES COMPONENT LOCATION
0 - GIVES ANGULAR POSITION
20 - RADIAL POSITION ON LONGITUDINAL DISTANCE POINT FROM REFERENCE POINT SHOWN IN SKETCH.

ALSOL IIA-3 (REHAB) HIGH FREQUENCY INSTRUMENTATION

Accelerometer Locations

Figure 55

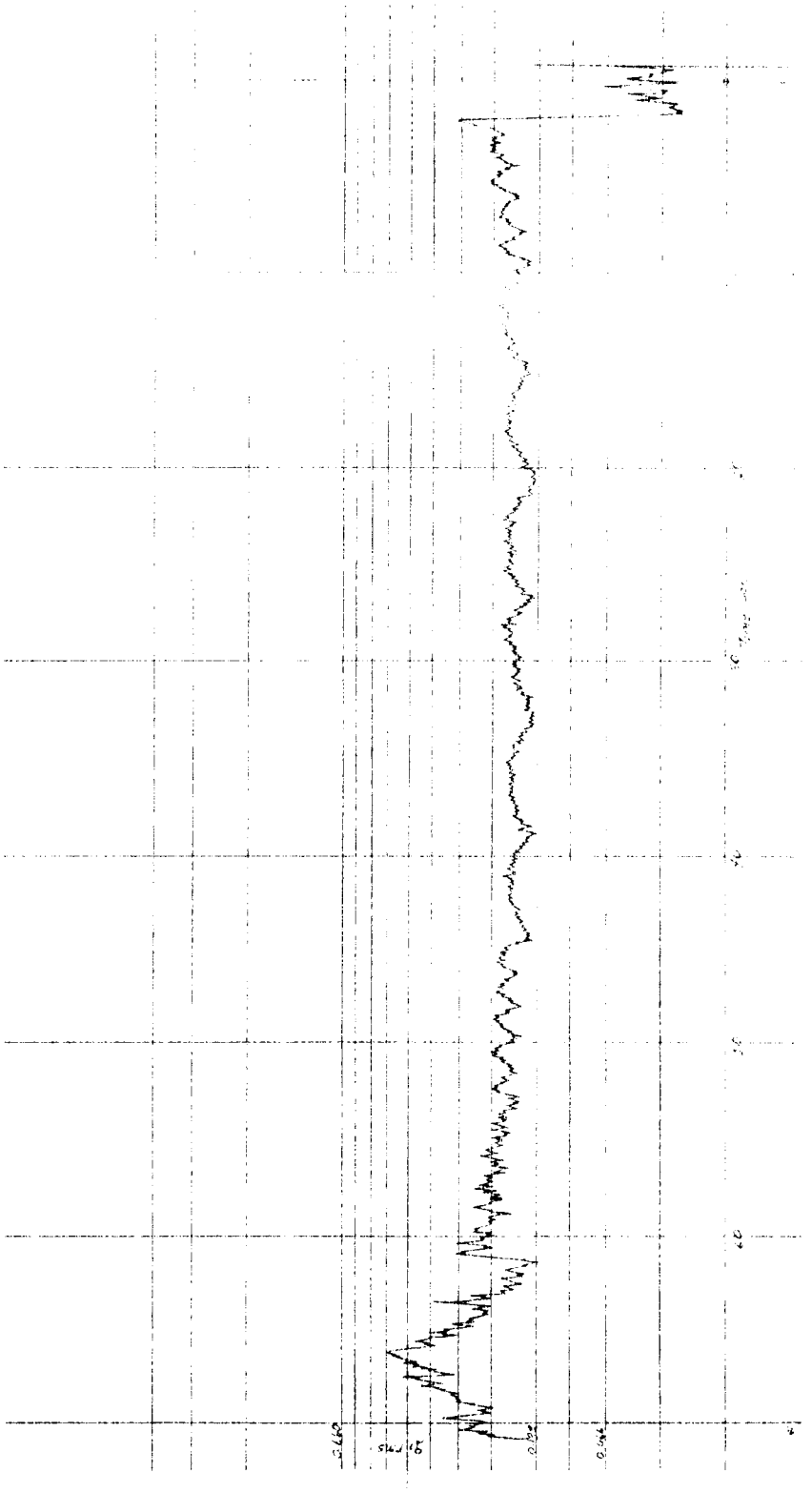

Vibration Data, Accelerometer GCFy-0-20.0

Figure 56

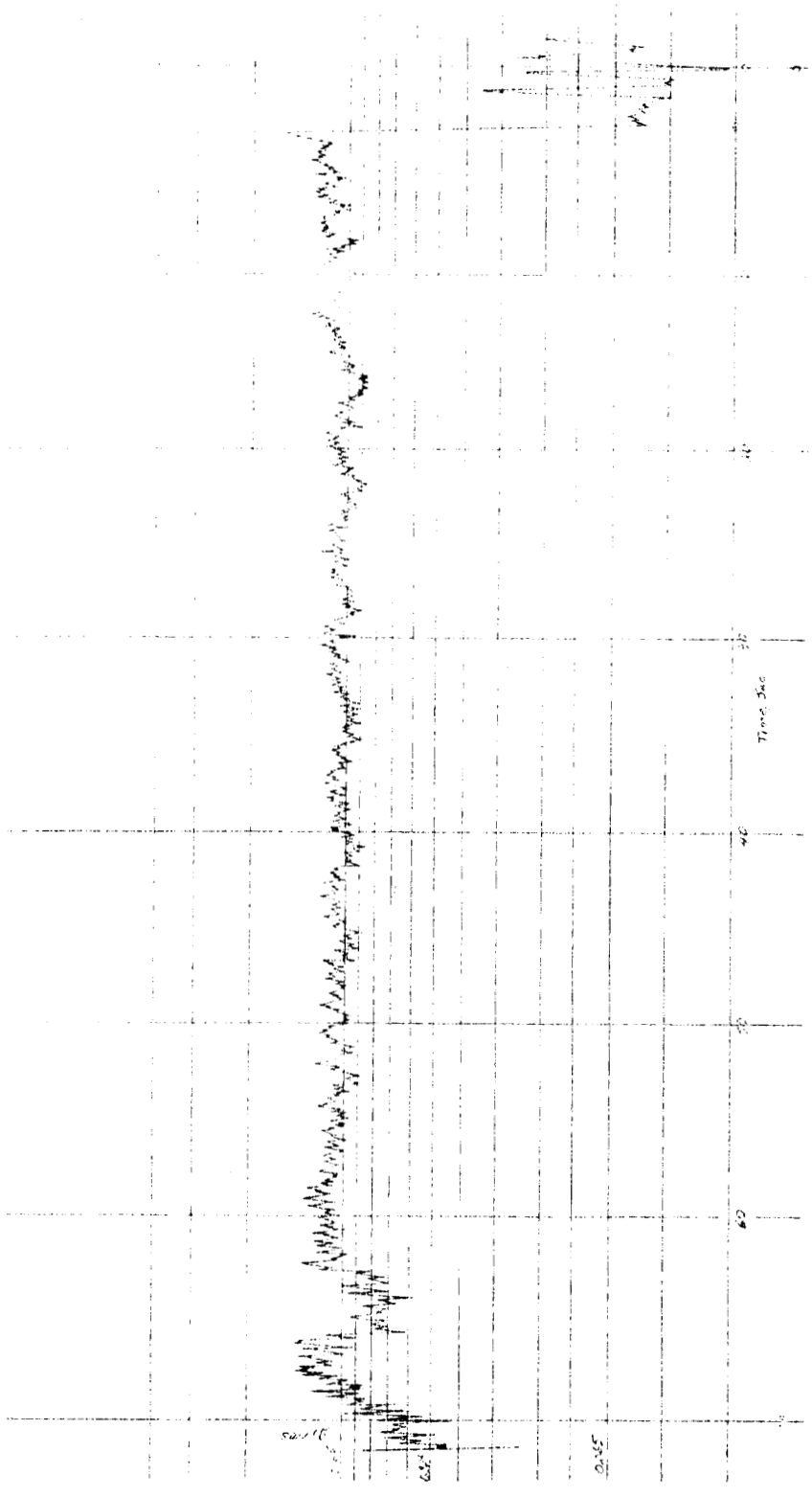

Vibration Data, Accelerometer GCFy-0-2, 0

Figure 57

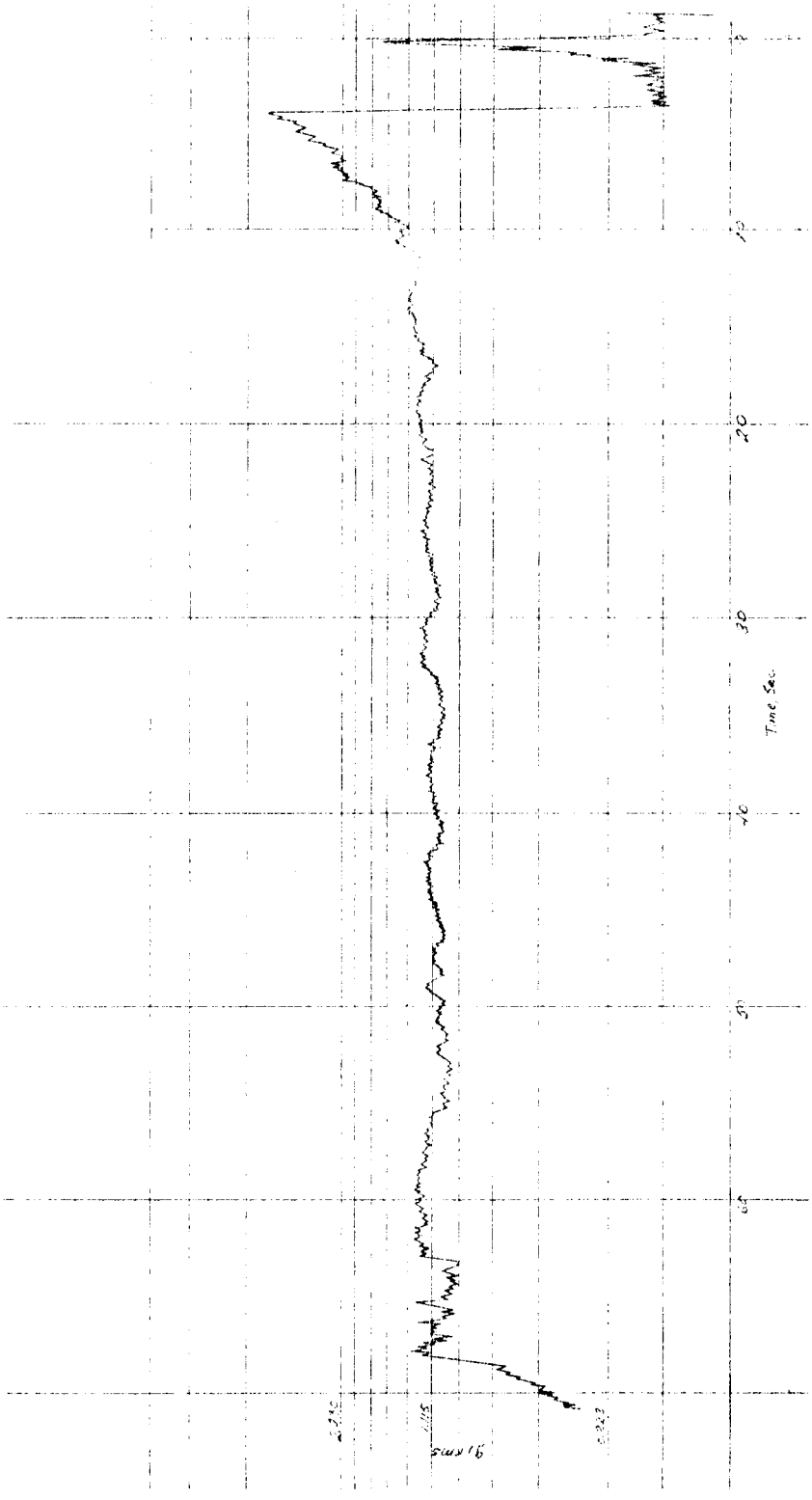

Vibration Data, Accelerometer GCAy-225-20

Figure 58

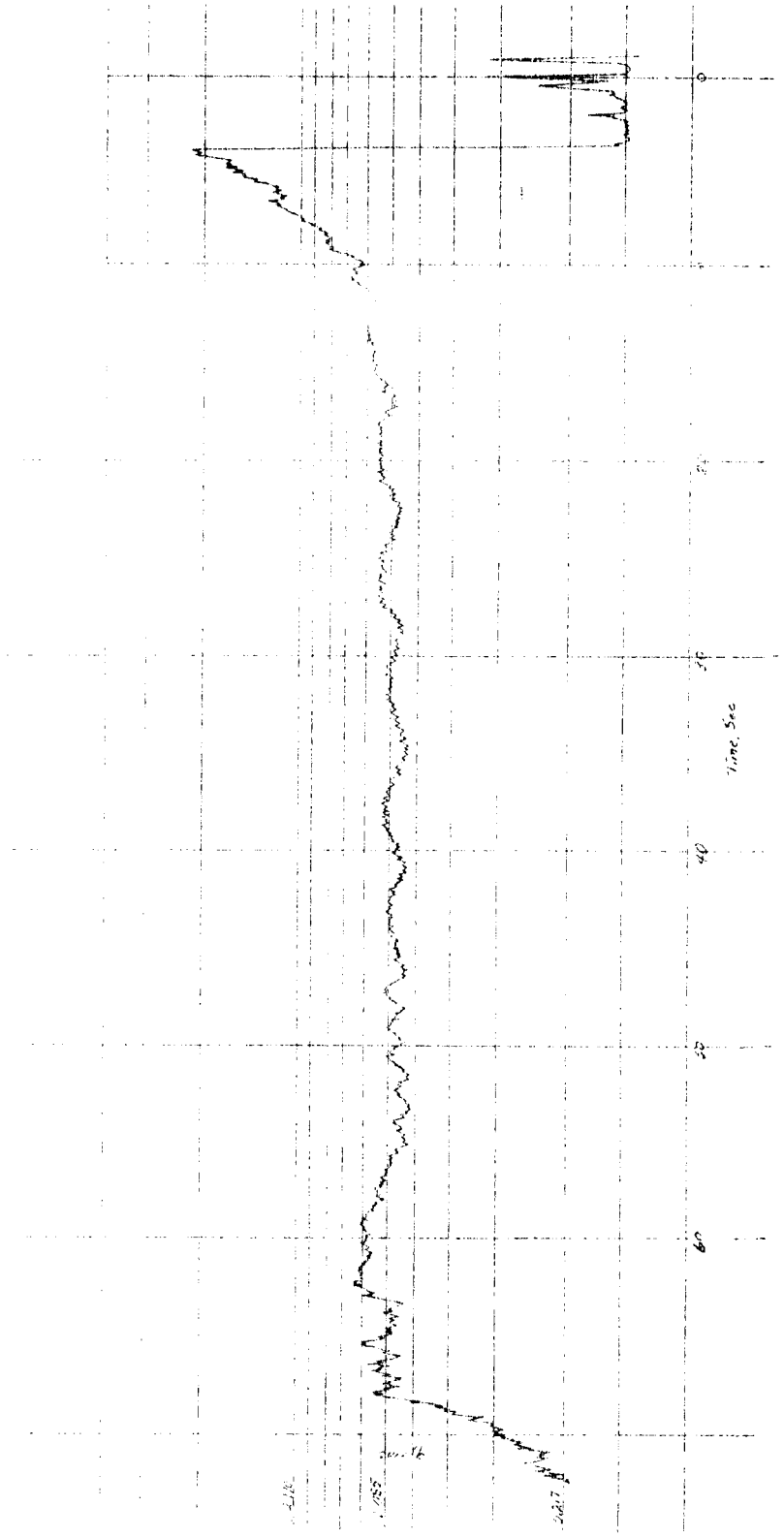

Vibration Data, Accelerometer GCAy-45-20

Figure 59

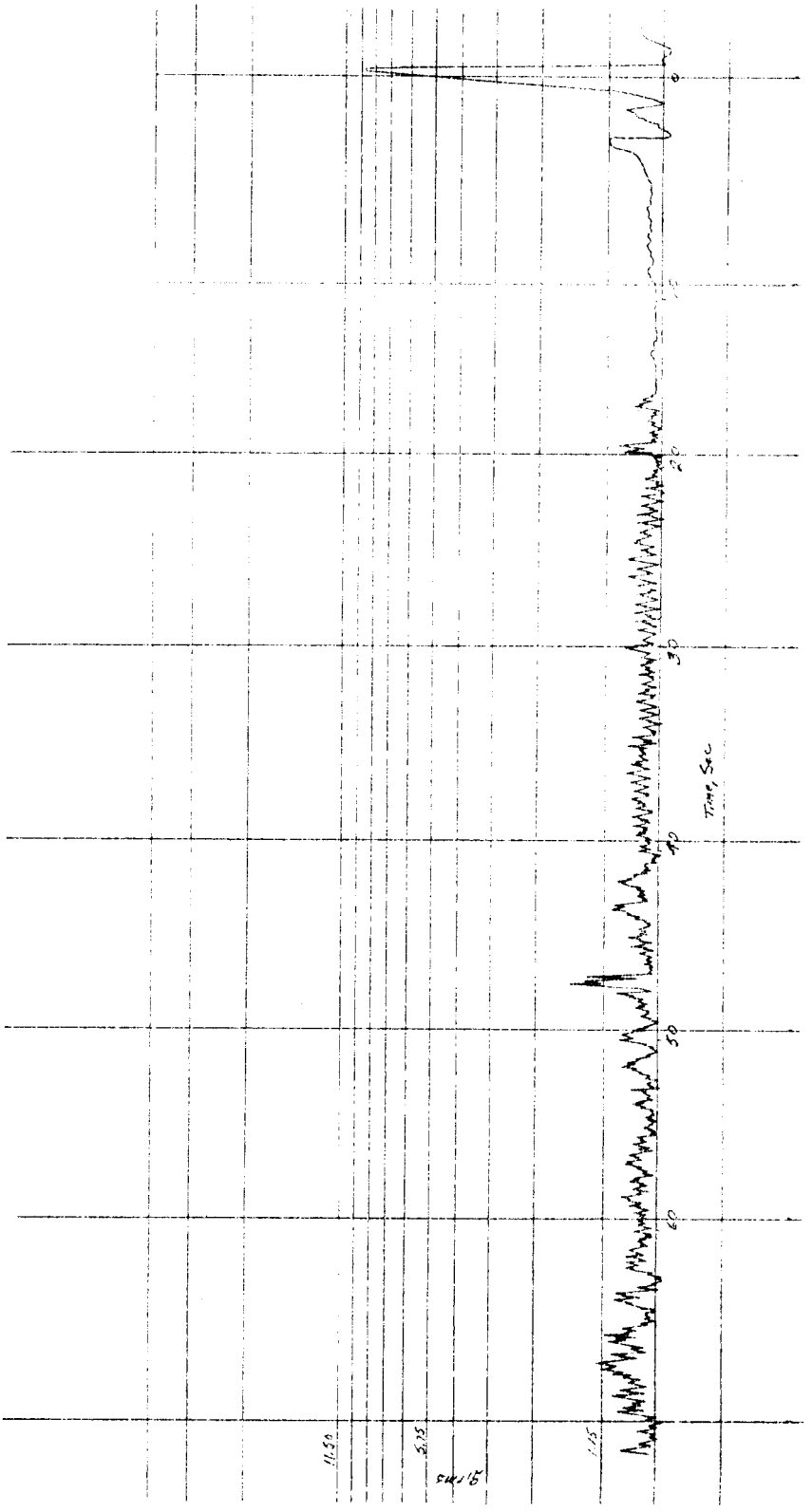

Vibration Data, Accelerometer G1GNy

Figure 60

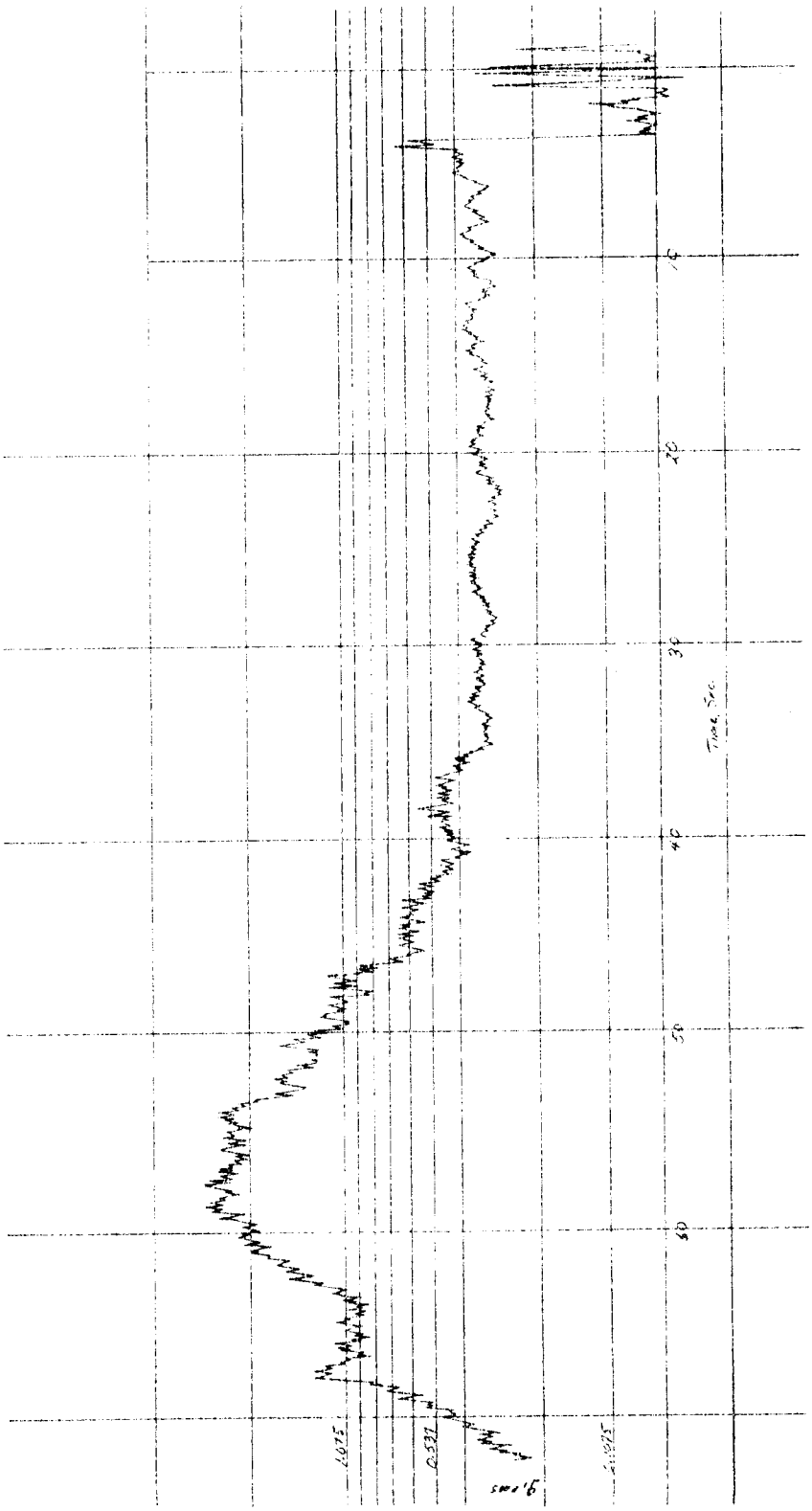

Vibration Data, Accelerometer GCCz-90-304

Figure 61

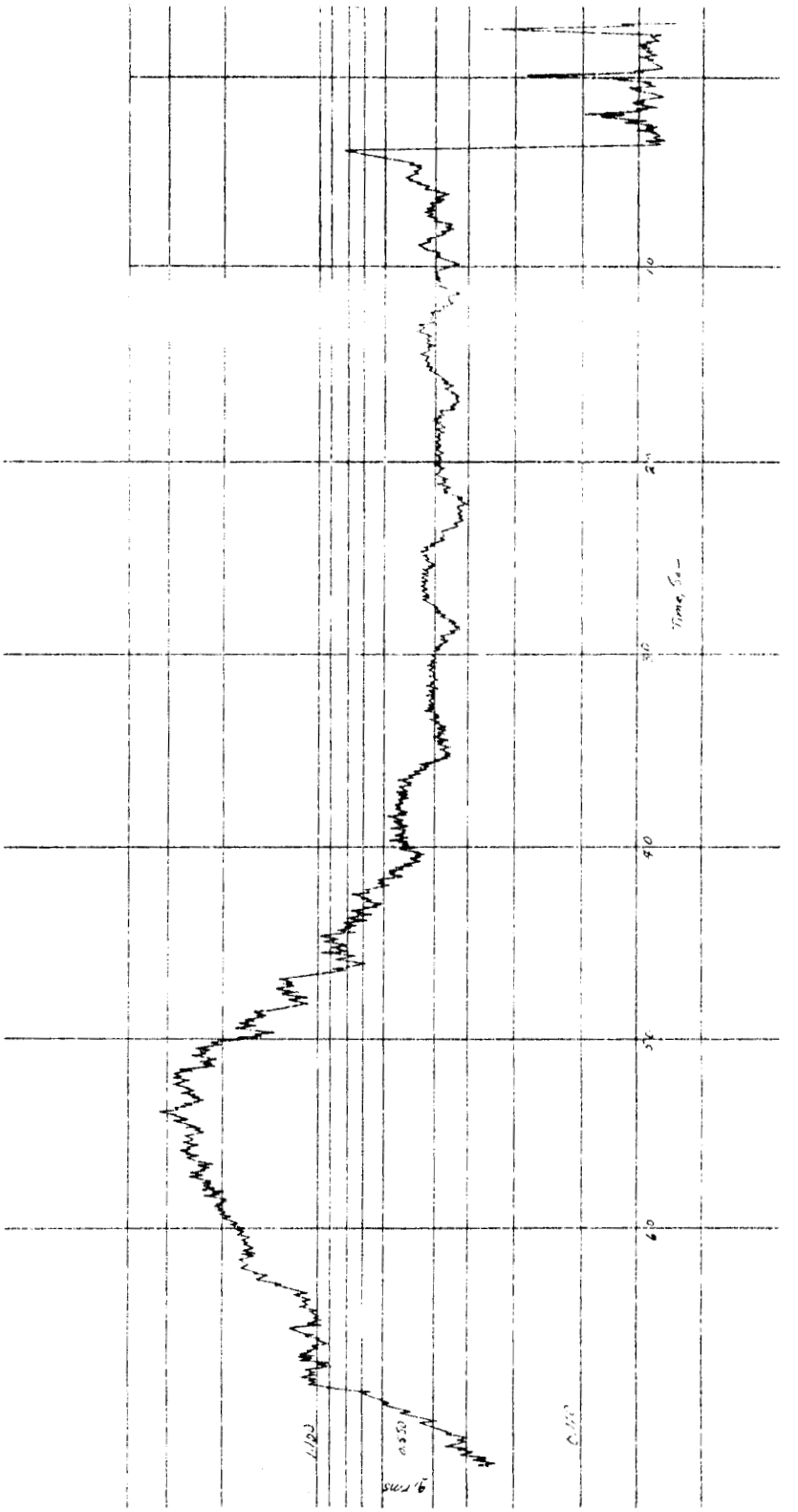

Vibration Data, Accelerometer GCCz-90-160

Figure 62

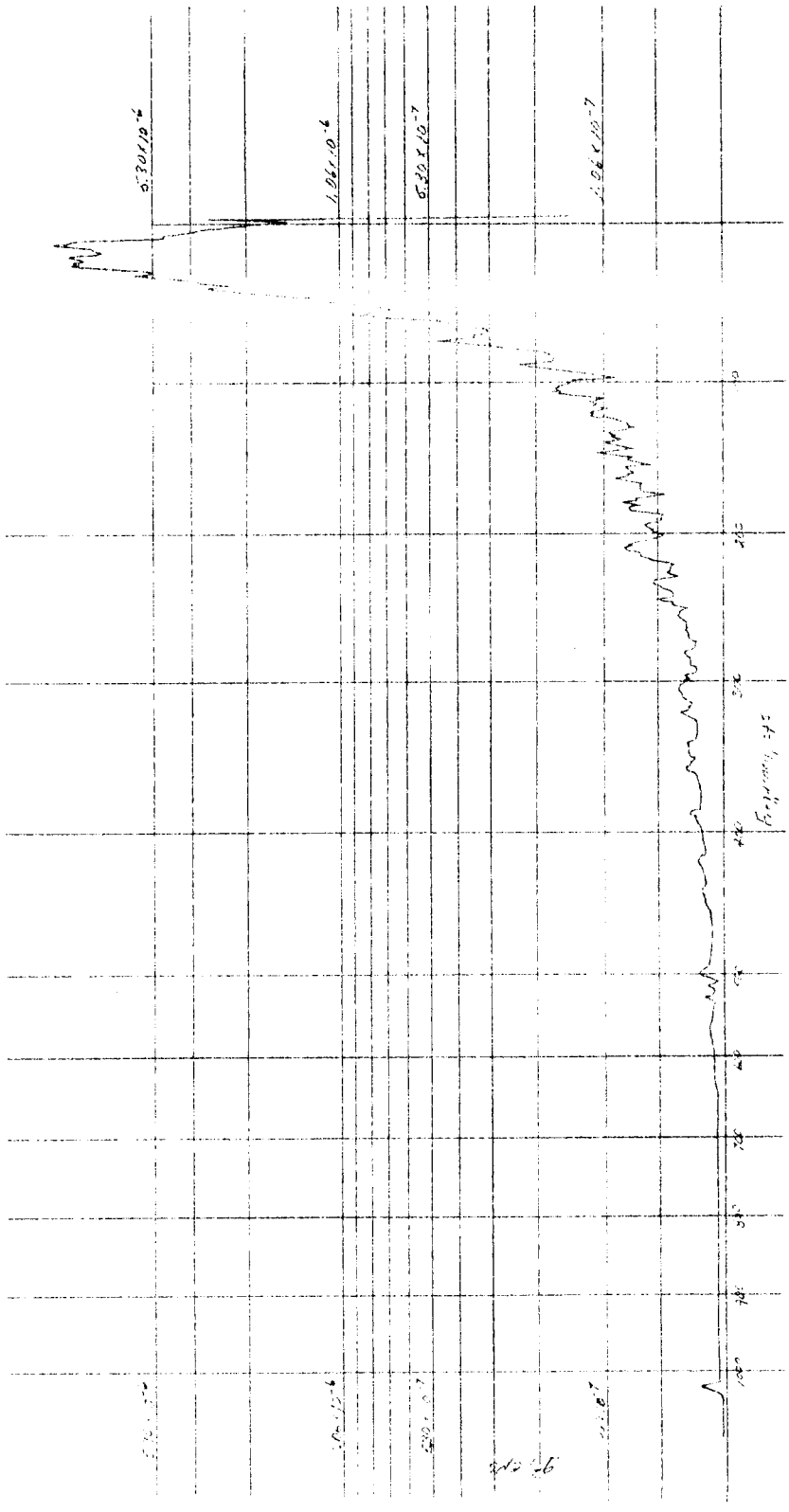

Sound Pressure Level, SPL-30-200

Figure 63

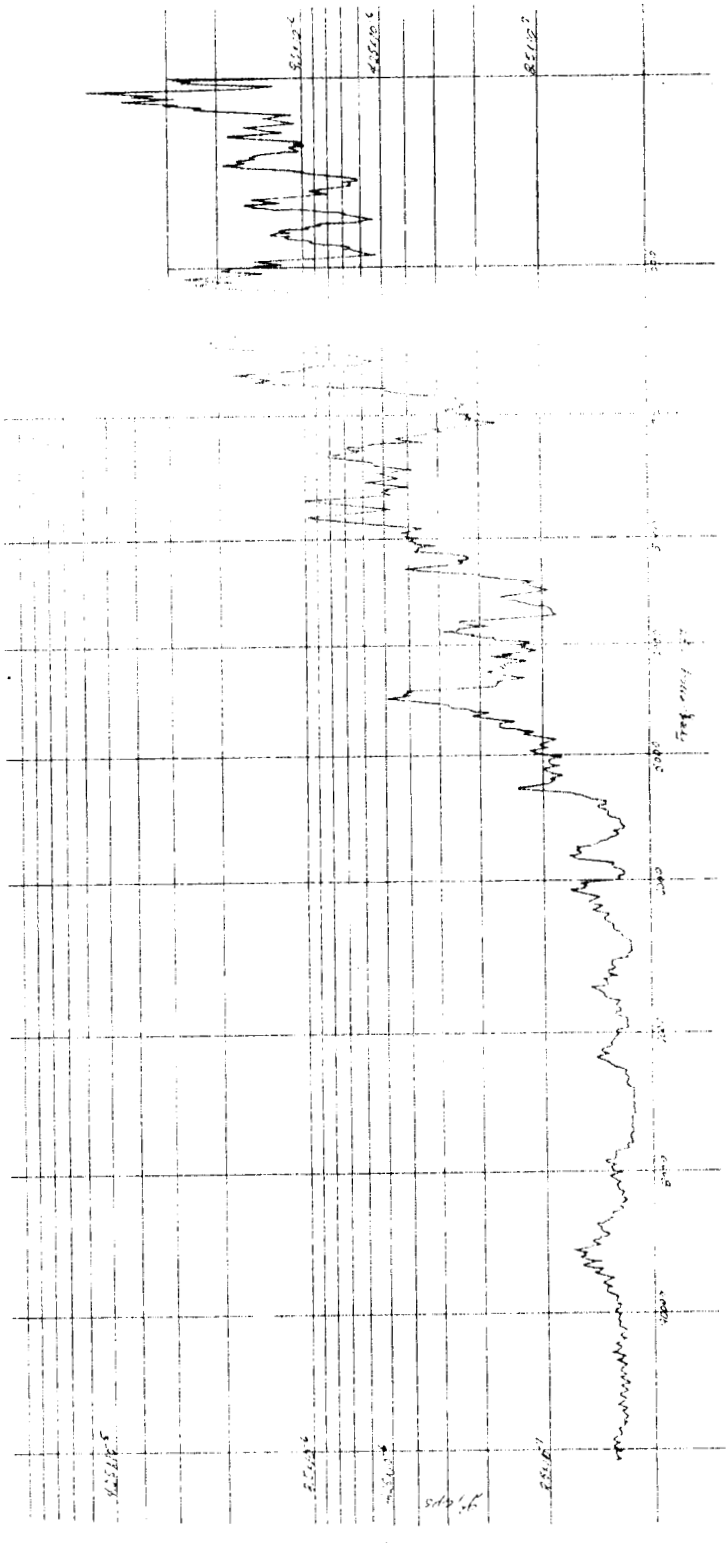

Power Spectral Density, Accelerometer Ch [illegible]-0-20

Figure 64

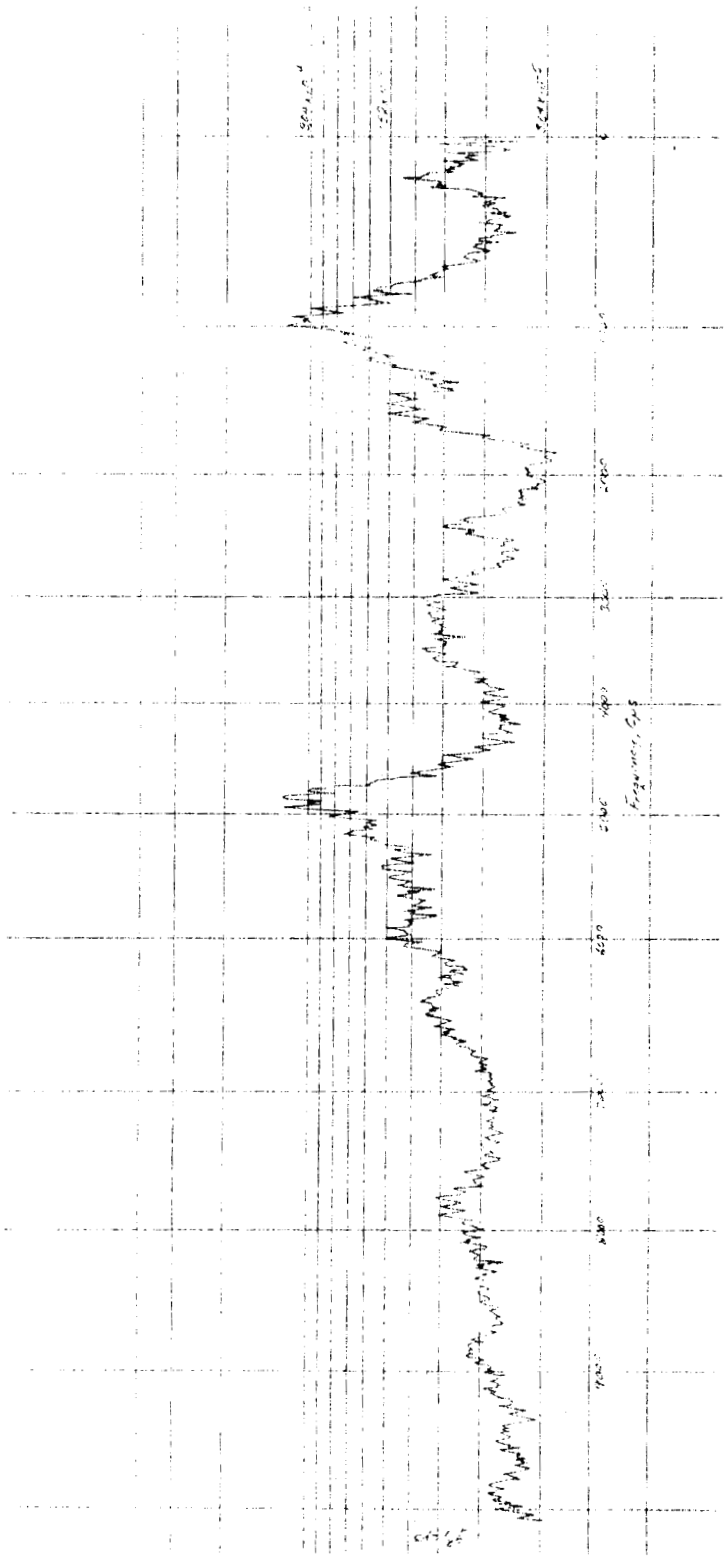

Power Spectral Density, Accelerometer GCAy-45-20

Figure 65

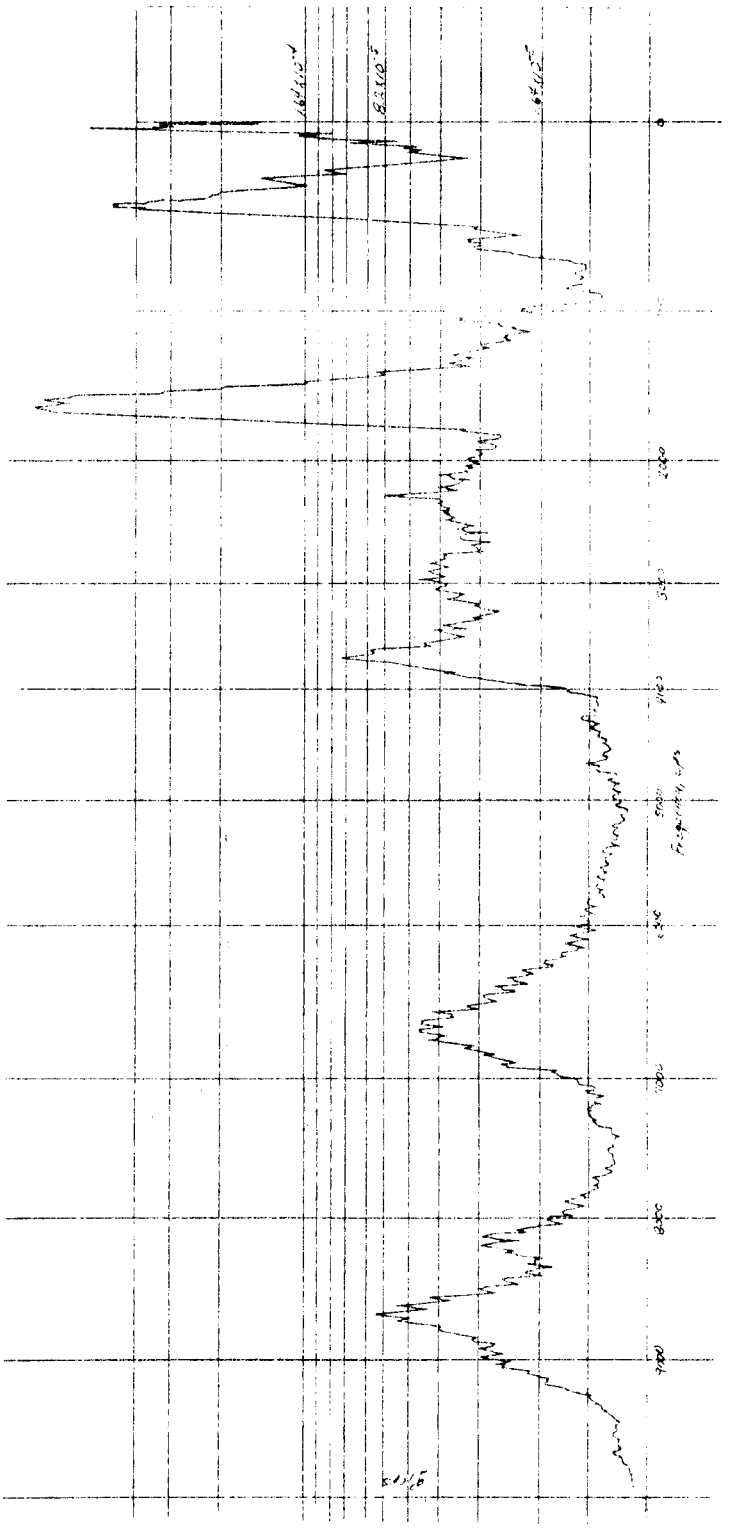

Power Spectral Density, Accelerometer GCFy-0-2

Figure 66

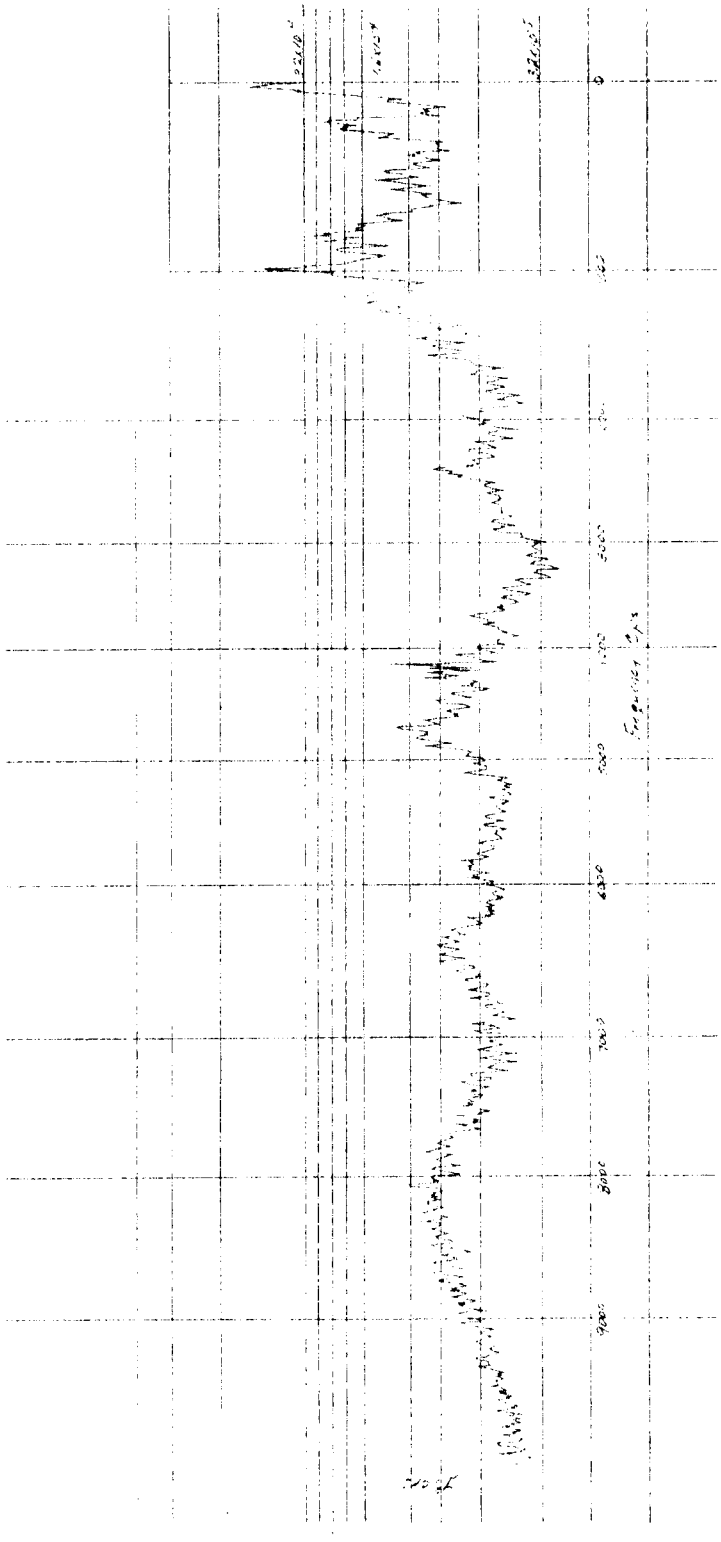

Power Spectral Density, Accelerometer GCAy-225-20

Figure 67

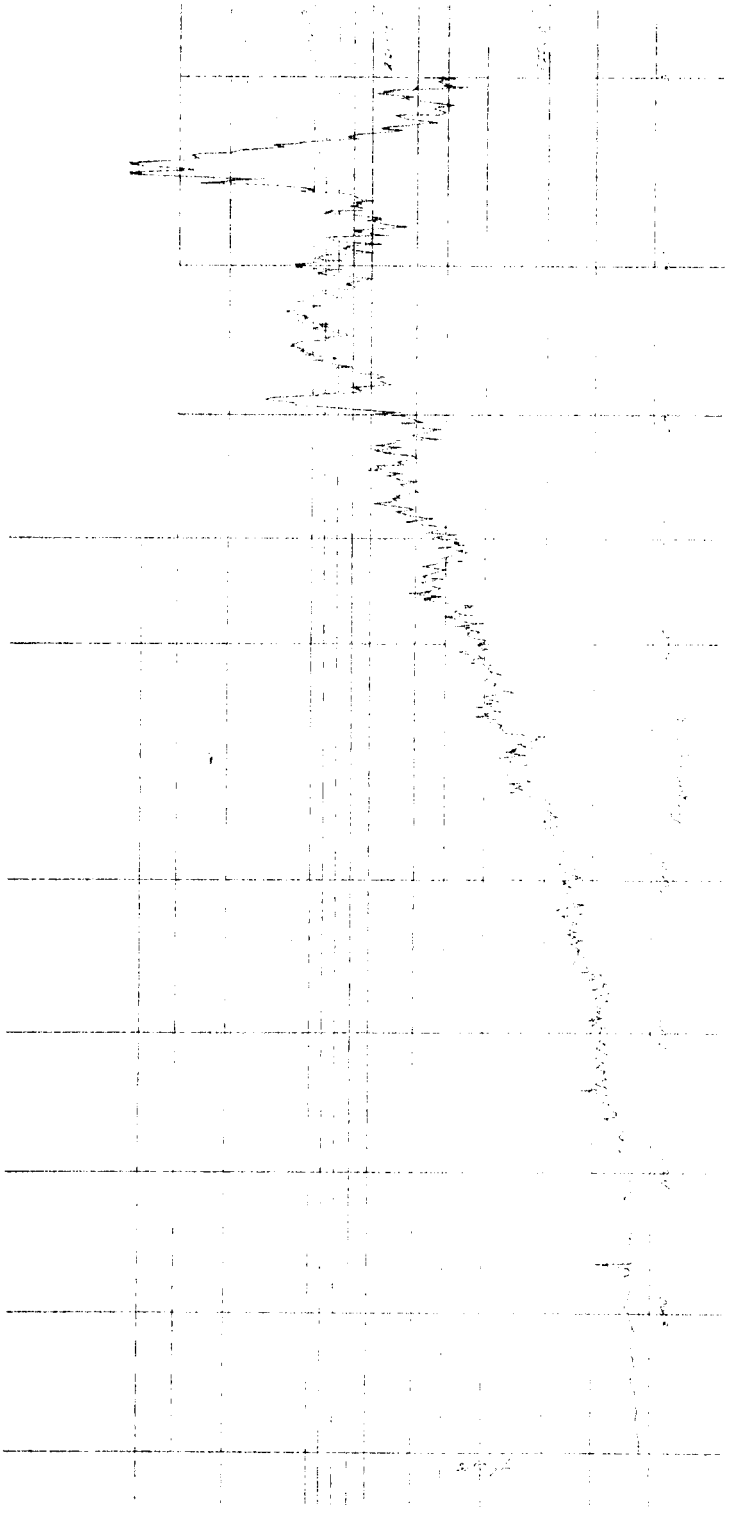

Power Spectral Density, Accelerometer GCCz-90-304

Figure 68

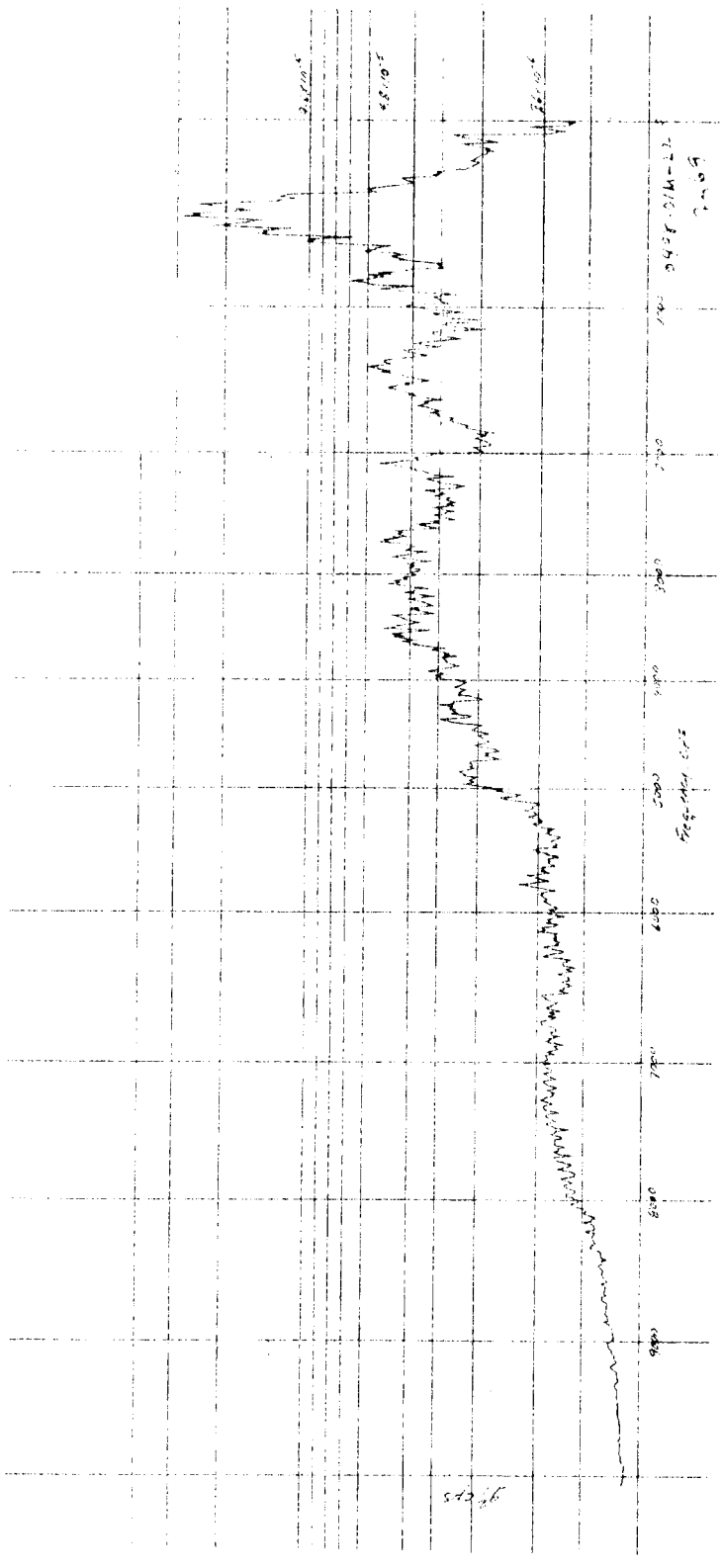

Power Spectral Density, Accelerometer GC1z-90-160

Figure 69